CHASING THE MUD: ANALYSING THE GEOMORPHIC IMPACT OF THE 19-21 JUNE 2015 RAINSTORM AND FLOOD EVENTS IN SOUTHERN NORTH ISLAND, NEW ZEALAND

A thesis

submitted in partial fulfilment

of the requirements for the degree

of

Master of Science in Physical Geography

at

Massey University, Palmerston North,

New Zealand

by

Erica Malloy

2021

Abstract

Heavy and prolonged rainfall during the 19-21 June 2015 storm event, triggered the largest recorded flood in the Whanganui River and resulted in widespread flooding in adjacent Whangaehu and Turakina drainage basins. In addition, this high intensity rainstorm triggered many thousand landslides in the soft-rock hill country of these catchments, impacting productivity of vast areas of the landscape within the region.

The principal objective of this research was to analyse and better understand the internal dynamics of the catchment sediment cascade and explain the manifestation of geomorphic change within the Whanganui, Whangaehu and Turakina catchments during the intense disturbance event of June 2015. To accomplish this, a geomorphic and sedimentological assessment of channel, floodplain and slope response to the 19-21 June rainstorm and flood events was undertaken to examine erosion, transportation and deposition zones that developed during this event. To facilitate a better understanding of the processes and mechanisms operating during this major storm event, this research provides an assessment of sediment sources and sinks that developed during the storm in the lower Whanganui, Whangaehu and Turakina catchments. It is surmised that the extreme nature of this rainstorm activated the landscape to a degree whereby slope-channel environments were highly connected.

Using GeoEye satellite imagery, the distribution and extent of landsliding was mapped, and slope-channel connectivity quantified. Additionally, regions of overbank flood deposition within the flood corridors of these catchments were mapped and the areal extent quantified. Physical terrain attributes, such as slope aspect and angle, vegetation cover and rock type were analysed in relation to landsliding to assess the influence these factors had in determining slope instability. To evaluate the flow and sediment regime of these fluvial networks during the 19-21 June rainstorm event, field mapping and sampling of flood deposits was conducted, and an assessment of the thickness and character of these flood drapes was undertaken. Subsequent analysis of flood deposit samples incorporated grain size analysis so that a better understanding of the hydraulic processes that transported these eroded sediments could be formed. Additionally, sedimentary analysis facilitated the development of new and local knowledge of the processes that produced distinct vertical layering within the flood drape deposited during the 2015 flood event. A linkage is made between the developing flood hydrograph, event sediment flux hydrograph and the stratigraphic layering which was found at various sites within the June 2015 flood drape of the Whanganui River.

Acknowledgements

Firstly, I would like to thank my supervisors, Professor Ian Fuller and Dr Sam McColl for their encouragement, advice, and guidance throughout my research. They planted the seed for this project for which I am eternally grateful, and I could not think of a better place to have been 'chasing the mud' but in my hometown of Whanganui. I would also like to sincerely thank Professor Mark Macklin from the University of Lincoln, United Kingdom, for bestowing his wisdom, knowledge and contagious enthusiasm and passion for all thing's river related.

I am indebted to James Brassington for providing me with pre-and post-event GeoEye satellite imagery which allowed for the spatial mapping of landslides and flood drape. These images formed a large part of this research and I am truly grateful for his time and effort in supplying this data.

Also, I would like to thank Eric Breard and Anya Moebis for their guidance on laser particle size analysis (LPA) techniques and Ian Ferkurt for providing the equipment to allow me to undertake a lengthy process of my grain size analysis at home. I would not have been able to conduct my LPA analysis if Ian had not facilitated this.

Andrew Steffert, Brent Watson, Willie McKay, and Peter Blackwood from Horizons Regional Council for supplying me with data for my research.

I would also like to extend my gratitude to Whanganui River Enhancement Trust for providing me with funding throughout my research. Additionally, I would like to acknowledge and deeply thank Mrs Berys Clark for awarding me the Lovell and Berys Clark Scholarship. I am honoured to have been the recipient of these scholarships and am immensely indebted to them for their generous financial support.

Finally, a heartfelt thank you goes out to my family who have been a constant source of support throughout my learning journey. My greatest motivation and inspiration to continue my studies has been my daughter. I would like to instill in her the importance of following her ambitions and show her that with hard work and perseverance she can achieve her dreams.

Table of Contents

Chapter 1 – Introduction

1.1 Background

Heavy and prolonged rainfall during the 19-21 June 2015 rainstorm event caused widespread landsliding and flooding within the Lower North Island, New Zealand. A slow moving warm, moist north-west flowing weather system over the region resulted in over one months' worth of rain falling over the Whanganui, Whangaehu and Turakina regions within a 2-day period and generated the largest flood on record in the Whanganui River. Additionally, the heavy rainfall that fell on already saturated ground produced widespread landsliding within the region with the most extensive areas of hill slope erosion correlating with the most intense 24 hr rainfall totals. The Whanganui, Whangaehu and Turakina catchments were among the most severely damaged regions, with many thousands of shallow soil and debris slides and flows occurring within these drainage basins during this disturbance event. Additionally, extensive streambank erosion and coupled landsliding, combined with extremely high discharges, produced sediment-rich overbank flows which inundated the flood corridors of these drainage basins, subsequently depositing a thick flood drape which blanketed farmland, properties, and infrastructure. Around 400 residents within the floodplain of the Whanganui River were evacuated or self-evacuated due to rising floodwaters and SH3, north and south of Whanganui, as well as SH4 were closed due to the impacts of this rainstorm event, leaving the city completely cut-off from external aid.

This study examines and seeks to better understand how our landscape evolves in response to extreme storm events and analyses the impact human activities such as deforestation and land use has on influencing geomorphological change. This research incorporates sedimentology, grain size analysis, ground survey techniques and spatial analysis to investigate the geomorphic response of the Whanganui, Whangaehu and Turakina catchments to the June 19-21, 2015 rainstorm and flood events.

Since European settlement in New Zealand over 150 years ago, substantial land cover modifications have occurred whereby indigenous forest in hill country has been cleared to allow for expansion of agricultural and farming practices. This land cover transformation has influenced hillslope susceptibility to erosion and has increased sedimentation rates within hill country regions which has subsequently had detrimental knock-on effects within the fluvial environment (Dymond *et al,* 2005). It is widely recognised that deforestation reduces slope stability and significantly enhances erodibility, frequently leading to increased rates of soil erosion and landsliding (Marden *et al,* 2005; Marden *et al,* 2012). Large volumes of sediment liberated through increased soil degradation and slope failure are consequently incorporated into the fluvial system which has the potential to enhance the level of sediment connectivity within a catchment (McCabe *et al,* 2013). The rapid onset and accelerated rates of erosion on pastoral hill country since the clearance of large tracts of indigenous forest has necessitated the retirement and/or reforestation

of substantial regions of pastured hill country in New Zealand (Marden *et al,* 2014). Landslide distribution that resulted from the 19-21 June 2015 rainstorm within the three catchments of interest was evidently related to land use and vegetation cover with results showing that relative to grassland hill slopes, landslide damage was much less extensive on slopes covered by exotic forest or native bush.

With the prevalence and magnitude of storms predicted to increase in some regions of New Zealand due to climate change, it is important to understand both the response of the landscape and the complex processes that govern geomorphic change during these extreme disturbance events. Within regions of highly erodible hill country, the history of erosion is a key indicator to the expected response of the landscape to anthropogenic factors such as land-use and future climatic events (Marden *et al*, 2014). Fundamental processes of fluvial geomorphology, such as flow regimes, sediment sources, transfer and depositional zones have not been studied in depth within these catchments. By examining various components within these fluvial systems, such as hillslopes, the channel network, and floodplains, and how these geomorphic compartments are linked together through processes that move sediment and water between them, this research provides an insight into how these process-response systems interact and respond to change during extreme rainstorm events and gives an indication as to how this landscape may respond in the future as climate and land-use evolves.

By analysing and documenting physical terrain characteristics which influence hill slope instability, this research seeks to increase knowledge of various landscape factors that considerably contribute to soil degradation and slope failures during large rainstorm events within the Whanganui, Whangaehu and Turakina catchments. By analysing the connectivity between hill slopes and the fluvial network within these catchments, this research demonstrates that change in one part of a catchment leads to transformation in other regions of that drainage basin. Furthermore, this research facilitates knowledge of hillslopes prone to erosion in the three catchments of interest so that response to future climatic changes and land-use practises can be better understood and prepared for.

In addition, as flooding is the most common natural disaster in New Zealand and with around two-thirds of the country's population living in flood prone regions (Renwick *et al,* 2016), including large portions of the Whanganui, Whangaehu and Turakina communities, it is paramount that current knowledge of hydrological conditions, both past and present, is refined in order to judiciously manage water resources into the future.

1.2 Objectives of Research

The principal aim of this research was to examine and better understand the internal dynamics of the catchment sediment cascade and explain the manifestation of geomorphic change within the Whanganui, Whangaehu and Turakina catchments during the June 2015 storm event. It is surmised that the extreme nature of this

rainstorm event activated the landscape to such a degree whereby the slope-channel domains were highly connected and due to the weak, relatively uncompacted and fine grained nature of the dominant rock types within these catchments, the propagation of these eroded sediments throughout the fluvial systems was highly efficient. Three major objectives were implemented in order to achieve this aim and investigate this hypothesis.

- Firstly, zones of erosion and deposition were mapped, and the areal extent of these regions was quantified. The intention of mapping hill slope erosion was to distinguish between coupled versus buffered landslides to assess the degree of catchment connectivity within the flood corridors of these watersheds.
- Secondly, this research aimed to analyse landsliding in relation to physical terrain attributes such as rock type, land cover and land use, slope aspect and slope angle to assess the relationship between these terrain characteristics and the distribution and extent of erosion. In doing so this project will provide new insights into the coupling between fluvial erosion and landsliding within the three adjacent drainage basins and illustrate the fundamental role that endogenous terrain factors have in determining landslide susceptibility during intense rainfall events.
- Objective three seeks to provide new and local knowledge of the processes of overbank deposition that occur throughout the course of major flood events within the three fluvial systems of interest. To achieve this sediment sampling and grain size analysis was undertaken and GIS mapping and quantification of the areal extent of the flood drape was conducted. During field work sampling of the June 2015 flood drape, stratigraphic layering was found at several sites and this research sought to better understand the hydraulic processes that produced these distinct sedimentary variations.

Chapter 2 – Study Region

2.1 Introduction

The three areas of interest chosen for this research are located within adjacent drainage basins, the Whanganui, Whangaehu and Turakina catchments, which lie within the lower North Island, New Zealand (Figure 1). Flood corridors (Figure 2) within the lower Whanganui, Whangaehu and Turakina watersheds were selected due to the extensive geomorphological changes that occurred during the 19-21 June 2015 rainstorm event. These flood corridors encompass lower catchment steep hill country, deeply incised valley gorges as well as piedmont and floodplain zones that surround the main fluvial systems of the drainage basins. Figure 1 illustrates the diversity in shape and size between the three catchments of interest with these factors influencing both the amount of, and speed with which, runoff reaches the fluvial network.

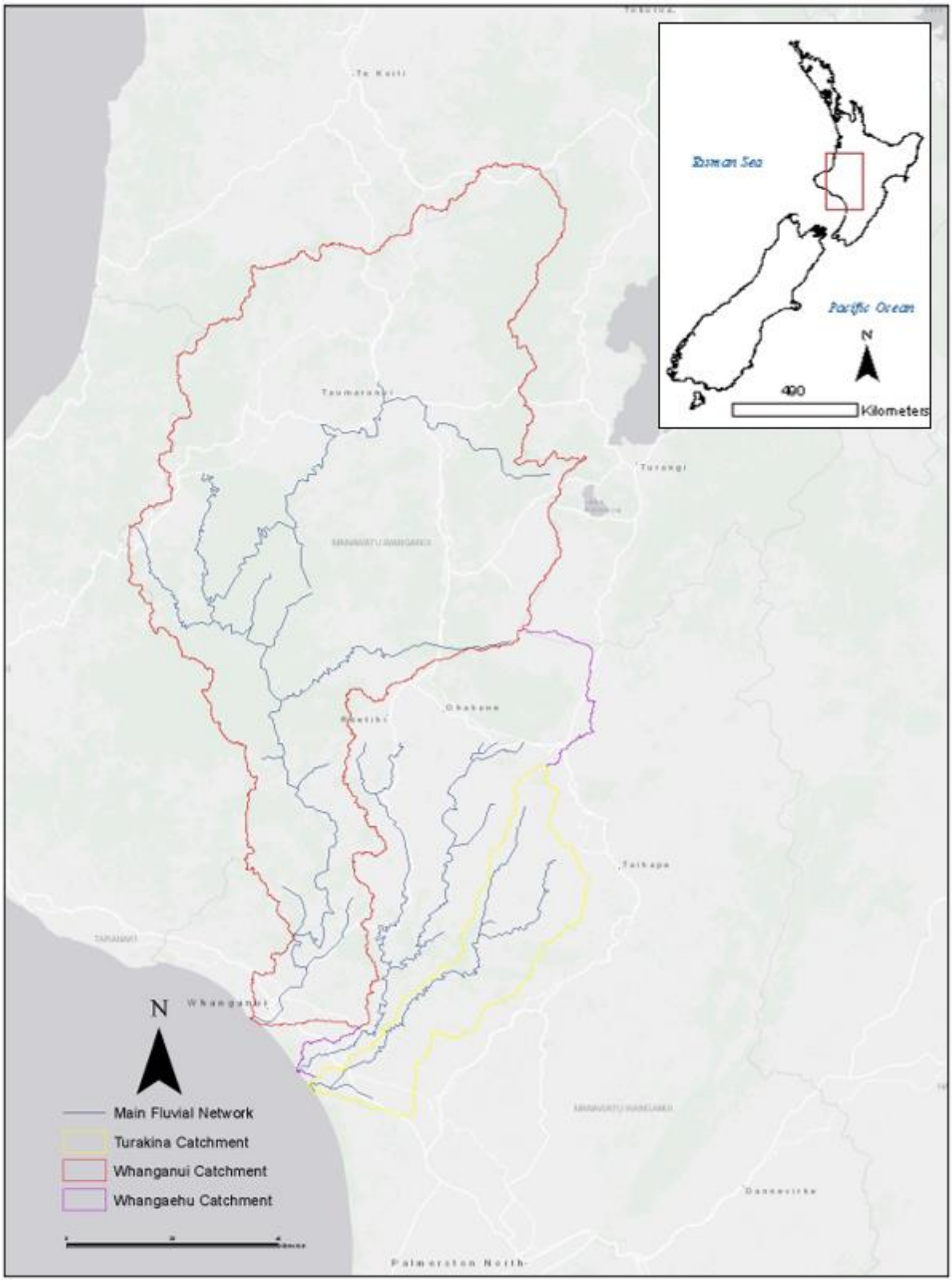

Figure 1. Location of the Whanganui, Whangaehu and Turakina catchments, lower North Island, New Zealand and major rivers within these watersheds.

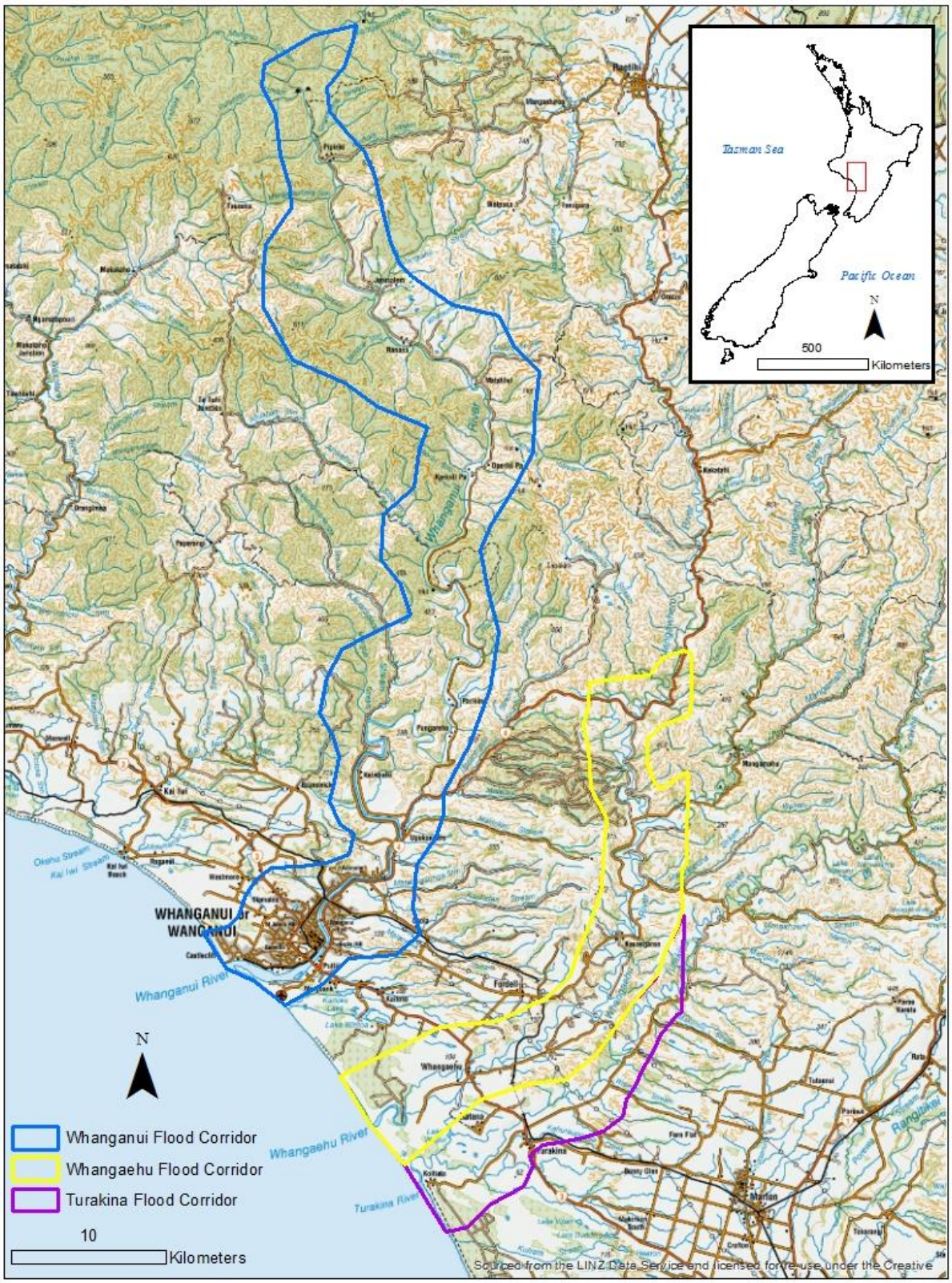

Figure 2. Location of the three areas of interest, here named the Whanganui, Whangaehu and Turakina flood corridors.

2.2 Regional Geology

The Whanganui, Whangaehu and Turakina catchments are encompassed within the landward edge of an incomplete back-arc basin, in Southern North Island, New Zealand (Figure 3). This sedimentary basin contains a comprehensive sequence of

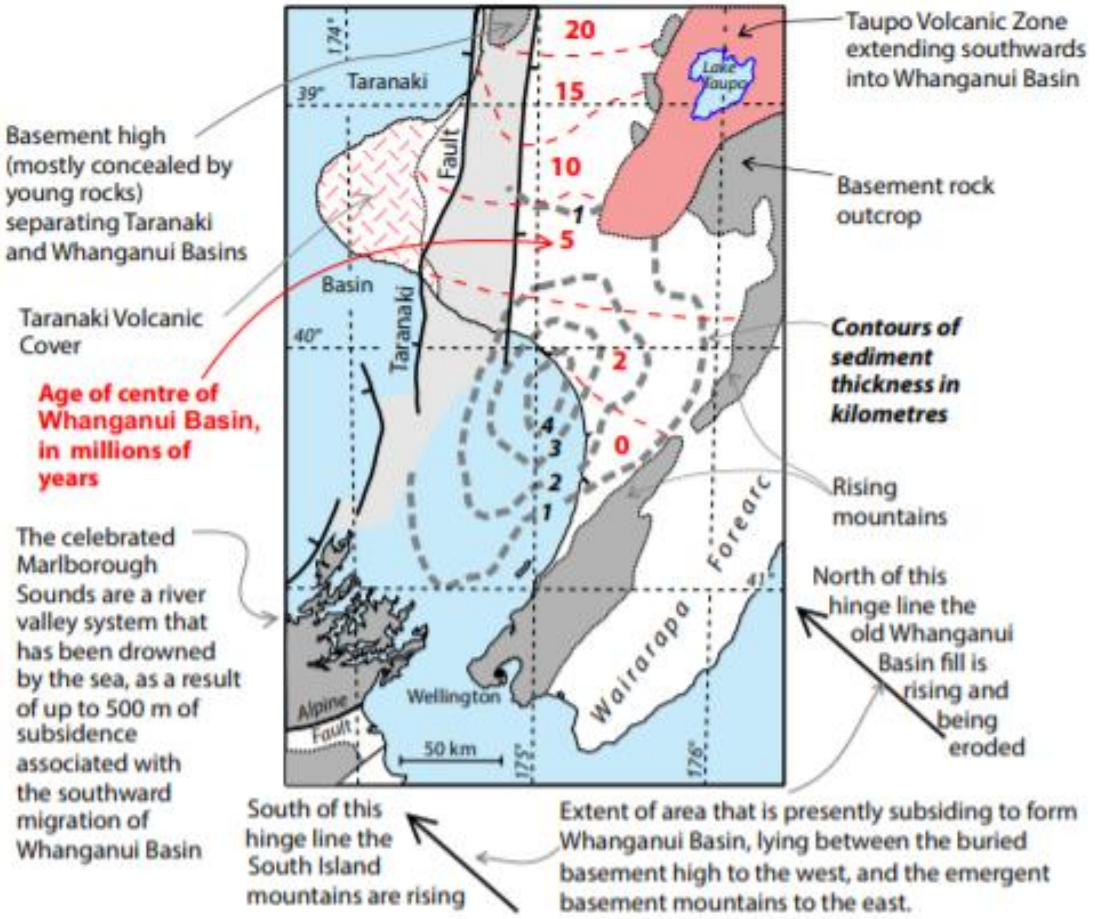

Whanganui Basin is a long-lived, major sedimentary basin. It has existed for 25 million years, moving steadily southward. Its origin is linked, in some way that is poorly understood, with the active volcanic arcs situated to the north of it.

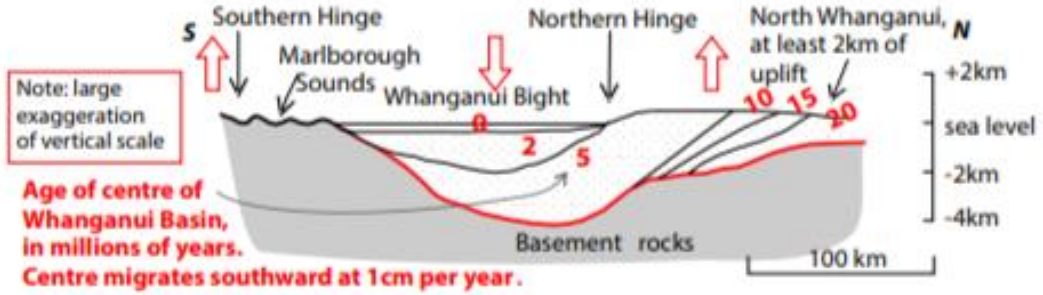

North - south profile through Whanganui Basin to show how the basin has migrated steadily southward for 20 million years. During that time it has maintained a position adjacent to the southern limit of the active volcanic arc.

Figure 3. Location and development of Wanganui Basin (Ballance, 2017).

interfingering shallow marine and terrestrial sediments that were deposited throughout the entire Quaternary Period (Pillans, 1994). The base of the Rangitikei Supergroup represents a major regional subsidence event, referred to as the "Tangahoe pulldown", and marks the initiation of the Wanganui Basin as a separate depocenter (Townsend *et al,* 2008). The Wanganui Basin formed during the Pliocene and has since received abundant synorogenic deposits which reach a maximum thickness of approximately 5000 m (Fleming, 1953). Over the past 5myr interglacial-glacial climatic cycles have generated a characteristic sedimentation pattern within the Whanganui Basin whereby regular oscillations between deposition of shallow marine gravel, sandstone and shell beds and relatively deeper outer continental-shelf marine siltstones and mudstones has taken place (Ballance, 2017). The northern margin of the Wanganui Basin has been progressively uplifted over geological timescales and has generated a steady influx of sediment to the south of the basin. High sea-cliffs along the coast west of Whanganui City reveal the gentle south-westward dip (between 2° and 8°) of relatively soft Tertiary age strata within the northern section of the Wanganui Basin (Fleming, 1953). Due to tectonic uplift, these thick sedimentary deposits were never deeply buried and compacted, producing a relatively low-strength suite of mud dominated deposits (Ballance, 2017). Gradual uplift, in combination with sea-level fluctuations and abundant deposition of terrestrial sediments, has resulted in a broad flight of 12 named marine terraces which extend more than 20km inland and rise to a height of more than 300m near Kai Iwi Beach, to the west of Whanganui (Pillans, 1990). These wave-cut platforms are aligned approximately parallel along the current coastline so that the main river channels and terraces are incised through these marine landforms at an oblique, near perpendicular, angle in their route to the sea. Regional uplift, in combination with local folding and faulting of strata has influenced the drainage pattern of the main rivers within the Wanganui Basin (Figure 4). 3D seismic data reveals that up until approximately 5Ma, the Whanganui river system ran to the north west, draining into the Tasman Sea in the region north of New Plymouth. Subsequent tectonic uplift of the Waikato region caused a reversal of this fluvial system, diverting the course of this fluvial system to the south east where it currently meets the Tasman Sea at Whanganui (T. Stern, personal communication, March 20, 2017).

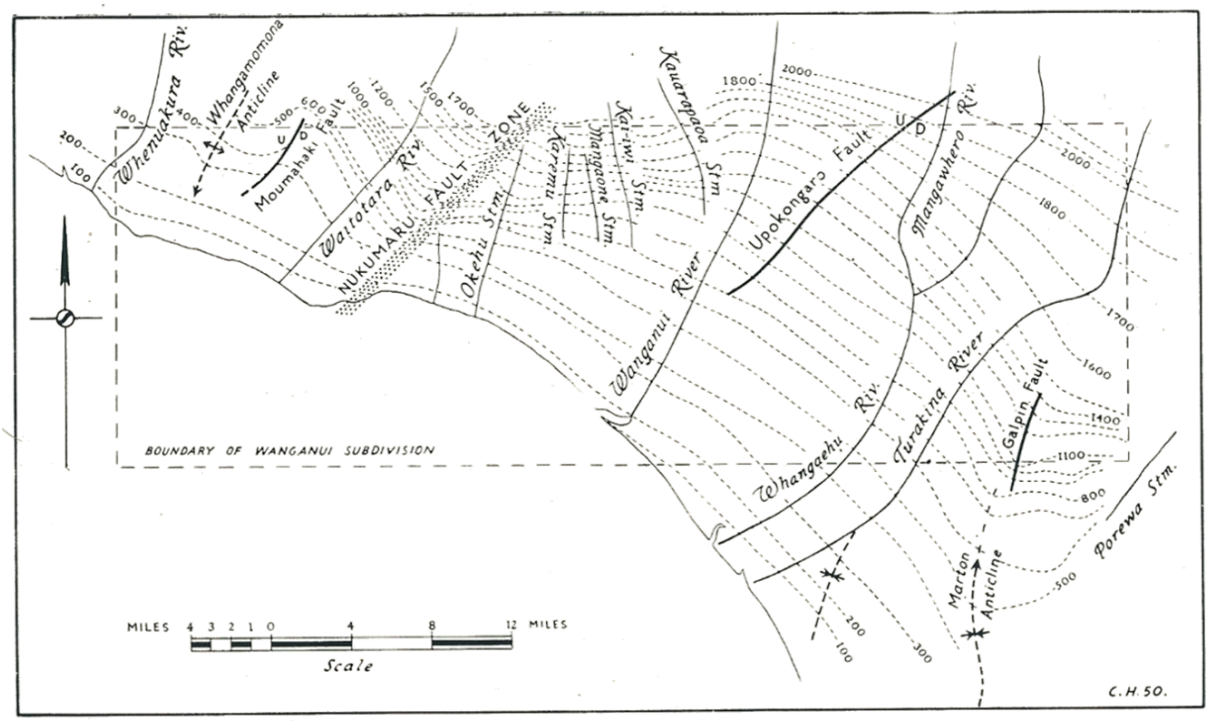

Figure 4. Landward section of the Wanganui Basin showing locations of major structural features within the coastal plain of the Whanganui, Whangaehu and Turakina areas. The main rivers are consequent upon the seaward slope of the deformed peneplain of the coastal lowland, shown by generalised summit contours. Folding and faulting of the coastal lowland has guided the streams that cross it (Fleming, 1953).

Relatively weak Neogene deposits laid down during Pliocene and Pleistocene marine transgression are the predominant sediments found in the Whanganui, Whangaehu and Turakina regions (Hancox *et al,* 2005a). Late Quaternary alluvial gravel and sand, as well as marine, estuarine and lagoon deposits dominate the coastal margin. Additionally, dune sand, swamp deposits, peat and lake silts are common within the coastal plain. Inland, early Quaternary marine gravel, silt conglomerate, sand and limestone predominate, with high inland terraces composed principally of alluvial gravel and sand. Dominant surface rocks of the steep hill country environment are consolidated to weak marine and non-marine mudstone, sandstone, conglomerate, and limestone of the Miocene-Pliocene Epochs. Volcanic rocks and lahar deposits are prevalent within the eastern and northern reaches of the Whanganui and Whangaehu catchments and are common within the fluvial bedforms of the main river systems, having been eroded, reworked, and deposited downstream of their original source region (Figure 5). The comparatively soft, weak sediments within these watersheds were raised and folded during the Quaternary, so that inland, a relatively mature landscape has evolved having been planed by erosion and deeply dissected by the fluvial system so that the hill country region encompasses a characteristic steep, sharp terrain.

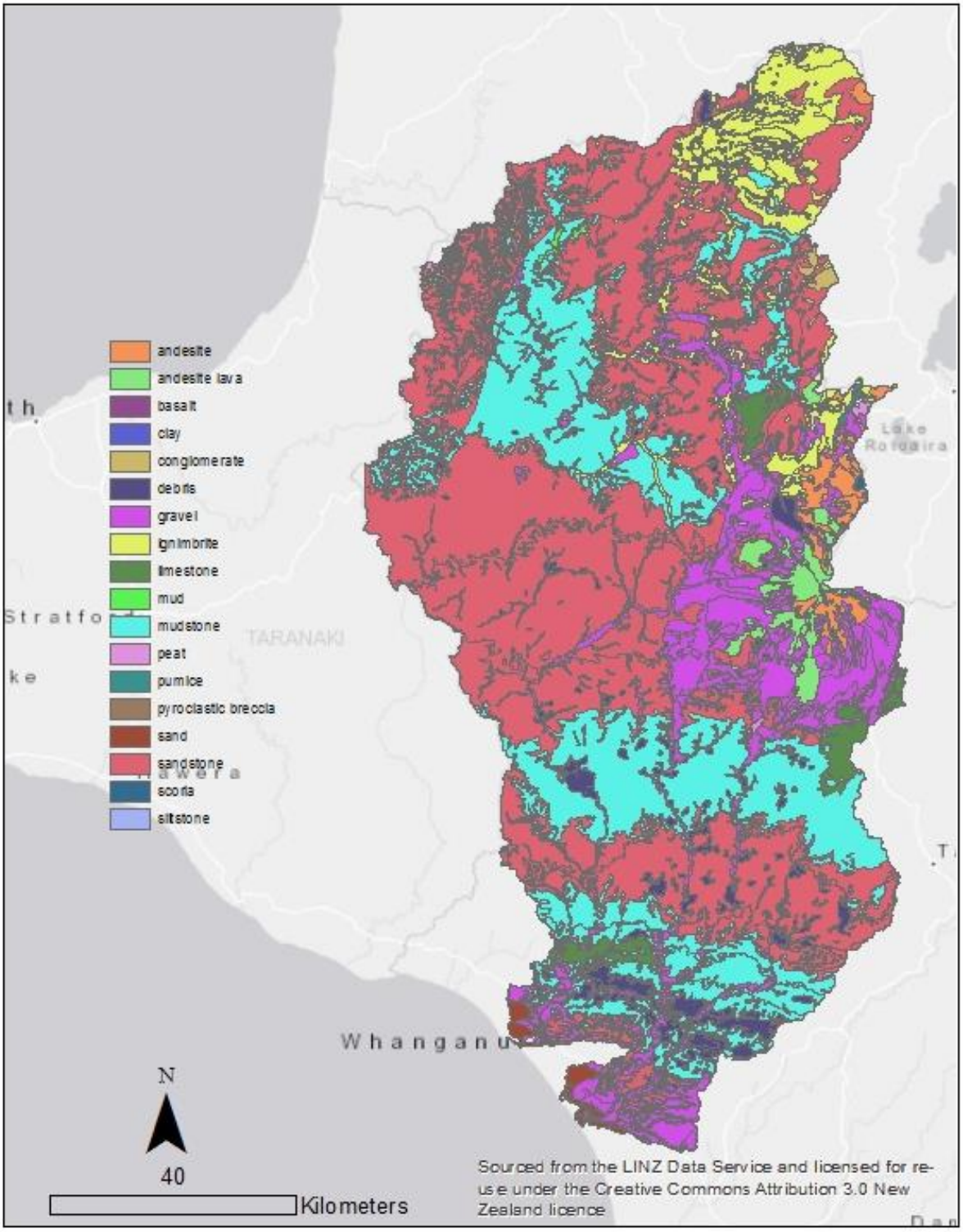

Figure 5 Stratigraphic age and lithology within the Whanganui, Whangaehu and Turakina catchments (GNS Science, 2014).

2.3 Whanganui River Catchment

The Whanganui River drainage basin, bound to the south by the Whangaehu and Waitotara watersheds, to the east and north by the Waikato River system and to the west by the Waitara Catchment, encompasses an area of approximately 7,112 km^2 and drains into the Tasman Sea at Port Whanganui. Although a large portion of this drainage basin was affected by the 19-21 June 2015 rainstorm, a relatively small section of the lower Whanganui Catchment was chosen for this research (Figure 2). This region is situated where the highest intensity rainfall fell during the 19-21 June 2015 rainstorm and subsequently encompasses a zone where some of the worst erosion, flooding and sedimentation occurred. The Whanganui flood corridor encompasses a relatively narrow zone of the lowland coastal plain, piedmont, and surrounding steep hill country zones as well as the floodplain of the Whanganui River. This flood corridor is approximately 505 km^2 and incorporates several settlements lying adjacent to the Whanganui River, including Pipiriki, Jerusalem, Atene, Parakino, Kawhaiki, Upokongaro and Whanganui. For the purposes of this study, and due to imagery constraints, an area of 219 km^2 was utilized in the landslide mapping analysis section.

2.3.1 Geomorphology

The Whanganui Catchment comprises a diverse landscape, encompassing the volcanic terrain of Tongariro National Park to the northeast of the watershed, as well as the relatively flat to gently rolling pastured landscape of the coastal fringe and the steep rugged hill country that covers around 60 percent of the total drainage basin (Tonkin & Taylor, 1978). The relatively soft Tertiary strata that underlies much of the Whanganui drainage basin has resulted in a complex and highly dense river network, that has deeply incised the landscape so that the Whanganui River, and its main tributaries, are confined within very narrow and steep sided valleys (Figure 6). A suite of paired fluvial strath terraces can be delineated well inland from the river mouth and were developed during Pleistocene glacial episodes (Manville *et al,* 2009). Dendritic drainage systems, such as the fluvial network of the Whanganui Catchment, develop in terrains where there are no distinctive geological controls and the drainage configuration facilitates a relatively smooth conveyance of sediment due to the lack of structurally controlled impediments (Brierly *et al*, 2005). The form of this morphological system generates high rates of flow-sediment interaction through the distribution of available energy during high rainfall events. In the upper to middle catchment regions, channels tend to dissect deeply into bedrock and have little or no floodplain development in the narrow valleys. The main alluvial plain of the Whanganui River lies adjacent to the lowest reach of the channel, upon which a large portion of Whanganui City is located (Figure 7). Taupo Pumice Alluvium (~1.8 ka) underlies a substantial area of the current Whanganui floodplain to a thickness of several metres (Fleming, 1953; Manville *et al,* 2009; Watson *et al,* 1998).

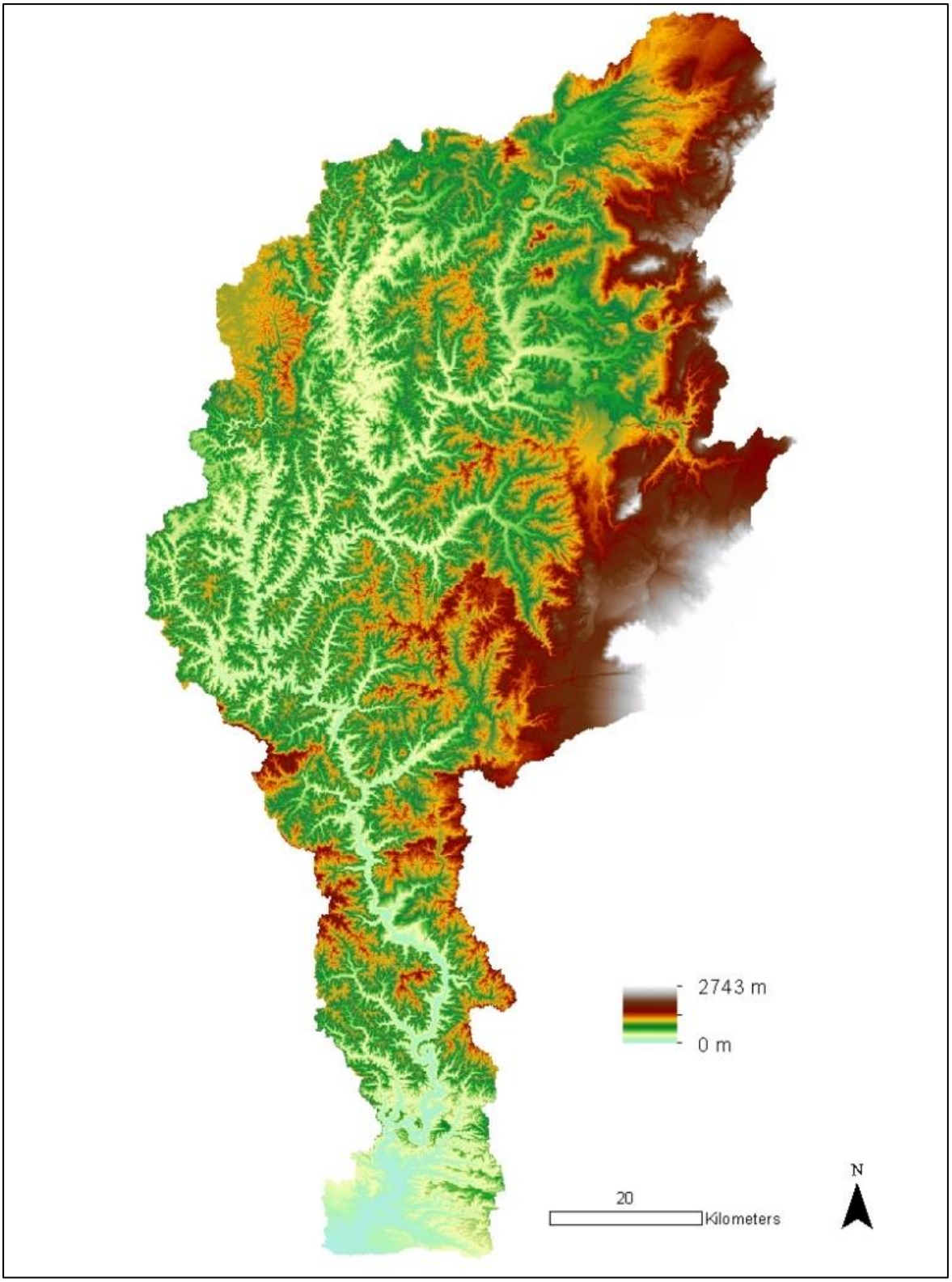

Figure 6. 15 m digital elevation model (DEM) of the Whanganui drainage basin. This model shows the dendritic drainage pattern within the catchment and the relatively high relief surrounding the fluvial network. (DEM courtesy of Koordinates).

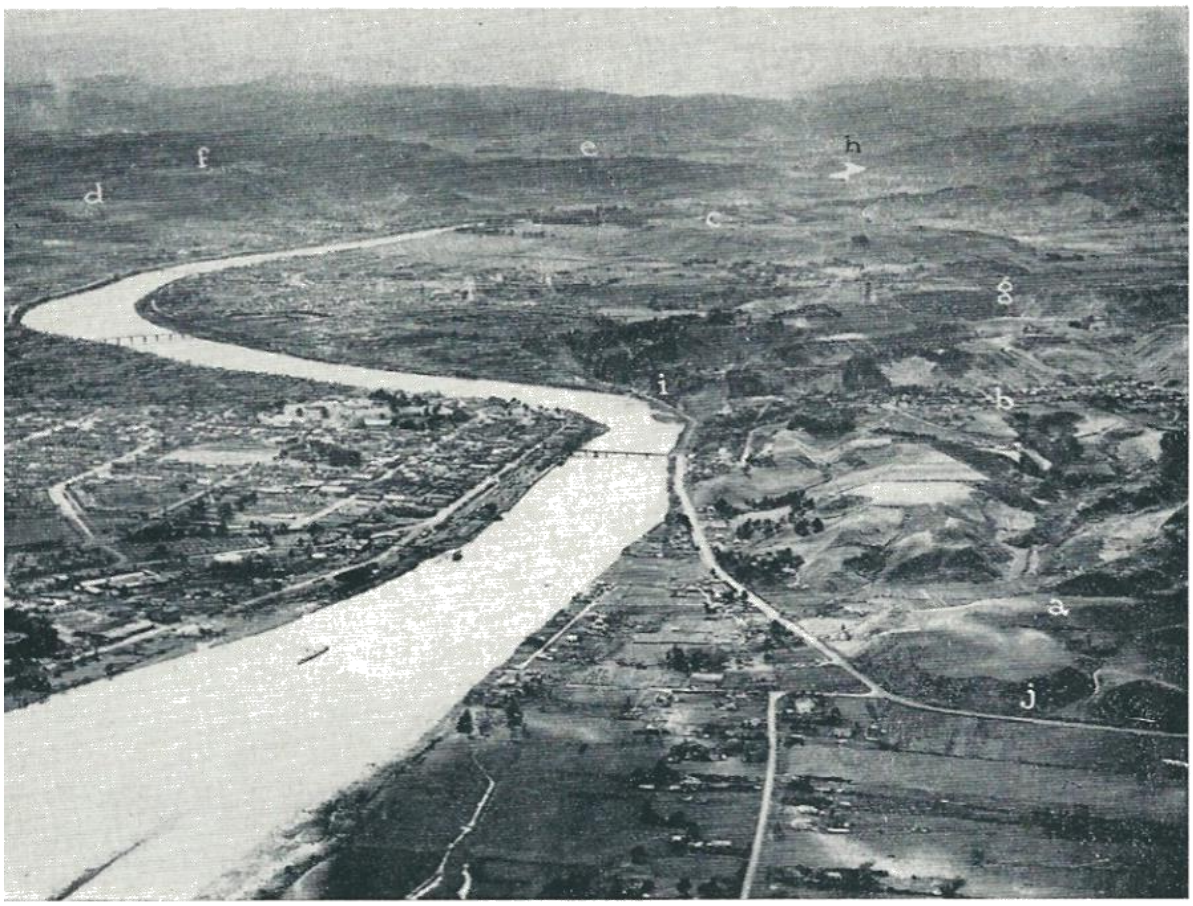

Figure 7. Aerial view of the Whanganui township, looking up the Whanganui Valley from near the river mouth. The city is built on the dune covered Aramoho Terrace. Terraced forms dominate the landscape; the most conspicuous terraces at Putiki (a), Durie Hill (b), Mt Churton (c), behind Aramoho (d), and at Mission (e), are parts of the Rapanui Terrace. Mt Jowett (f), and Ikitara (g) are parts of the Brunswick Terrace. Castlecliffian sediments, overlying Nukumaruan at Makirikiri (h), are exposed in valley walls, for instance at Shakespeare Cliff (i), and Putiki (j) (Fleming, 1953).

The Whanganui Catchment morphology is synonymous to an inverted funnel in that water during significant flood-producing events is contained within narrow gorges prior to reaching the piedmont zone and coastal plain whereby floodwaters then disperse rapidly across the floodplain at Whanganui city. These geomorphological factors combined with the location of homes and infrastructure on the Whanganui River floodplain often have negative consequences for residents of the city during intense rainfall and subsequent flood events.

2.3.2 Rock Type and Geology

A diverse suite of rock types underlies the Whanganui flood corridor (Figure 8). Bedrock in the steep hill country within the upper reaches of the flood corridor is predominantly composed of early Pliocene sandstone and mudstone as well as Holocene landslide deposits. The middle reaches of the area of interest is underlain by younger middle Pliocene repeated sequences of pebbly to well sorted sandstone and mudstone with poorly fossiliferous siltstone and limestone also common. The piedmont and coastal lowland are dominated by moderately weathered undifferentiated poorly sorted loess-covered alluvial gravel deposits,

Middle to Late Pleistocene river sediments (sand, silt, pumice, and clay) and Holocene windblown dune deposits.

Figure 8. Lithological map of the Whanganui flood corridor (based on the GNS Science 250k geological units' layer in the GNS QMap series, 2014).

2.3.3 Landcover and Land Use

Milling of the native forest and ensuing pastoral development within the Whanganui Catchment began in the late 1880's after the European population began to settle inland (Tonkin & Taylor, 1978). The Whanganui National Park currently protects one of the North Islands largest remaining tracts of podocarp-hardwood lowland forest and encompasses 742 km^2 of land surrounding the middle and lower reaches of the Whanganui River (Department of Conservation, 2006). The relatively steep, rugged terrain of the inland drainage basin has restricted land use development and current land use practices reflect the limitations imposed by relief (Tonkin & Taylor, 1978). A distinct variation between contemporary landcover and land use of the coastal lowland zone and landcover and land use within the hill country further inland exists within the Whanganui flood corridor. Landcover of the coastal plain predominantly consists of the built-up urban region of Whanganui township and surrounding pastural regions (Figure 9 and 10). Further inland, canopy cover is provided by large expanses of indigenous forest, closed canopy pine plantations, and Manuka and Kanuka scrub. Relatively smaller tracts of exotic grassland and open canopy pine forestry are interspersed (Figure 11).

Figure 9. Photo taken of slopes surrounding the Whanganui River at Crowley House north of Whanganui city on 20th June 2015 at 13:52. This photo was taken during the relatively early stages of the June 2015 rainstorm and flood event in the lower Whanganui catchment. Shallow landsliding is visible on pastured slopes in the distance and runoff in the foreground (photo courtesy of Crowley family, 2015).

Figure 10. Photo taken of the slopes surrounding the Whanganui River at Crowley House north of Whanganui city on 21tst June 2015 at 15:51. Extensive shallow landsliding resulted from the intense rainfall that fell over this area during 20-21 June 2015. The above two photos reveal the during and after effect of this rainstorm on the pastured slopes surrounding Crowley House (photo courtesy of Crowley family, 2015).

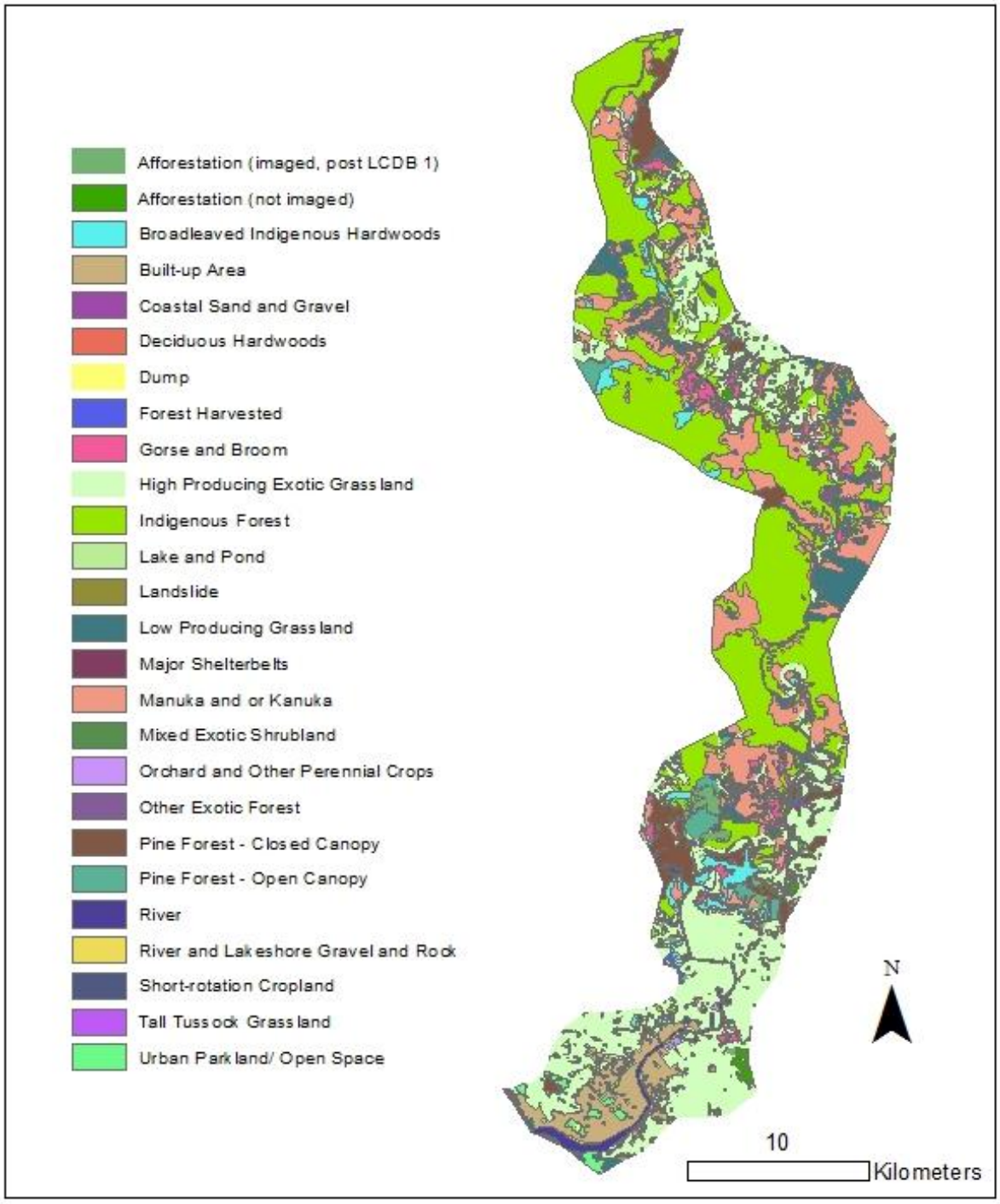

Figure 11. Vegetation cover within the Whanganui flood corridor (based on the New Zealand Land Cover Database (LCDB) from Land Resource Information Systems portal, 2017).

2.3.4 Whanganui River

The Whanganui River is a major fluvial channel in the North Island, New Zealand. To many Maori this is a river of sacred power - their *awa tupua* and in Maori understanding the Whanganui River is considered a person – a *tupuna,* or ancestor (National Geographic, 2019). On March 20, 2017 New Zealand recognised in law that this river is a living being – "Te Awa Tupua – the river and all its physical and metaphysical elements – is an indivisible, living whole, and henceforth possesses "all

the rights, powers, duties, and liabilities" of a legal person" (National Geographic, 2019).
The total length of the Whanganui river, from its headwaters on the flanks of Mount Tongariro, is approximately 305 km (Shand, 2001) and is the second longest river in the North Island. Principal tributaries include the Ongarue and Ohura rivers to the north, the Whakapapa and Manganui-a-te-Ao rivers rising from Mt Ruapehu in the east and the Whangamomona and Tangarakau rivers to the west. Whilst eastern tributaries erode through volcanic strata, western tributaries have dissected sedimentary mudstone and sandstone formations so that downstream alluvial deposits consist of a broad suite of fluvially transported sediments.
From its source, the Whanganui River flows north-west for approximately 60 km, before turning south near Taumarunui where it winds a sinuous course to drain into the Tasman Sea at Port Whanganui (Beaglehole, 2015).
At Whanganui, the mean flow of the river is estimated to be 229.0 m/s (cumulative catchment average) and the annual sediment yield is calculated to be 4,699,800 tonnes (Hume *et al,* 2015). The river has a very low gradient throughout much of its lower reach and large volumes of seawater flow into and out of the channel over a tidal cycle (Blackwood *et al,* 2016). The tidal range is estimated to extend 42 km up-river (J. Watson, personal communication, February 1, 2016).
The relatively low-strength muddy sedimentary rocks within the Wanganui Basin, in conjunction with tectonic uplift leading to steep slopes and deep river incision, is dynamite when it comes to erosion and slope stability, particularly in deforested regions of the catchment (Balance, 2017). A further consequence of these environmental factors is the preservation of vast areas of river terraces in the vicinity of Whanganui city (Figure 7).

Recording of flow data in the Whanganui River began in 1957 and a continuous record is available between 1957-2014 from the Paetawa recorder site (Table 1). In 2006, a new gauging station was installed at Te Rewa to provide continuous flow records which are equivalent to those at Paetawa due to the sites encompassing essentially the same catchment areas (Blackwood *et al,* 2016).
Flood records from gauging stations frequently have insufficient length to adequately identify the actual temporal context of extreme hydrologic events like large floods (House *et al,* 2002) and in New Zealand, current flood frequency analysis often relies on instrumental records which are frequently less than 100 years in length. Flood research constantly requires the calculation of peak discharge for a particular return period that is significantly longer than the available gauged record. Documented records provide another means of extending the flood history of fluvial systems (Table 2). For the Whanganui, peak discharges of historic floods have been estimated through hydraulic modelling of flood level information found in photographs and newspaper articles (Blackwood *et al,* 2016). Major documented flood events and the corresponding discharges are outlined in Table 2. Historic photographs of flooding in the Whanganui River are shown in Figure 12.

Table 1. Whanganui River at Paetawa and Te Rewa Annual Maxima 1957-2015 (Blackwood et al, 2016).

YEAR	DISCHARGE (CUMECS)	RANK	YEAR	DISCHARGE (CUMECS)	RANK
1957	2359	27	1987	1430	55
1958	3845	4	1988	1872	39
1959	1470	51	1989	1937	37
1960	1816	43	1990	4106	2
1961	2259	31	1991	2589	21
1962	2285	30	1992	1760	46
1963	1163	58	1993	2151	32
1964	2906	13	1994	2996	11
1965	3272	8	1995	2745	15
1966	2047	34	1996	2516	24
1967	2586	22	1997	1466	52
1968	2836	14	1998	3815	5
1969	1063	59	1999	2683	18
1970	1502	50	2000	3804	6
1971	2346	28	2001	2483	25
1972	1798	45	2002	1848	40
1973	2612	20	2003	2482	26
1974	2971	12	2004	3293	7
1975	3134	9	2005	1239	57
1976	1965	36	2006	1830	41
1977	1821	42	2007	1582	49
1978	3071	10	2008	2326	29
1979	2546	23	2009	1440	54
1980	1933	38	2010	2130	33
1981	1590	48	2011	2729	17
1982	1441	53	2012	2617	19
1983	1648	47	2013	3947	3
1984	1390	56	2014	2003	35
1985	1805	44	2015	4755	1
1986	2739	16			

Table 2. Whanganui River at Paetawa historic floods (Blackwood et al, 2016)).

YEAR	DISCHARGE (CUMECS)	YEAR	DISCHARGE (CUMECS)
1858	4293	1904	4325
1864	4293	1926	3856
1875	4293	1935	3700
1883	3856	1936	3732
1891	4231	1939	4011
1897	3917	1940	4689

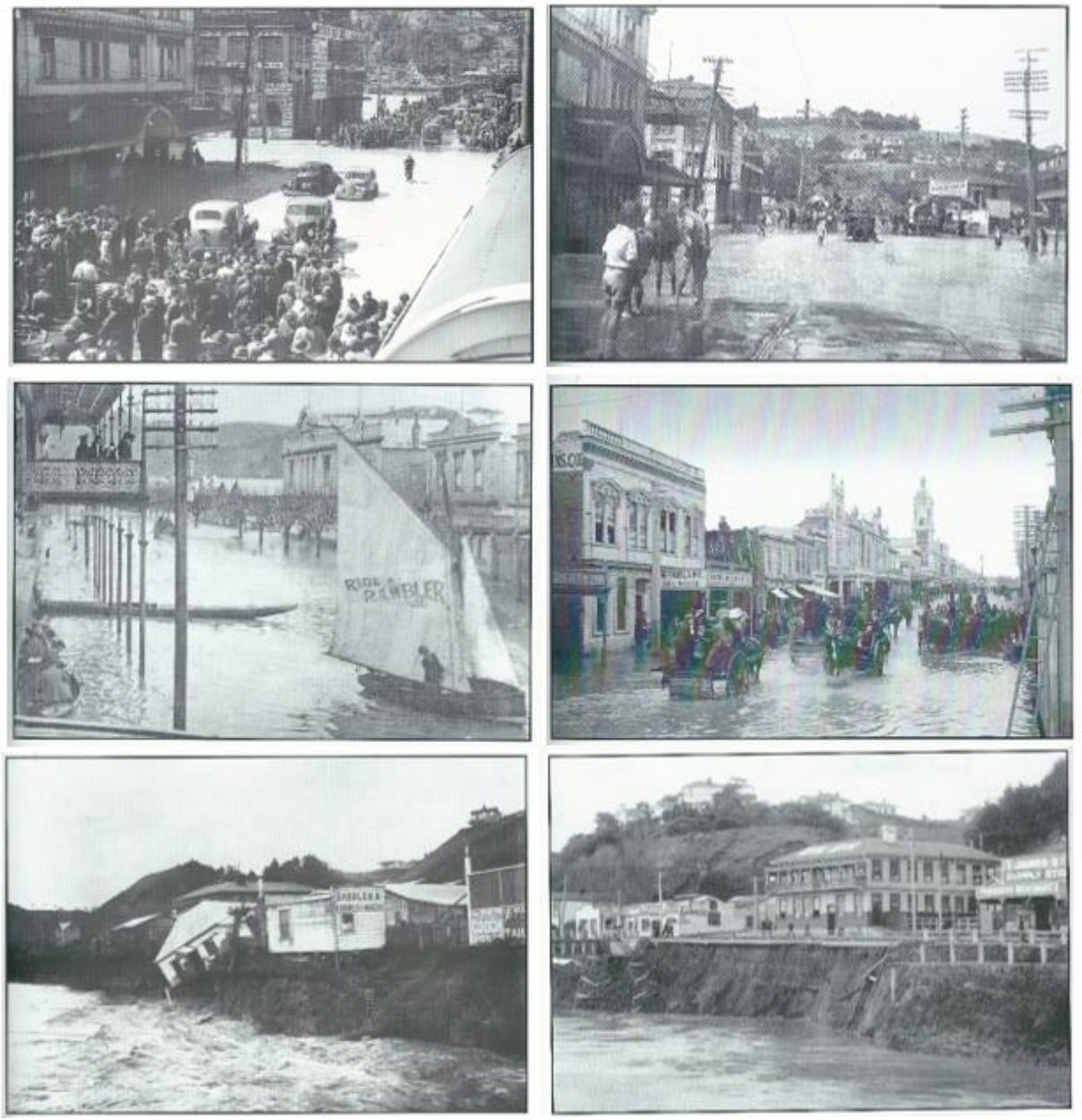

Figure 12. Top left, 1940 Flood at the corner of Taupo Quay and Victoria Avenue (Hanton & Anderson Print, 1995). Top right, vehicles and pedestrians still cross the intersect at Victoria Avenue and Taupo Quay despite floodwater inundation during the 1940 flood event (Hanton & Anderson Print, 2005). Middle left, 1904 flood shown from beside Fosters Hotel, Taupo Quay (Hanton & Anderson Print, 2009). Middle right, lower Victoria Avenue during the 1904 flood event (Hanton & Anderson, 2001). Bottom left, streambank erosion that resulted from the 1904 flood event along Anzac Parade. Erosion undercut several buildings in front of the Red Lion Hotel (Hanton & Anderson Print, 1995). Bottom right, bank erosion along the same reach as depicted in the earlier photograph on bottom left (Hanton & Anderson Print, 2009). This section of the Whanganui River is prone to streambank erosion due to a combination of the morphology of the channel, whereby flow is restricted by a narrowing of the channel immediately upstream of this section and flow naturally undercuts the outer concave bank which consists of unconsolidated alluvium.

Intense and prolonged rainfall during the 19-21 June 2015 storm event, triggered the largest flood in instrumental, as well as documented history in the Whanganui River and resulted in widespread flooding in adjacent Whangaehu and Turakina drainage basins (Figures 13, 14, 15 and 16).

Figure 13. Whanganui River mouth during the June 2015 flood event (Smith, 2015).

Figure 14. June 2015 flooding of the Whanganui River along the outer bank of the broad bend directly upstream of Town bridge. The houses inundated above are situated along Anzac Pde (Conley, 2015)

Figure 15. June 2015 flooding of the Whanganui River at Dublin St bridge (Conley, 2015).

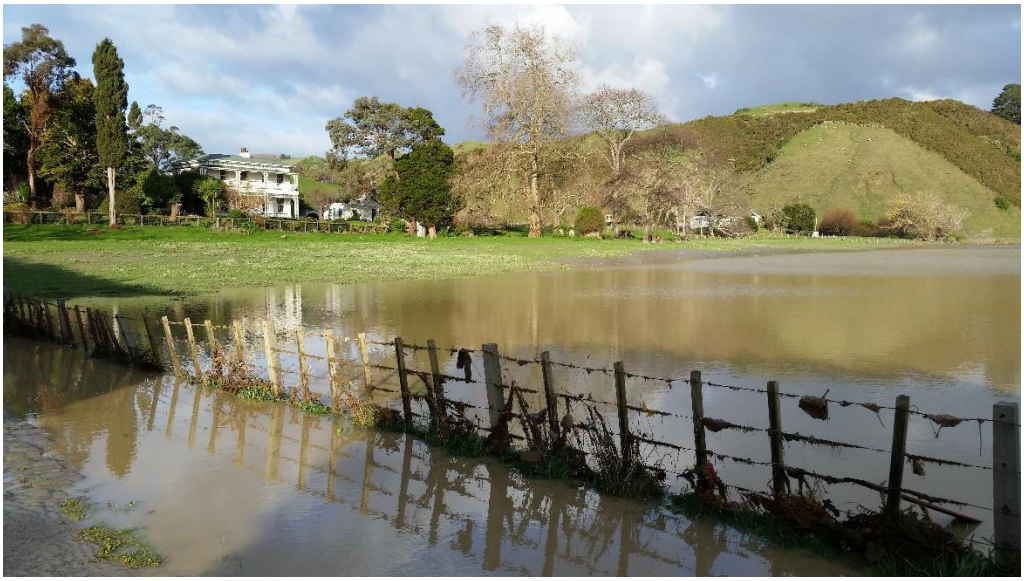

Figure 16. Photo taken 21st June 2015 at 15:07 of flooding of the Whanganui River at Crowley House north of Whanganui city. SH4 is to the left of this photograph. Picture shows the sediment rich flood waters which inundated the first river terrace at the front of the property. Flood debris is visible along the fence line in the foreground (photo courtesy of Crowley family, 2015).

Figure 17 shows the sediment plumes discharging from the three drainage basins of interest during the 2015 rain induced flood events indicating relatively coupled environments within all three catchments.

Figure 17. USGS operated Landsat 8 Operational Land Imager (OLI) imagery of the Whanganui, Whangaehu and Turakina river mouths taken (left) approximately 3 weeks prior to the 19-21 June rainstorm event on 28 May 2015. (right) Shows the sediment plumes from these fluvial systems during the storm event on 20 June 2015. (Imagery courtesy of USGS LandsatLook).

Fuller *et al* (2019) investigated palaeofloods in the Whanganui River using floodplain sedimentary archives taken at two sites, Atene, and Crowley House (Figure 16), in the lower Whanganui catchment. At Atene, an age-depth model identifies three discrete phases of sedimentation with higher-than-average flood activity

documented at 1450-1125, 950, 650-500, and 400-325 cal. yr BP, with these periods associated with enhancement of the Southern Hemisphere Westerly Wind circulation and the El Nino Southern Oscillation (ENSO) (Fuller *et al,* 2019). Cosmogenic analysis of cores taken from Crowley House reveal large floods were also more frequent during the late 1800s, reflecting a period of increased storminess and landcover change (Fuller *et al,* 2019).

2.4 Whangaehu Catchment

The Whangaehu drainage basin, bordered to the west and north by the Whanganui fluvial system and in the east and south by the Rangitikei and Turakina watersheds, drains approximately 1992 km^2 of steep hill country of the Central North Island to discharge into the Tasman Sea several kilometres southwest of Whangaehu Township (Figure 18). The Whangaehu study area encompasses a zone where some of the worst erosion, flooding and siltation occurred during the 19-21 June 2015 rainstorm. The Whangaehu area of interest, here named the Whangaehu flood corridor, is approximately 196 km^2 and encompasses a narrow strip of the coastal plain as well as the piedmont zone, floodplain and surrounding steep hill country.

2.4.1 Geomorphology

The Whangaehu river basin can be divided into three distinct geomorphological zones:

1. The Volcanic zone extends from the source of the Whangaehu River at Crater Lake, Mount Ruapehu, to the edge of the volcanic ring plain. From its origin, the channel is slightly dissected, occasionally diverging and generally flows in an easterly direction across a wide alluvial fan before turning southwest near Waiouru (Wells *et al,* 1980).
2. Dissected hill country extends southwards from the edge of the ring plain and comprises uplifted Tertiary marine siltstones and sandstones (Fleming, 1953). The river channel is characterised by a steeply incised meander pattern that is restricted by the narrowness of the valleys through which it runs (Wells *et al,* 1980). Near Mangamahu, the regional geology changes to relatively younger, less consolidated Quaternary sediments that consist predominantly of sand and silt deposits. The width of flood terraces increases considerably downstream of Mangamahu and entrenchment of the Whangaehu River channel is markedly reduced (De Ruyter, 2001).
3. The coastal plain is characterised by a comparatively narrow coastal fringe of flat to gently rolling pastured slopes that encompass a relatively wide alluvial flood plain that is confined within late Quaternary river terraces (Hodgson, 1993). Marine gravel, sand and silt of late Pleistocene predominate this zone (Wells *et al,* 1980).

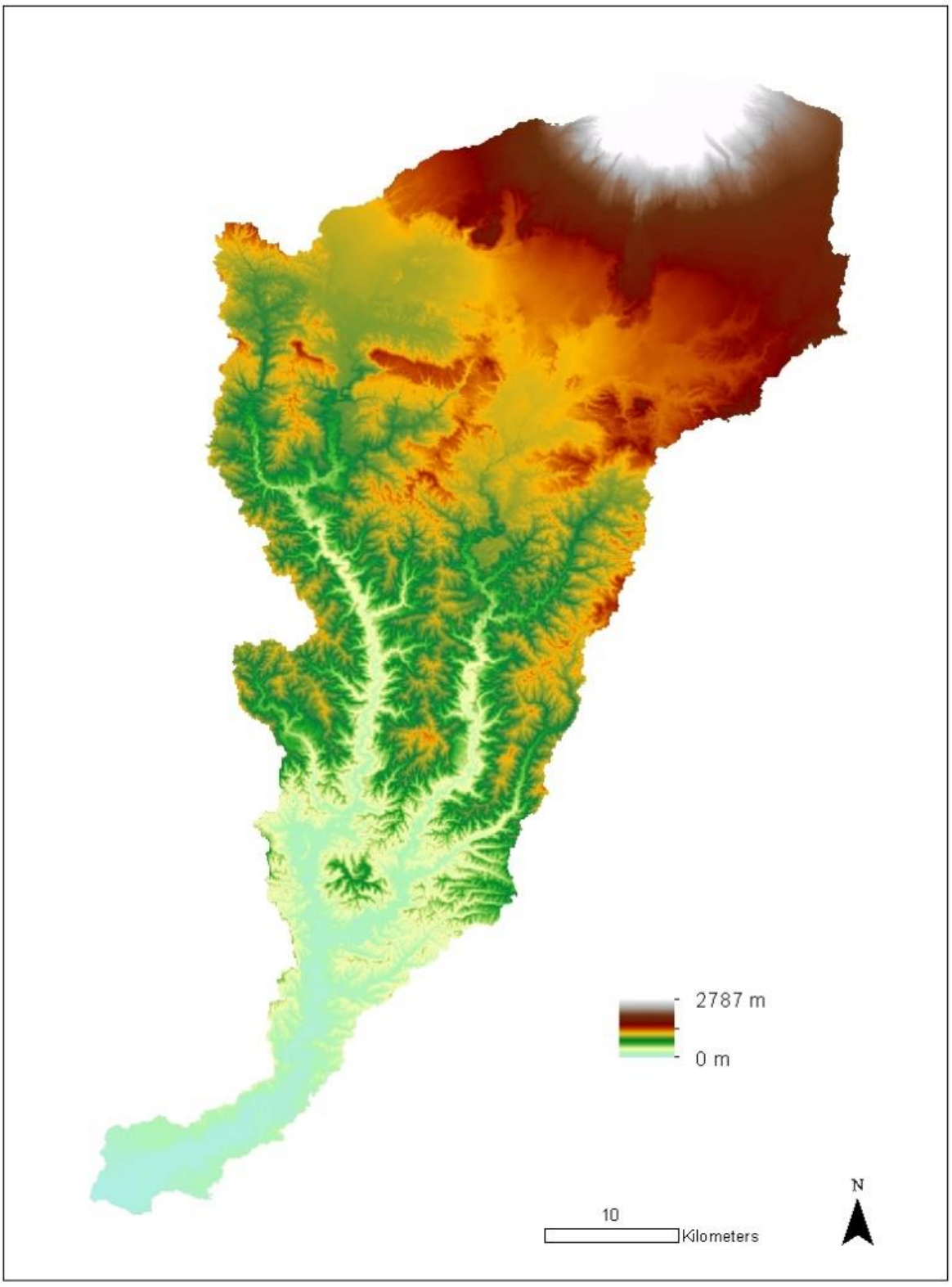

Figure 18. Digital elevation model of the Whangaehu drainage basin (DEM courtesy of Koordinates).

2.4.2 Rock Type and Geology

The upper Whangaehu flood corridor region is underlain by Late Pliocene mudstone, sandstone, conglomerate, and limestone formations with river deposits common along channel bank regions. Bedrock of the middle reaches of the Whangaehu flood corridor is mainly Early Pleistocene mudstone, sandstone, limestone, and conglomerate. Poorly to moderately sorted gravel with minor sand and silt underlies river terraces and includes minor fan deposits and loess. Principal deposits of the coastal plain consist of Holocene alluvial gravel, sand, silt, mud, and clay with local peat as well as active and stable windblown dune deposits (Figure 19).

2.4.3 Landcover and Land use

The upper Mount Ruapehu plateau is encompassed within the Tongariro National Park and is thus protected and managed accordingly (De Ruyter, 2001). Land use within lower plateau region includes forestry (native and exotic), farming and defence force reserve land (Philpott, 2007). Below the plateau, sheep and cattle farming are the predominant land use practices, with a focus on dairying within the fertile river terraces of the lower 30km of the catchment (De Ruyter, 2001). Within the Whangaehu flood corridor, high producing exotic grassland predominates with relatively small zones of closed and open canopy pine forests and crop land interspersed (Figure 20). *Salix* or willow is common along the streambanks of the lower Whangaehu River, planted to help control the water course and mitigate bank collapse and erosion.

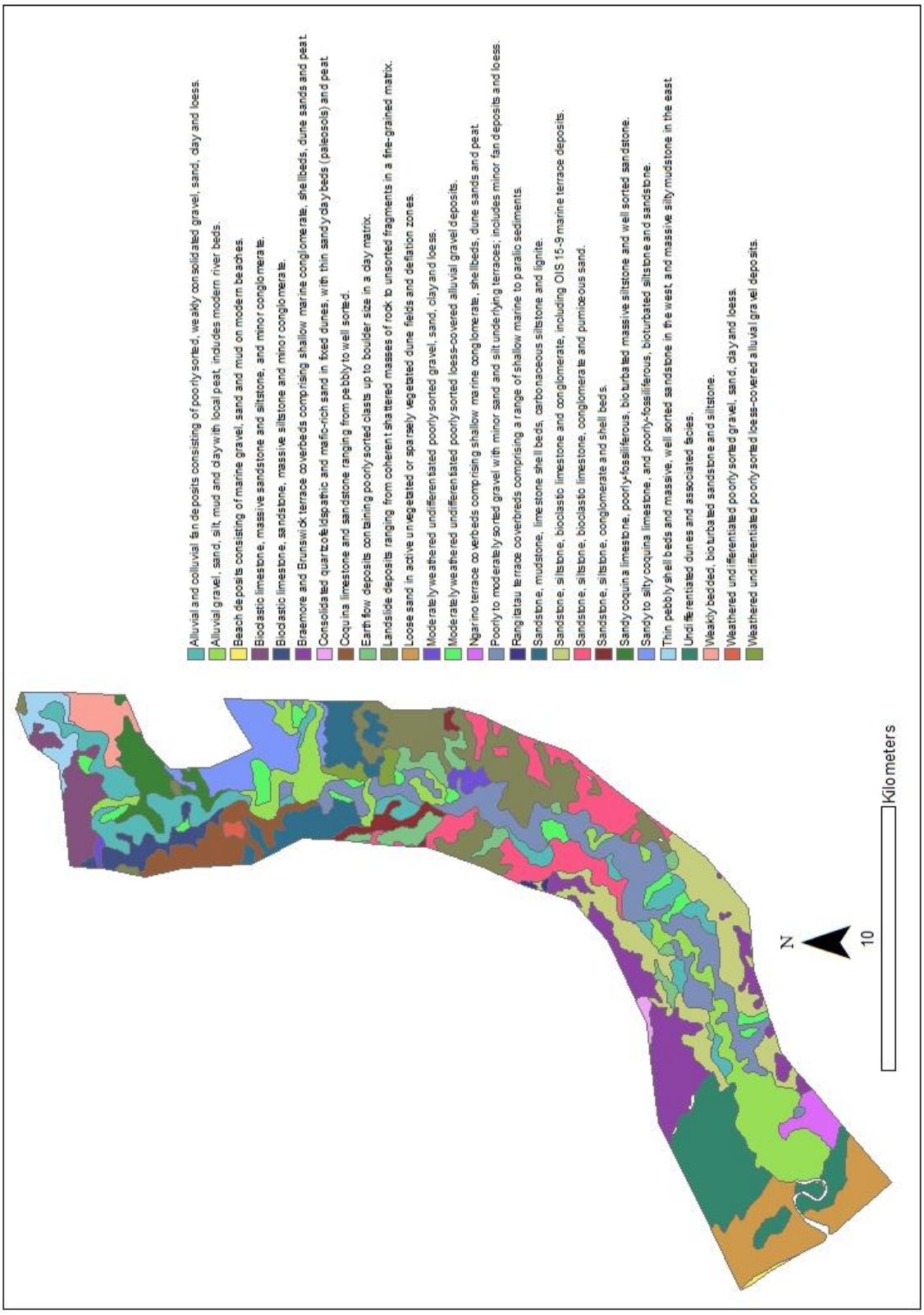

Figure 19. Lithological map of the Whangaehu study area. Based on the GNS Science 250k geological units' layer in the GNS QMap series (2014).

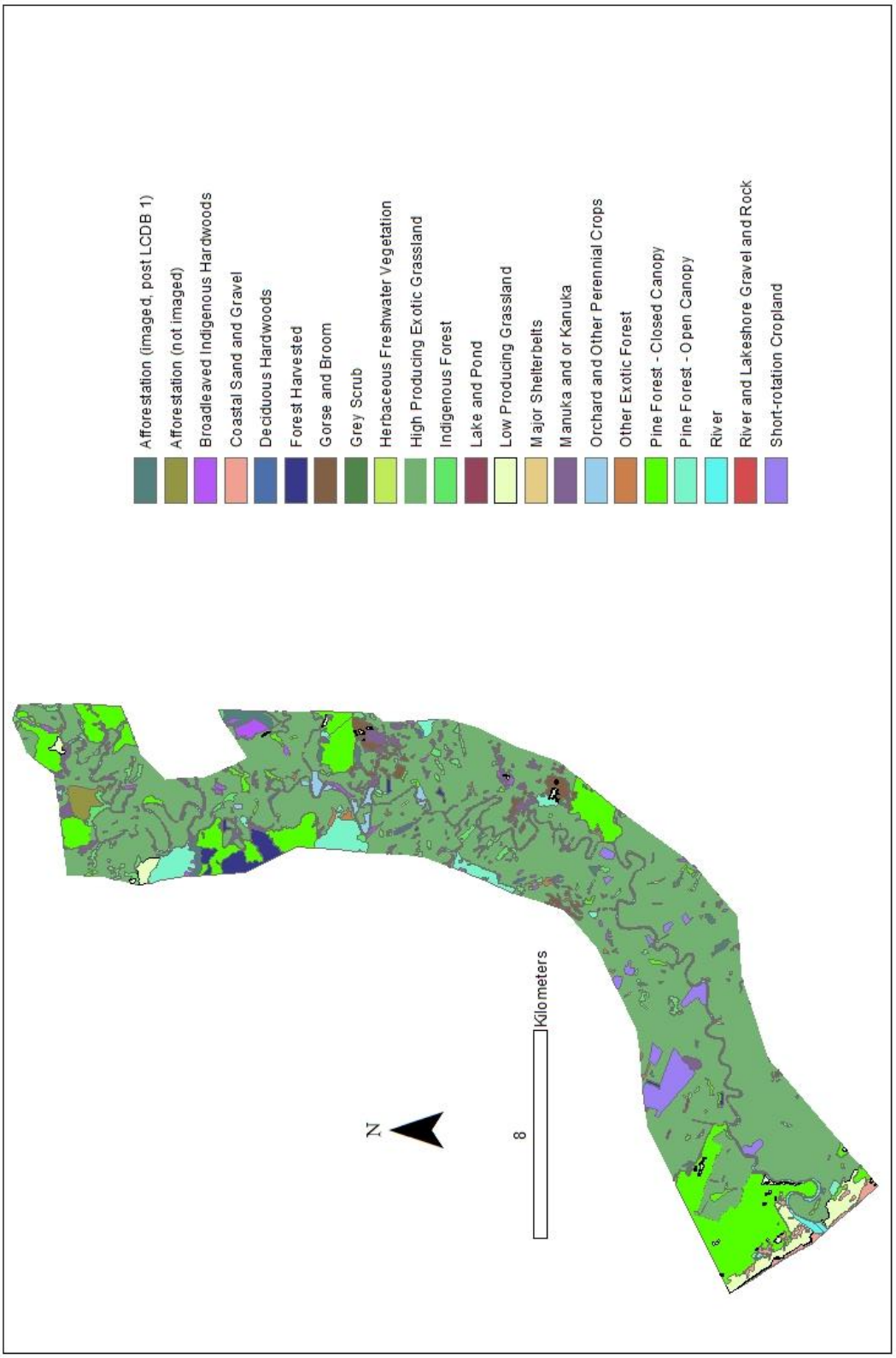

Figure 20. Vegetation cover within the Whangaehu area of interest. Based on the New Zealand Land Cover Database (LCDB) from Land Resource Information Systems portal.

2.4.4 Whangaehu River

The Whangaehu River is a major water course in the North Island, New Zealand and drains a basin adjacent to the Whanganui River. The source of the Whangaehu River is Crater Lake at Mount Ruapehu, and the upper catchment region drains the southern and eastern flanks of the mountain (Wells *et al,* 1980). The mainstem of the Whangaehu River is 202 km in length and drains a catchment basin of 1992 km^2. The drainage basin is bound to the east by the Turakina River and Rangitikei River catchments and to the west by the Whanganui River catchment. The Whangaehu River mouth lies 8 km southeast of Port Whanganui. The Whangaehu watershed has three main tributaries: the Makotuku River, the Tokiahura Stream, and the Mangawhero River. The Mangawhero River originates on the south-western flanks of Mt Ruapehu and flows through Ohakune in a course largely parallel to the Whangaehu River (De Ruyter, 2001). The confluence of the Mangawhero and Whangaehu rivers is situated 54 km upstream of the river mouth, between the Mangamahu and Kauangaroa settlements (De Ruyter, 2001). At Mangamahu, there is a distinct change in morphology of the fluvial network whereby river entrenchment downstream of this settlement markedly decreases and width of river terraces increases due to the change in underlying stratigraphy to less consolidated marine sediments which are more easily erodible (Bell, 2013).

Due to the impact that the June 2015 storm event had at the confluence of the Mangawhero and Whangaehu rivers whereby sediment rich flood waters backed up into the Mangawhero causing overbank flows to deposit a relatively vast blanket of flood drape at this junction, the lower reach of the Mangawhero River is included in the Whangaehu flood corridor.

2.5 Turakina Catchment

The Turakina drainage basin, bordered to the north and west by the Whangaehu Catchment and to the east by the Rangitikei watershed, drains approximately 956 km^2 of predominantly steep hill country within the lower Central North Island to discharge into the Tasman Sea at the beach settlement of Koitiata (Figure 21).

The Turakina study area, here named the Turakina flood corridor, is approximately 96 km^2 and encompasses a narrow region of steep hillslopes, lowland coastal plain and piedmont and floodplain zones and encompasses an area where some of the worst erosion, flooding and deposition occurred during the 19-21 June 2015 rainstorm.

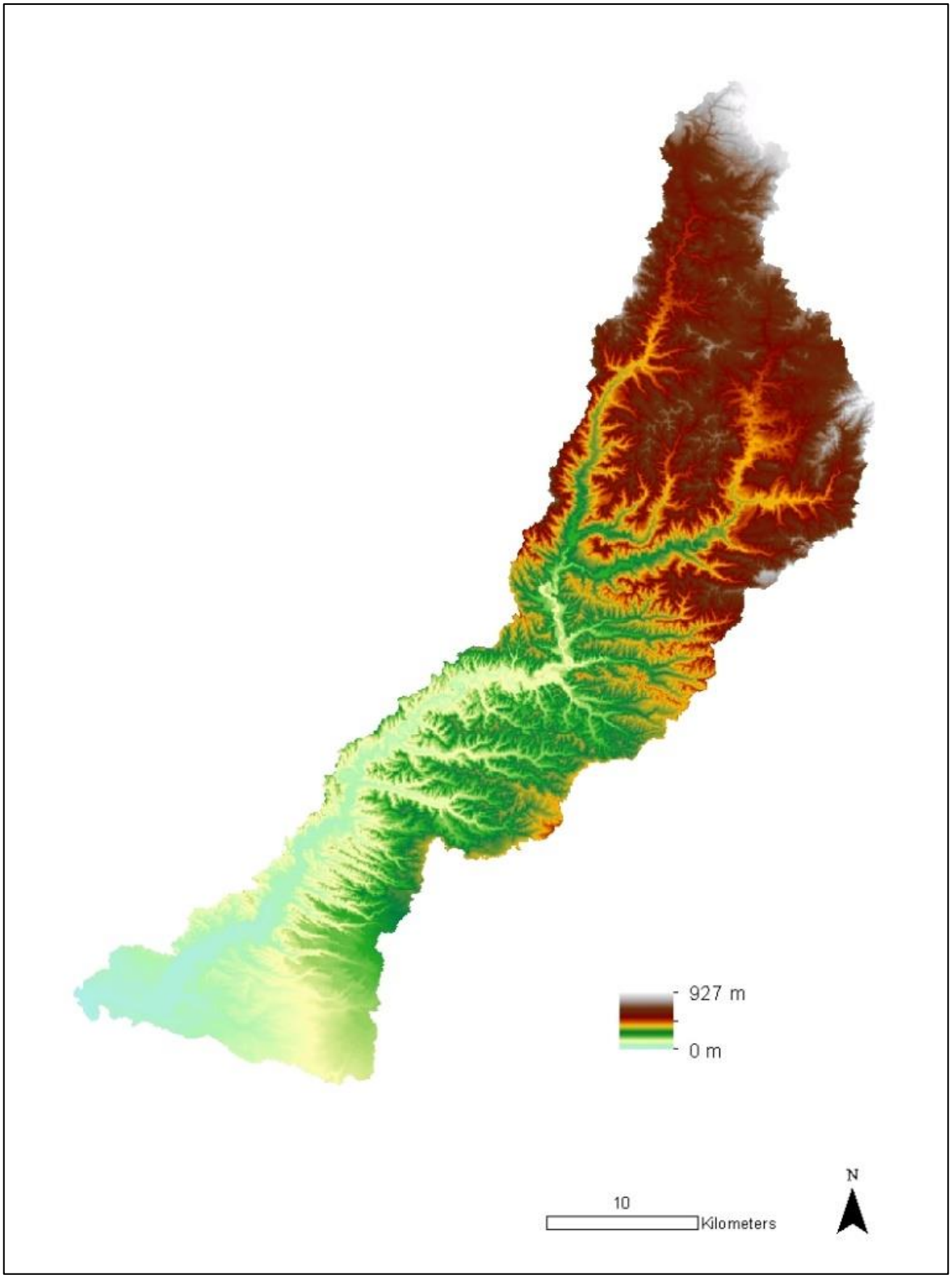

Figure 21. Digital elevation model of the Turakina drainage basin.

2.5.1 Geomorphology

The morphology within the Turakina flood corridor encompasses a narrow belt of alluvial deposits within the lower reaches of the Turakina River that has evolved into a relatively low gradient planar surface. The fluvial system becomes deeply entrenched further inland and is surrounded by steep slopes in the surrounding hill country.

2.5.2 Rock Type and Geology

The regional geology of the Turakina flood corridor is shown in Figure 22. The northern region of the area of interest is predominantly underlain by weak to very weak Mangaweka mudstone of the Kai Iwi Group with sandstone, siltstone, bioclastic limestone, conglomerate and pumiceous sand sub-rocks. Further down catchment the principal rock type is a relatively younger, less consolidated sandstone of the Shakespeare Group that contains increasing amounts of volcanic debris as well as intermittent beds of peat. The coastal lowlands consist of Braemore and Brunswick terrace coverbeds comprising shallow marine conglomerate, shellbeds, dune sands and peat.

2.5.3 Landcover and Land Use

Due to sheep and beef farming dominating the land use within the lower region of the Turakina Catchment (Horizons Regional Council, 2002) land cover within the Turakina flood corridor study area is predominantly high producing exotic grassland (Figure 23). Relatively small regions of low producing grassland, gorse and broom, and closed canopy pine forest are located within the sand and gravel deposits on the coastal plain. Pockets of *salix* or willow have been planted along the streambanks of the lower Turakina River to mitigate bank collapse and erosion.

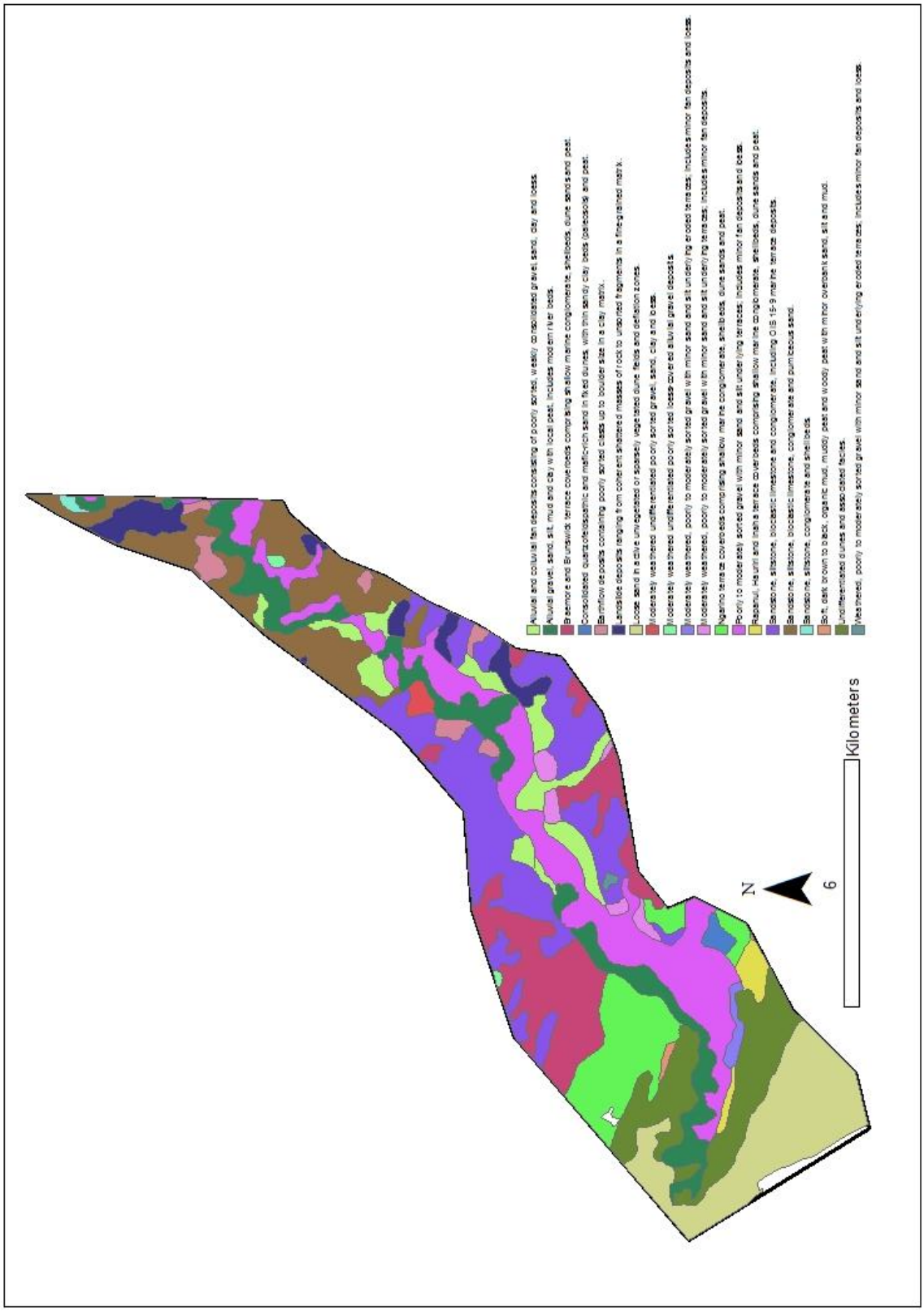

Figure 22. Lithological map of the Turakina study area. Based on the GNS Science 250k geological units' layer in the GNS QMap series (2014).

Figure 23. Vegetation cover within the Turakina area of interest. Based on the New Zealand Land Cover Database (LCDB) from Land Resource Information Systems portal.

2.5.4 Turakina River

The Turakina River is a major water course in the North Island, New Zealand and drains a basin adjacent to the Whangaehu River. The Turakina River has a total drainage basin area of 962 km^2 and is approximately 140km in length. The headwaters of the Turakina River originate in the low-lying hill country near the Rangiwaea Junction, south of Waiouru (Horizons Regional Council, 2002). Locally, the main river flows seaward at a relatively gentler gradient than the slope of the surrounding land surface (Fleming, 1953). The stream network within the Turakina Catchment commonly runs east-west, merging with the Turakina River, which culminates with the Tasman Sea approximately 16 km south east of Whanganui, near the small coastal settlement of Koitiata. The east-west flow is likely due to uplift along the Marton Anticline (van der Neut, 1996). Due to a man-made cut at the mouth of the Turakina River being created to direct water out to sea, a lagoon frequently exists in the natural riverbed of the channel (Figure 24).
The rainstorm and subsequent flood event in June 2015 caused the mouth of the Turakina River to cut a direct path to the sea. This migration of the Turakina river mouth also occurred during the flood event of 2004. Over time, the Turakina river mouth naturally migrates south along the coast again, cutting a less direct course. This process reflects the energy regime of the river during and after large flood events.

Figure 24. Four years after a major flood cut a direct path to the sea, the Turakina River-mouth has migrated several hundred metres to the south (left). This process will eventually result in the river re-joining its earlier channel which now forms a lagoon next to the settlement of Koitiata (upper left) (Coastal Systems Ltd, n.d).

2.6 Regional Climate of the Study Area

Climate within the Wanganui-Manawatu region is largely controlled by the presence of the Kaimanawa range and volcanic peaks in the north and the Ruahine and Tararua ranges in the east and south (Tait *et al*, 2005). The climate within the region is maritime and temperate with prevailing winds coming from the western quarter (Dymond *et al,* 2004). However, local topography can influence surface winds so that a considerable tendency for surface winds to blow from northern and north-easterly directions exists (Tait *et al,* 2005).

Annual rainfall for the greater region ranges between 5000 mm at the top of the eastern ranges to 800 mm along the coastal plain (Dymond *et al,* 2004). Hill country regions in the north of the area receive on average between 1400 to 1600 mm/year (Tait *et al,* 2005).

2.6.1 Synoptic Conditions of the 19-21 June 2015 rainstorm

On the 19-21 June 2015, the lower North Island, New Zealand, experienced a severe winter storm event which caused heavy rain to fall within the Horizons and Taranaki regions. The heavy rainfall, in conjunction with already saturated ground conditions attributable to a wet autumn, caused waterways to burst their banks as well as surface flooding in many low-lying regions and severe erosion in the hill country (Ministry for Primary Industries, 2015). This, in combination with a king high tide resulted in the worst flood on record in the Whanganui River and Civil Defence authorities declared a state of emergency in Whanganui and surrounding regions and hundreds of people were evacuated from homes due to rising flood waters.

The New Zealand MetService forecast predicted that a complex low over the Tasman Sea was expected to move east over the South Island and spread north into southern and central North Island on Friday, 19 June 2015 (Figure 25). These low, and associated fronts were expected to bring periods of stormy weather to these regions over the following days. The greatest rainfall amounts were forecast for the ranges of Westland where a total of 300mm of rain was expected to accumulate. In addition, 250mm was expected about the Tararua Range, with 200mm about Mt Taranaki, and 150mm about Tongariro.

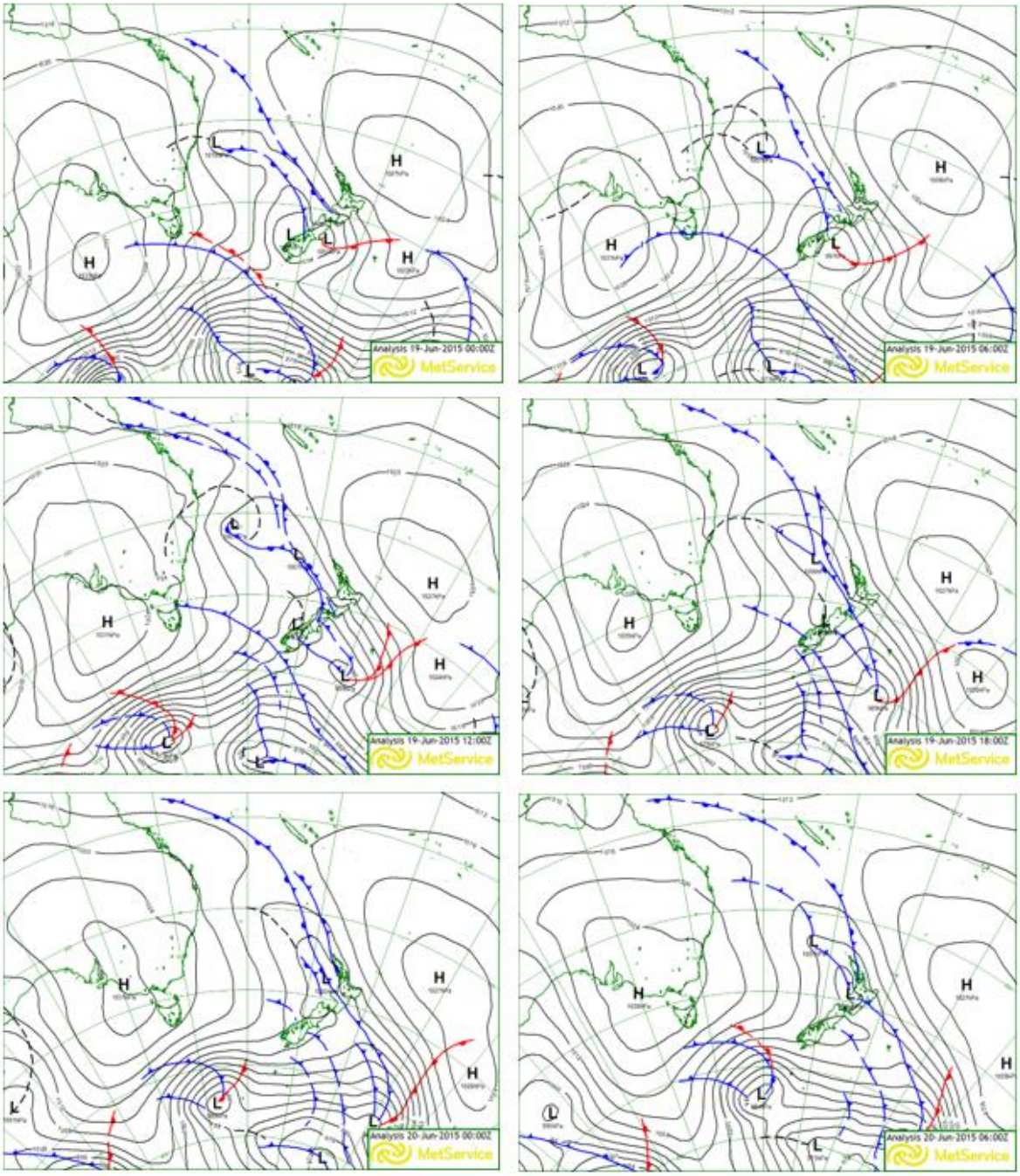

Figure 25. MetService weather forecasts during the 19-21 June rainstorm event. These maps show the progression of the 'two pronged' attack of the two main low systems over the lower North Island.

Chapter 4 – Methodology

4.1 Introduction

To facilitate analysis of how the landscape responded to the June 2015 rainstorm and flood events and the geomorphological processes that facilitated change, various geophysical survey methods were used along the three flood corridors of interest. These included: streambank profiling using RTK- dGPS, flood drape sample collection, sedimentology and grain size analysis and GIS techniques. In addition, multiple data sources were utilized including GeoEye satellite imagery, river flow, turbidity and sediment flux data was obtained from Horizons Regional Council and various physical terrain attributes shapefiles (vegetation and land-use, rock type, slope, and aspect) from Land Information New Zealand.

4.2 Flood Drape Sample Collection

The initial objective was to capture sufficient flood drape sample data to identify any potential variation in downstream fining as well as sediment grading across the floodplain and vertically within the flood drape itself. Thus, samples were taken at relatively regular intervals down the flood corridor and proximal as well as distal samples were taken at various sites along the flood corridors. Distinct layering was identified within the 2015 flood deposits at various sites (Figure 46) so discrete samples were removed from each layer.

Additionally, at each sample site, a cross section of the surface extent of flood deposits was measured and recorded using RTK – dGPS equipment to enable analysis of grain size data in relation to aerial extent.

Figure 46. Layering within flood drape samples at sites along the Whanganui River at Wg10 (left), Wg16 (middle) and Wg 20 (Pungarehu Marae).

4.3 Measurement of Flood Drape Elevations Above the Wetted Channel

The real-time kinematic (RTK) differential global positioning system (dGPS) survey technique was deployed along the flood plains of the Turakina, Whangaehu and Whanganui rivers to enable a more accurate spatial and quantitative estimate of the areas of flood drape deposition to be made. A Trimble R8 RTK- dGPS was utilized in this research to aid in mapping as well as quantifying the areal extent of the flood drape. This surveying facilitated measurements of height above, as well as width away from, the wetted channel that overbank deposition occurred. The GPS surveys also allowed for accurate location data of flood drape samples to be made.

The initial objective was to take sediment samples and undertake surveys at regular intervals of approximately 3-5km along the flood plains of the catchments of interest. This method had to be adapted due to various limitations, which included: limited access due to substantial flood damage to the streambank environment; and density of vegetation and steepness of terrain. Both greatly limited the usability of the RTK-GPS equipment in many upper regions of the areas of interest (see below). Along each transect, surveys were taken from the most distal (away from the wetted channel) point of the visible flood drape and concluded at the wetted channel. Points were taken at breaks in slope along each transect so that streambank flood drape cross sections could be plotted.

4.4 Grain Size Analysis

To aid in the assessment and interpretation of sediment transport processes and the flow regime of flood waters during the June 2015 flood event, samples of overbank deposits (Figure 47) were taken from the flood plains of the Whanganui, Whangaehu and Turakina rivers. Grain size analysis of flood drape samples was undertaken to ascertain the processes that caused distinct layering of overbank flood deposits to occur during the June 2015 flood event.

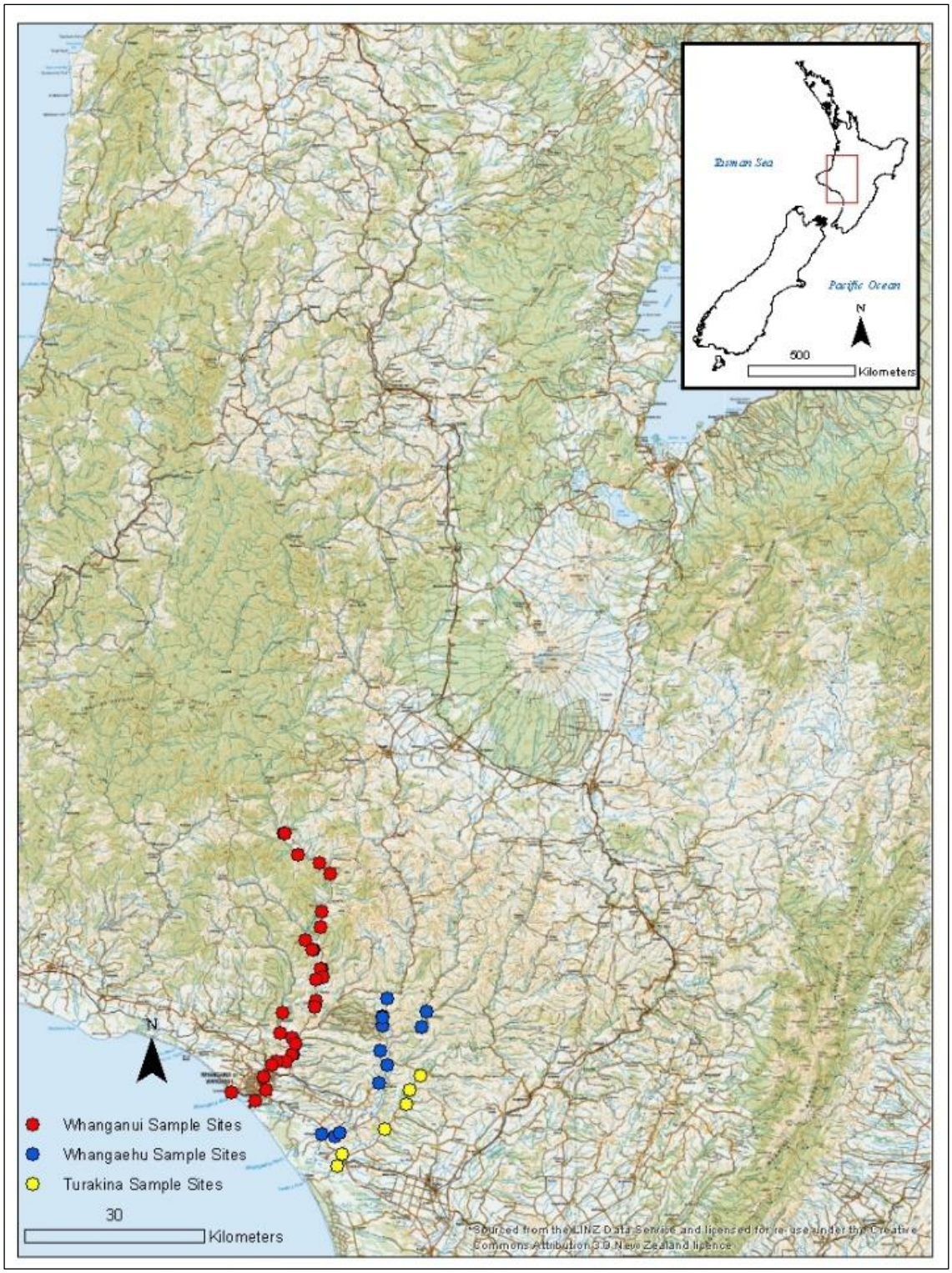

Figure 47. Flood drape sample and flood drape cross section survey sites within the Whanganui, Whangaehu and Turakina catchments.

The following methodology was followed to prepare each sample for laser particle size (LPA) analysis:

- To eliminate organic material from the flood drape samples, 3-4 grams of each sample was weighed out (roots and visible organic matter was removed) and placed into large beakers. Beakers were labelled with each site code so that samples were easily identifiable.
- Hydrogen peroxide (H_2O_2) (30%) was then added to each beaker. Enough H_2O_2 solution was added to just cover each sample. The reaction was quite strong in many of the samples, so several drops of copryl alcohol was applied when bubbling was near overflowing point.
- H_2O_2 was applied over a period of approximately 4-5 weeks so that the sediment remained moist. This process was vigilantly observed as there was a risk of the samples drying out which could have affected the outcome of the LPA if clay particles flocculated together.
- The process of eliminating organic matter was finally completed by utilizing a heat pad and fume hood over an approximately 6 hr period until no bubbling was heard or seen (Figure 48).

Figure 48. Final stage of the removal of organic material from flood drape samples was completed by simmering the sample and H_2O_2 mixture on a heat pad under a fume hood.

- Each sample was then centrifuged with deionised water to eliminate the H_2O_2 (a clear solution remained as opposed to a yellow solution).

- Each sample was divided into 6 centrifuge tubes and approximately 40 ml of deionised water was added. The centrifuge was run with the following settings: 9 – deceleration, 7,000 RPM, 4 minutes. The liquid was then decanted and discarded. The process was repeated until the solution ran clear.
- Following H_2O_2 removal, each sediment sample was then put into LPA glass cylinders and deionised water was added to $^3/_4$ fill each vial.
- Each cylinder was labelled with the sample site code for easy identification.

A Horiba LA-950 laser scattering particle size distribution analyser was then utilized in the analysis of the flood drape grain sizes. This instrument uses two beams of light of different wavelengths (LED: λ=405 nm; Laser: λ=650 nm) to precisely determine the distribution of grain size classes in fluid-solid dispersions.

The following methodology was followed to measure grain size:

- The water level of the deionised water tank was checked before, during and after sample processing.
- The deionised water tank tap was opened to depressurize the container prior to processing.
- The Horiba machine, printer and computer were turned on. The Horiba programme was then started.
- The slurry sampler method was utilized to run samples in suspension. Between 9-27 samples were placed in batches on the Horiba sample tray depending on how many had been centrifuged at the time.
- Three repeats of each sample were run.
- Results were then transferred to Excel spreadsheets for analysis

Additionally, rainfall, discharge and sediment flux data were sourced from Horizons Regional Council (HRC) to support in the analysis and interpretation of sediment transport processes that occurred during the June 2015 flood event. 48 hr rainfall totals within the Whanganui, Whangaehu and Turakina catchments, as well as 48 hr Average Recurrence Intervals (ARIs) for rainfall that fell over 19-21 June 2015 were provided (Figures 49 and 50) as well as discharge (l/s) (Figure 51) and sediment flux (Figure 52) data from the Te Rewa gauging station on the Whanganui River. The catchment area this monitoring site encompasses is approximately 6643 km² (note: flow is recorded by NIWA at Paetawa 2km downstream of Te Rewa). Sediment flux (kg/s) and turbidity data was acquired from HRC for the Whanganui River at Te Rewa monitoring site.

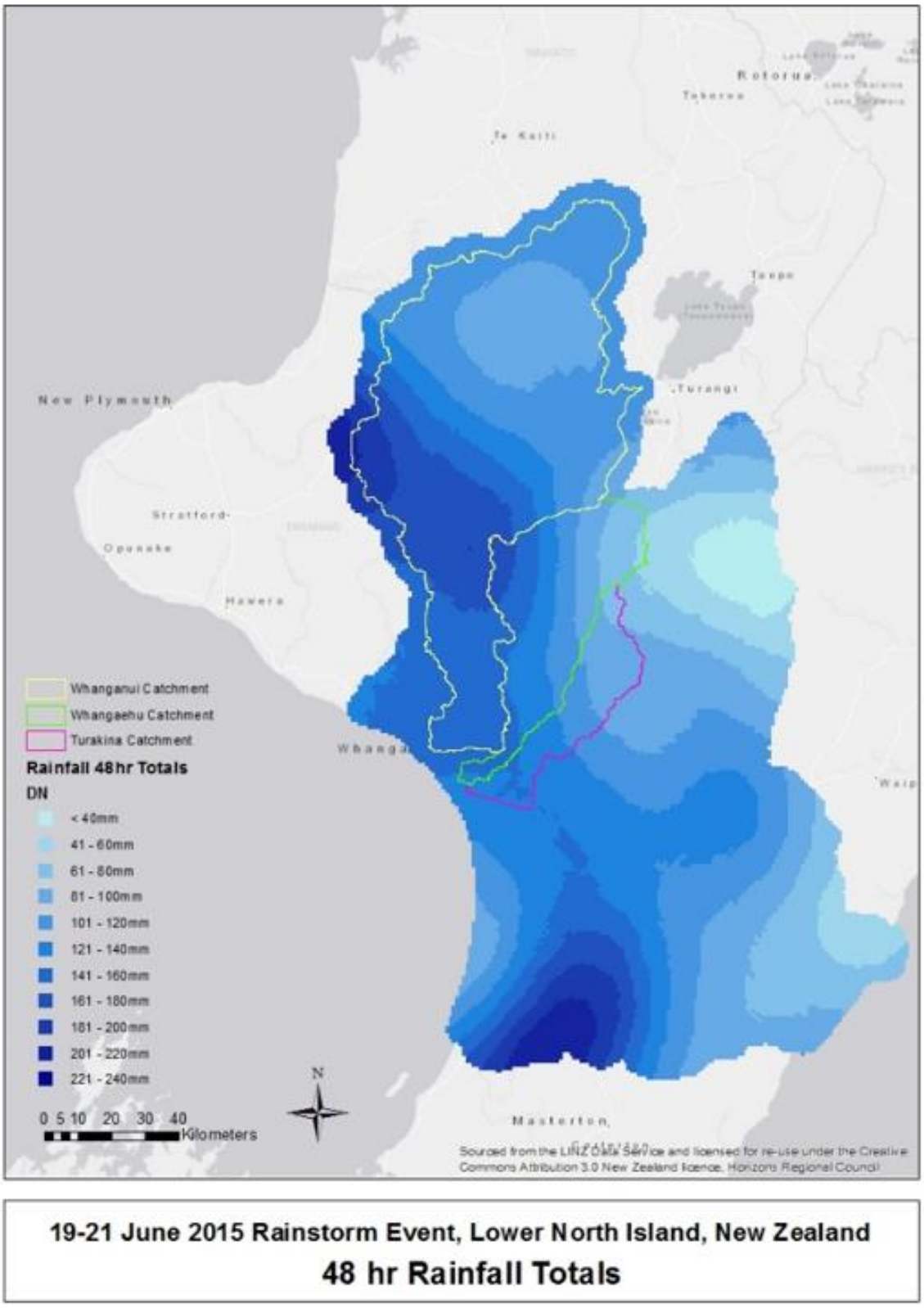

Figure 49. 48 hr rainfall totals within the Whanganui, Whangaehu and Turakina catchments (Rainfall totals data courtesy of HRC).

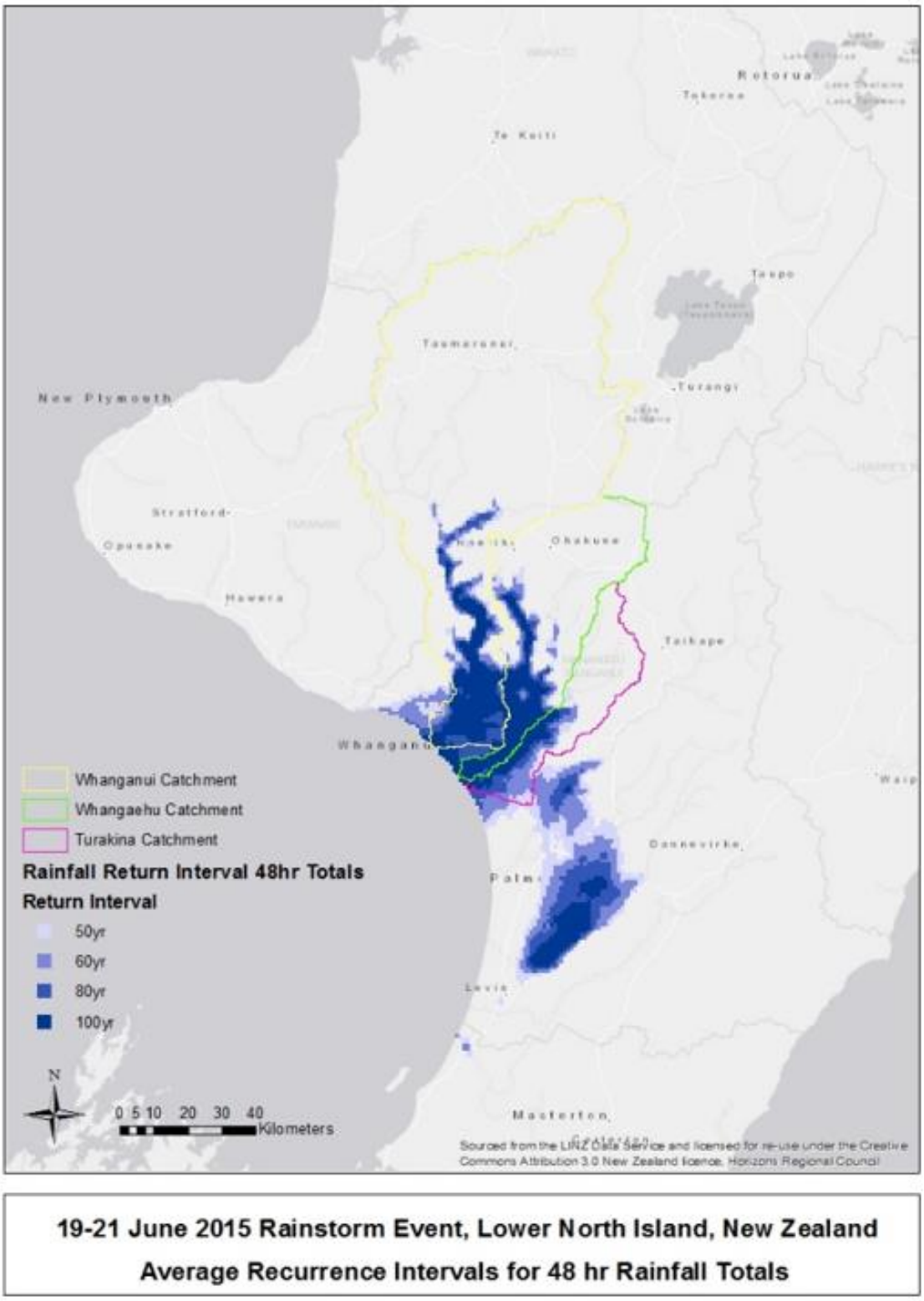

Figure 50. 48 hr Average Recurrence Intervals (ARIs) for rainfall that fell over 19-21 June 2015 within the Whanganui, Whangaehu and Turakina catchments. Notable rainfall is represented through selected regions of rainfall equal to or exceeding a 50 yr recurrence interval of NIWA's HIRDS V3 model (High Intensity Rainfall System V3). These regions of rainfall were created by spatially approximating 24 and 48 hr maximum rainfall amounts from rain gauges managed by various regional councils (Taranaki Regional Council, Hawke's Bay Regional Council, Horizons Regional Council as well as Greater Wellington Regional Council), one privately owned rainfall gauge and MetService (Meteorological Service of New Zealand Limited). The rainfall regions with calculated values matching recurrence intervals of NIWA's HIRDS V3 model were allocated recurrence interval values ranging from 1.58 to 100 years. Only recurrence intervals of greater than 50 years are shown above. The accuracy of the modelled recurrence intervals should be considered indicative only (ARI data courtesy of HRC).

The catchment area this monitoring site encompasses is approximately 6643 km² (note: flow is recorded by NIWA at Paetawa 2km downstream of Te Rewa). Sediment flux (kg/s) and turbidity data was acquired from HRC for the Whanganui River at Te Rewa monitoring site (Figure 41).

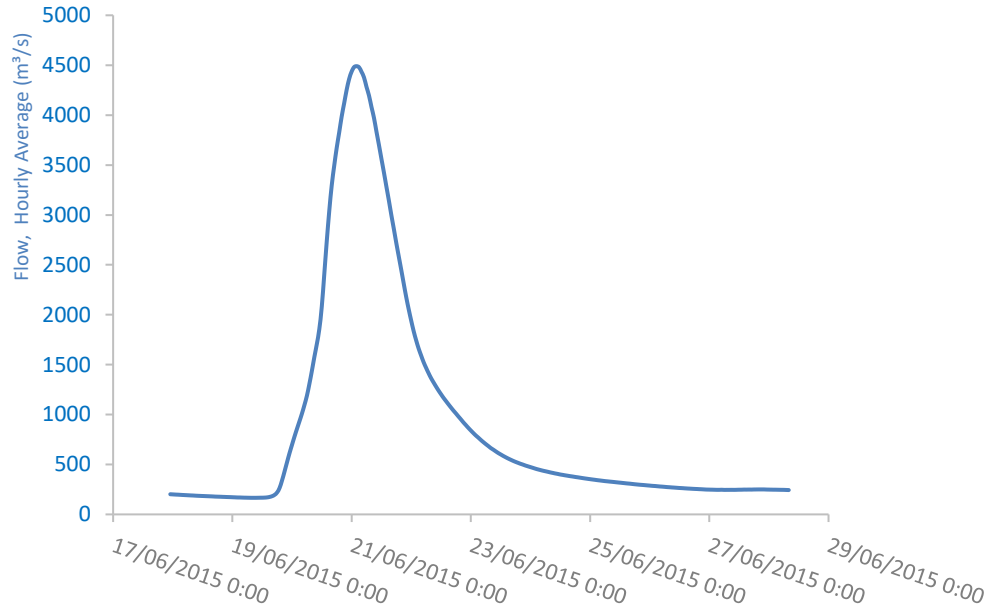

Figure 51. Flood hydrograph for the June 19-21, 2015 flood event (data courtesy of HRC).

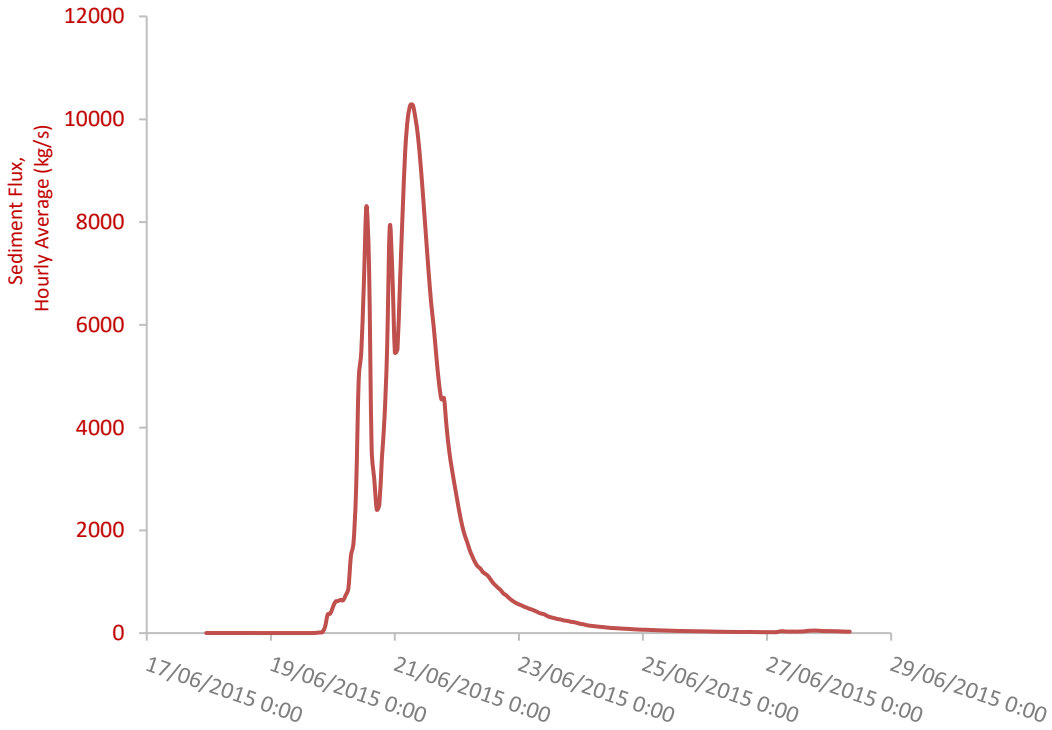

Figure 52. Sediment flux during the June 19-21, 2015 flood event (data courtesy of HRC).

4.5 Landslide and Flood Drape Mapping

Landslide analysis was completed through manual digitization and statistical analysis within ArcMap. The primary data source for the manual digitization of landslides in this project comprised a narrow GeoEye (5 m) scene, captured on 12 July 2015 (post-event) which encompassed the lower Whanganui, Whangaehu and Turakina drainage basins. This scene comprised 96 individual images that together, encompass the middle to lower Whanganui, Whangaehu and Turakina drainage basins. Figure 53 shows a mosaic of the GeoEye imagery with the Turakina flood corridor polygon overlaid. The Land Information New Zealand (LINZ) New Zealand river centrelines and New Zealand major rivers shapefile layers were downloaded from the Koordinates website to help distinguish landslides that were coupled with the fluvial system from those that were not.

To analyse the relationship between the physical terrain attributes of interest (land cover, slope angle and slope aspect, and rock type) and landslide distribution and extent, several datasets were acquired through publicly available sources. The New Zealand Land Cover Data Base (LCDB) provided a cropped multi-temporal digital thematic map of land cover and land use (LCDB v4.0 (Deprecated)) which was used to assess the relationship between landsliding and land cover. This map was downloaded from the Land Resource Information Systems (LRIS) portal. A Palmerston North 15 m DEM, as well as the Taumarunui 15 m DEM were downloaded from the Koordinates website. These were utilized in the creation of slope and aspect layers. The NZL_GNS_250K_geological_units' layer was utilized in the analysis of landsliding which occurred within different rock types in the flood corridors of interest. This dataset is part of the QMAP Geological Map of New Zealand Project and was produced by GNS Science. A flood corridor boundary polygon was created around each of the three corridors of interest (Figure 52 shows the Turakina flood corridor) to keep a consistent area for mapping and statistical analysis. Due to the image sources used in this study having different coordinate systems, the Data Frame coordinate system was set to NZGD 2000 New Zealand Transverse Mercator prior to input of any data.

Figure 53. Mosaic of GeoEye-1 3 band imagery captured 12 July 2015. Black polygon defines the Turakina flood corridor of interest. Northwest of the lower Turakina Catchment, the floodplain of the Whangaehu River is visible.

Polygons were digitized manually around each landslide and were separated into two discrete classes. Coupled and buffered landslides were individually mapped (Figure 54) and was based upon visual assessment of vegetation coverage, freshly exposed regolith and debris deposits. Following research methods by McCabe *et al,*

(2013) landslides were classified as coupled if debris deposits appeared to enter the fluvial system, whereas landslides whose debris deposits were not connected to the stream network were classed as buffered. The Land Information New Zealand (LINZ) NZ River Centrelines shapefile layer was downloaded from the Koordinates website to help distinguish landslides that were coupled with the fluvial system. However, careful consideration was taken to identify areas where ephemeral streams were likely to have been generated during the storm event. Landslides that appeared to have reached these 'transient' streams and did not appear to have debris tails remaining at the base of the source region were mapped as coupled landslides. For example, a large meander cutoff along the Whanganui River at Atene is typically a dry abandoned channel. However, during the June 2015 rainstorm and flood event it appears that this usually dry relic streambed was partially inundated at the downstream neck so that one of the landslides on the slopes surrounding this meander cutoff was coupled with the channel. Additionally, a large build-up of fresh flood drape was deposited at the downstream confluence of this meander cutoff (Figure 55). To help verify regions of fresh landsliding and slope-channel coupling within the three flood corridors of interest, photographs were taken in the field of landsliding along the three main river channels (Figure 56).

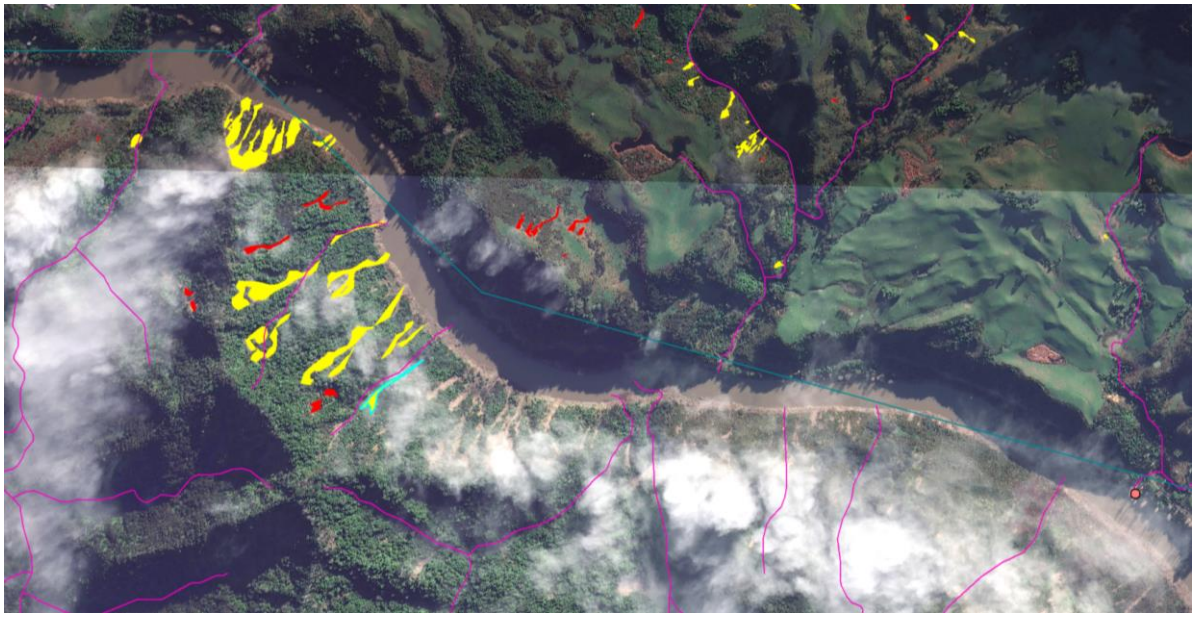

Figure 54. Manual digitization of landsliding along the Whanganui River was completed within ArcMap. Coupled landslides are in yellow and buffered are in red. Digitization is here seen partially completed in this zone. New Zealand major rivers centrelines (blue) and New Zealand river centrelines (maroon) were used to help identify the fluvial network within the three flood corridors of interest (data from Land Information New Zealand).

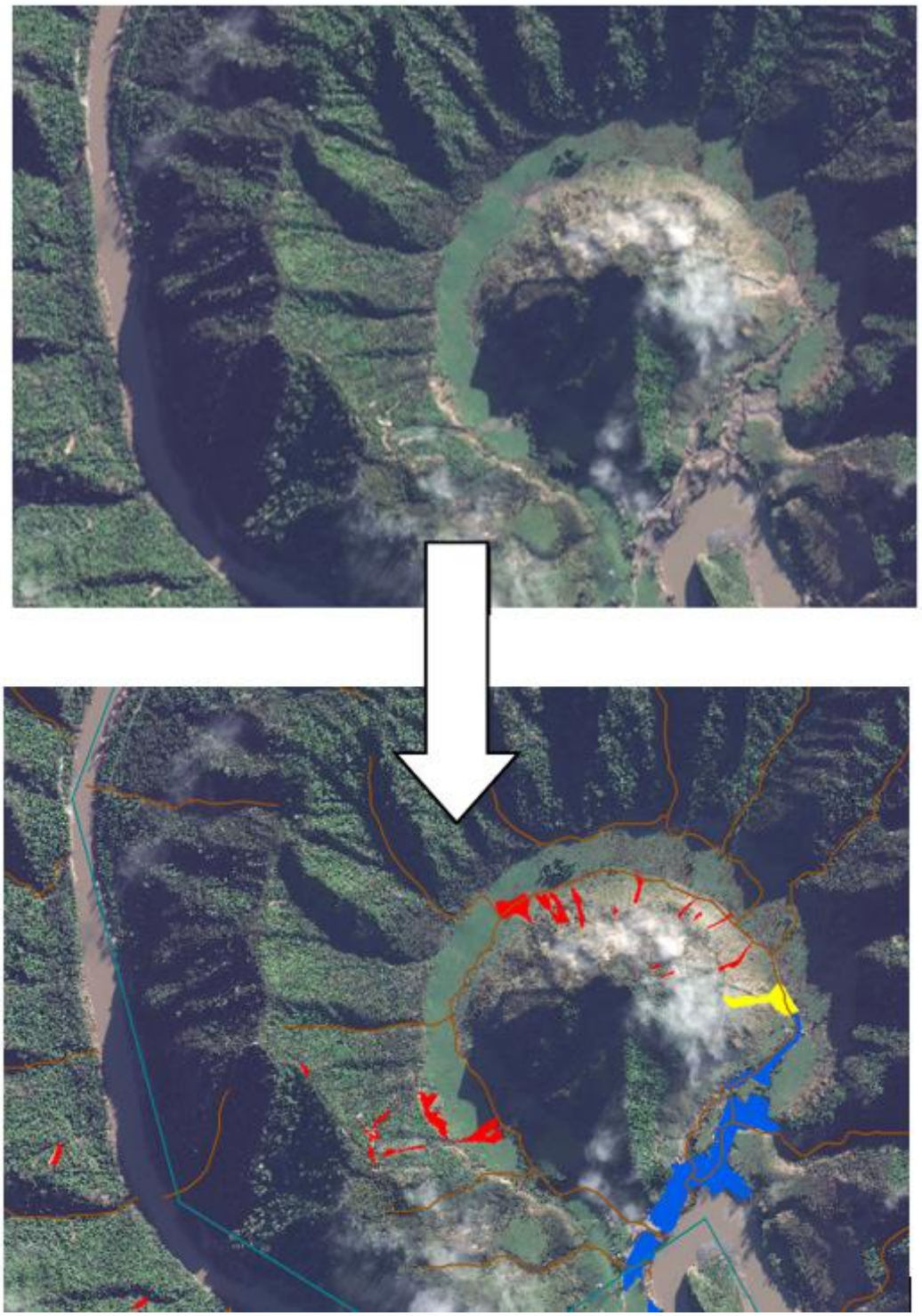

Figure 55. Meander cutoff along the Whanganui River. Top aerial view shows areas of landsliding and sedimentation. This abandoned channel appears to have been during the June 2015 flood event so that many of the landslides have been mapped as coupled (yellow). Buffered landslides are here mapped red and flood drape is mapped in blue. NZ rivers centreline in brown.

Figure 56. Photographs taken along the Whanganui River at flood drape sample sites to aid in the identification of slope-channel coupling of landslides. All photographs were taken near Atene. Bottom left shows a large relic landslide that was partially remobilised during the June 2015 rainstorm event. Whanganui locals spoke of a large landslide which dammed the Whanganui River channel many years ago – a landslide of the magnitude shown here at bottom left would have had the potential to do this (Author, December 2015).

Additionally, over-bank deposits were manually digitised by visually identifying fresh deposits along lowland and floodplain zones (Figure 57) and these areas quantified. Again, photographs were taken in the field to aid in the visual assessment of these areas (Figure 58).

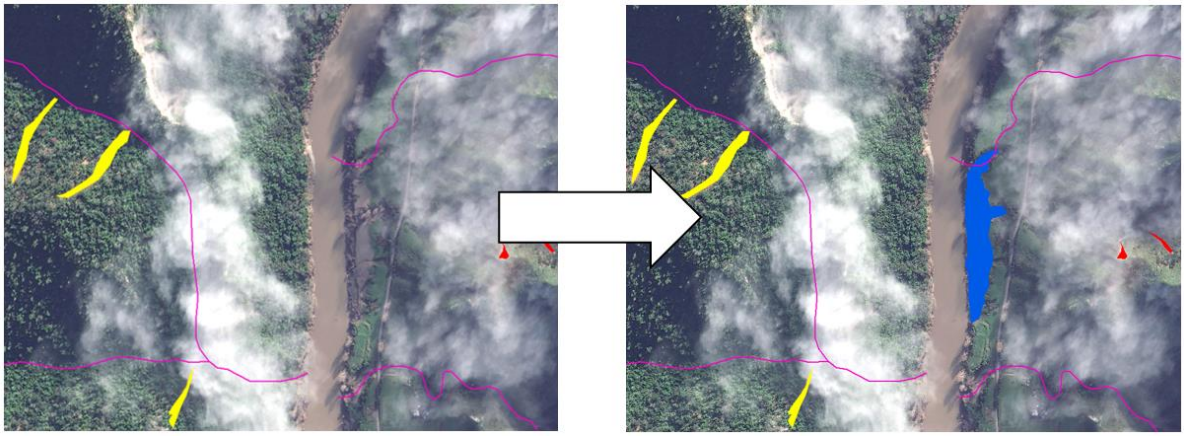

Figure 57. Flood drape mapping along the Whanganui River channel. Aerial view on the left shows an area of sedimentation along the main channel. Image to the right depicts the flood drape mapped in blue. Coupled (yellow) and buffered (red) landslides are also shown and the NZ river centrelines is in maroon to help distinguish the fluvial network.

Figure 58. Flood drape photographs taken during December 2015 – January 2016 field work at Taupiri Stream (a meander cutoff at Atene – the original bed of the Whanganui River) (top left), at Wg16 (top right), Wg17 (bottom left), and Wg18 (bottom right) (Author, December 2015).

The planimetric area of each landslide class as well as the flood drape layer, was calculated through the creation of an "Area" field within each attribute table and using the "Calculate Geometry" tool.

To determine the surface area of the digitized landslide and flood drape classes, a new field entitled 'area' was added into the attribute tables of each class in the three flood corridors. The 'calculate geometry' was then used to compute the area (m^2) of each digitized landslide and flood drape polygon. This data was then extracted to text file format and copied into Excel for further statistical analysis.

To analyse the relationship between the terrain attributes of interest (rock type, land cover, slope angle and slope aspect) and landslide distribution and extent, several datasets were acquired through publicly available sources. The New Zealand Land Cover Data Base (LCDB) provided a cropped multi-temporal digital thematic map of land cover and land use (LCDB v4.0 (Deprecated)) which was used to assess the relationship between landsliding and land cover. This map was downloaded from the Land Resource Information Systems (LRIS) portal. The Palmerston North and Taumarunui 15 m DEMs were utilized in the assessment of the relationship between landsliding and slope and aspect. The slope raster was created in ArcMap using the Slope (Spatial Analyst) Tool whilst the aspect raster was created via the Aspect (Spatial Analyst) Tool. The NZL_GNS_250K_geological_units' layer within the GNS Science QMap database was utilized in assessing the relationship between landslide distribution and extent and rock type. In order to analyse the distribution of each landslide in regard to the above physical attributes, tools within ArcMap were used to extract data from each terrain attribute layer. To enable this, each landslide polygon layer was converted to a point layer using the Feature to Point tool in ArcMap (Figure 59). The Intersect tool in the Overlay dropdown menu in Analysis tools was used to derive landslide and rock type as well as landslide and landcover data. Landsliding in relation to slope angle and slope aspect was analysed by extracting data via the Spatial Analyst Tools in ArcMap. The Extract Multi Values to Points tool in the Extraction dropdown menu was utilized in this process. Thereafter, attribute tables for all of the above physical terrain characteristics analysed in this study were exported as text files and then copied into Excel for further processing.

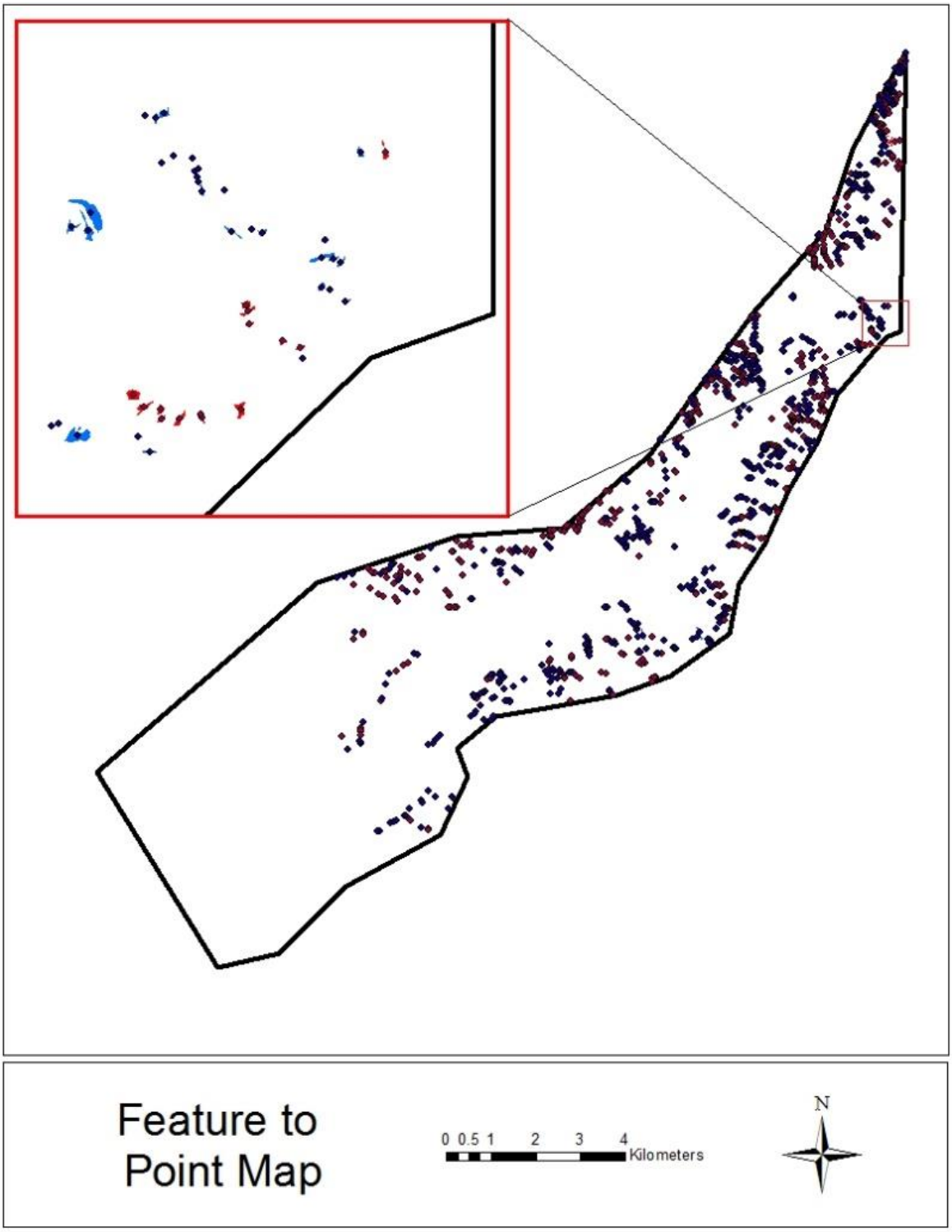

Figure 59. Landslide polygon to point map within the Turakina flood corridor. Inset shows an area where landslide polygons (coupled: red; buffered; blue) have been converted to point features.

Chapter 5 – Results of Spatial Landslide Mapping

5.1 Introduction

Analysis of satellite imagery, as well as observations made in the field reveal the dominant hillslope erosion process that occurred during the June 2015 storm event was rainfall-triggered shallow landsliding. Many of these shallow landslides were coupled with the channel network and resulted in vast quantities of sediment being transported through the fluvial systems of each catchment and being draped over the landscape within floodplain zones.

5.2 Spatial Mapping of Landslides

The spatial distribution of coupled and buffered landslides, as well as flood drape regions is graphically summarised in Figure 60. The manually digitized map of landslides, produced from the GeoEye satellite imagery, produced over 4500 individual landslides within the three flood corridors encompassed in this research.

5.2.1 Landslide distribution and area

A total study area of over 511 km^2 was utilized in the mapping of landslide extent and distribution. A total landslide area of 4,424,602 m^2 (0.87% of total land area) was mapped, of which 2,811,632 m^2 (64%) were identified as being coupled with the channel. Spatial analysis data of coupled and buffered landslides within each of the three flood corridors is summarised in tables 6, 7 and 8.

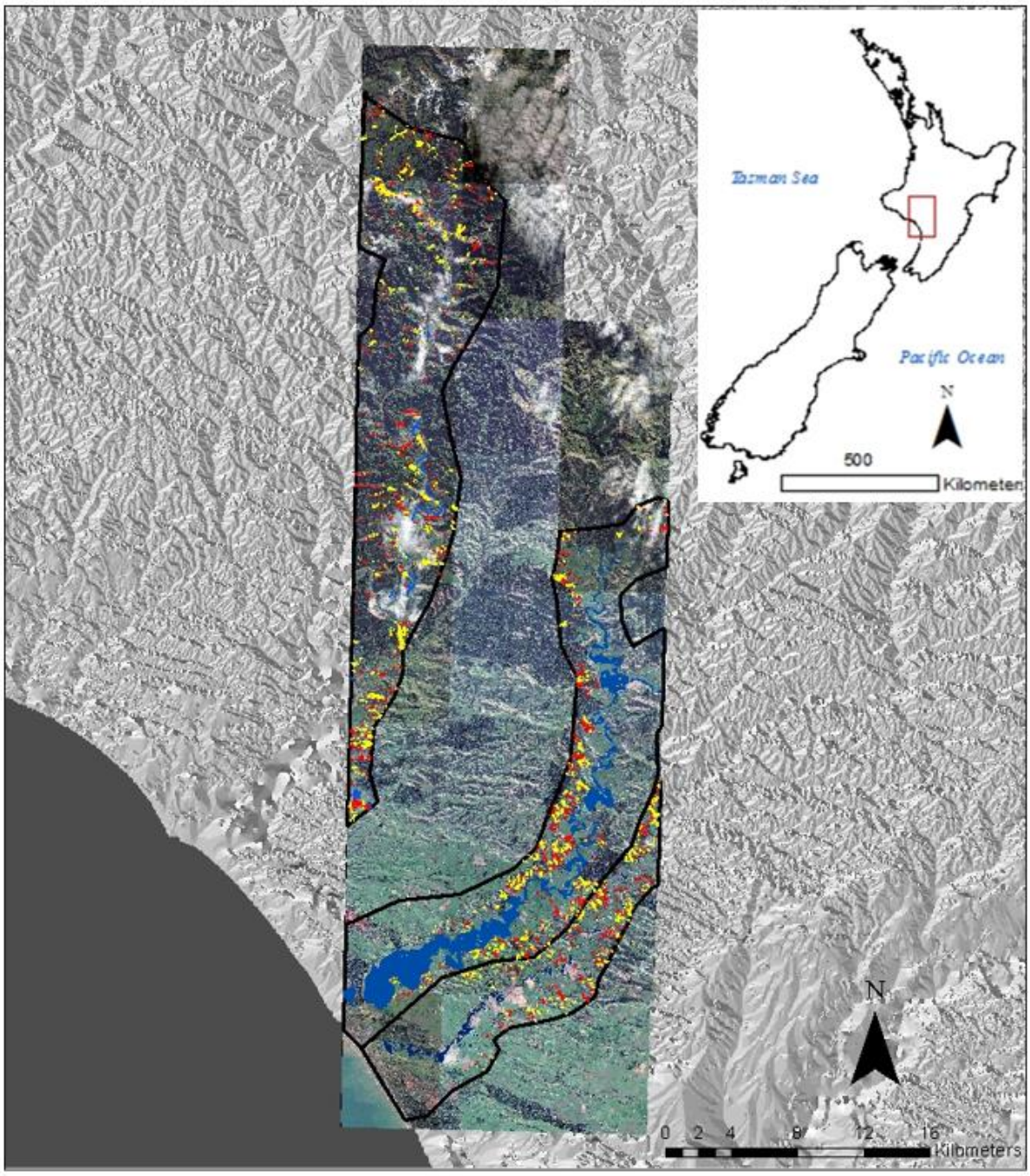

Figure 60. Manually digitized landslide and flood drape polygons within the Whanganui, Whangaehu and Turakina flood corridors. Coupled landslides: red; Buffered landslides; yellow; Flood drape: blue; Flood corridor polygons: black.

Table 6. Statistical data for the digitized mapping analysis within the Whanganui flood corridor.

Polygon Total Area (km^2)	218.78
Flood Drape Area (km^2)	0.6389
Total Coupled Landslides	820
Total Area of Coupled Landslides (m^2)	1334139
Total Buffered Landslides	1132
Total Area of Buffered Landslides (m^2)	607150

Table 7. Statistical data for the digitized mapping analysis within the Whangaehu flood corridor.

Polygon Total Area (km^2)	196.85
Flood Drape Area (km^2)	19.78
Total Coupled Landslides	530
Total Area of Coupled Landslides (m^2)	960655
Total Buffered Landslides	870
Total Area of Buffered Landslides (m^2)	660471

Table 8. Statistical data for the digitized mapping analysis within the Turakina flood corridor.

Polygon Total Area (km^2)	95.74
Flood Drape Area (km^2)	3.39
Total Coupled Landslides	539
Total Area of Coupled Landslides (m^2)	516838
Total Buffered Landslides	619
Total Area of Buffered Landslides (m^2)	345349

5.2.2 Landslide connectivity

Although the total number of coupled landslides was substantially less than buffered landslides within all flood corridors, the total aerial extent of coupled landslides was considerably higher compared to buffered landslides. Many relatively large, coupled landslides were mapped (and photographed in the field) along slopes confining the Whanganui River (Figures 61 and 62).

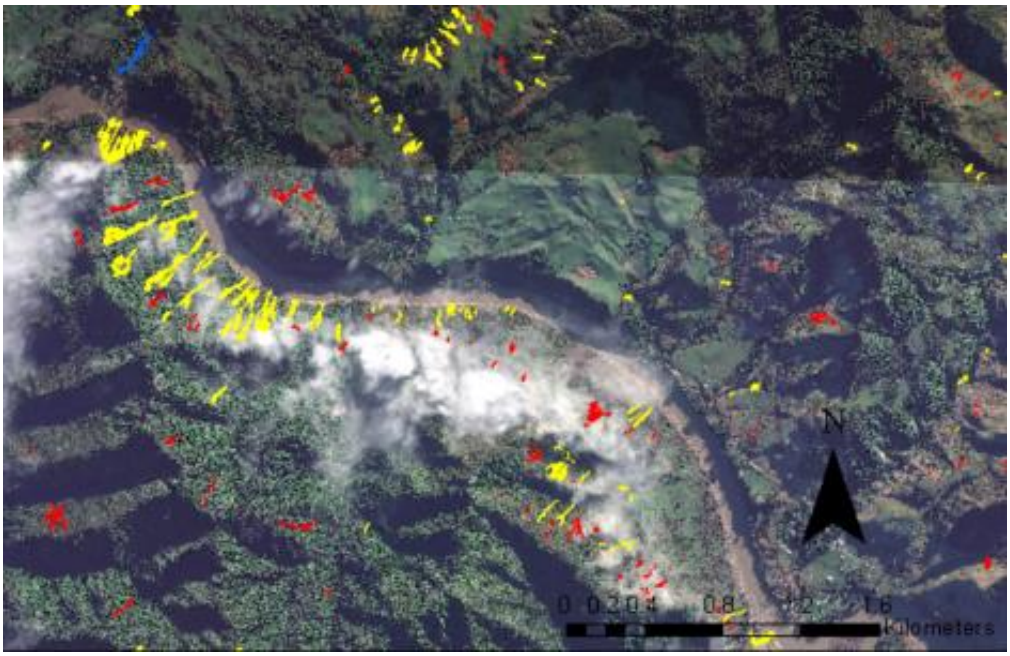

Figure 61. Manual digitization of coupled landslides (yellow polygons) along the main channel, as well as smaller tributaries, of the Whanganui River. Buffered landslides are in red and flood drape is in blue.

Figure 62. Coupling of landslides along the main channel, as well as smaller tributaries, of the Whanganui River (Author, December 2015).

5.2.3 Landslide distribution in relation to physical terrain characteristics

Slope angle and slope aspect data, as well as rock type and landcover were overlaid with the distribution of coupled and buffered landslides to assess the extent to which these physical terrain attributes influenced landsliding during the June 2015 rainstorm event.

5.2.3.1 Slope

Slope angle classes in this study are based on those defined in the Land-Use Capability Survey Handbook (Ministry of Works, 1969) which have been grouped into the following classes, as outlined in Table 9.

Table 9. Slope Classes used for this study based on Land Use Capability Slope Classes.

Slope Classes used for this study	
0° - 15°	Flat to Gently Rolling
16° - 25°	Strongly Rolling to Moderately Steep
26° - 35°	Steep
> 36°	Very Steep

Slope classes and the proportion of landslides which occurred within these slope ranges for the three flood corridors in this research are displayed in Figures 63, 64, and 65. The Whanganui flood corridor analysis shows failures on natural slopes occurred within all slope angle class ranges. However, a majority of landslide affected slopes were within angles ranging from 16° to > 36° with the *strongly rolling to moderately steep* and *steep* classes predominating slopes affected by landsliding within the Whanganui area of interest. The Whangaehu flood corridor analysis shows failures on natural slopes occurred within all slope angle class ranges. However, a small minority of landslide affected slopes were within terrain classed as *very steep*. The *gently rolling, strongly rolling to moderately steep* and *steep* classes have a relatively even proportion of slopes affected by landsliding within each of these classes. The Turakina flood corridor analysis shows failures on natural slopes occurred within all slope angle class ranges. However, a majority of landslide affected slopes were within angles ranging from 0° - 25° with the *gently rolling* and *strongly rolling to moderately steep* classes the predominant slopes affected by landsliding within the Turakina area of interest. The *very steep* slope class contained a minority of landslide affected slopes with approximately 1% of all landslides being within the > 36° slope angle range.

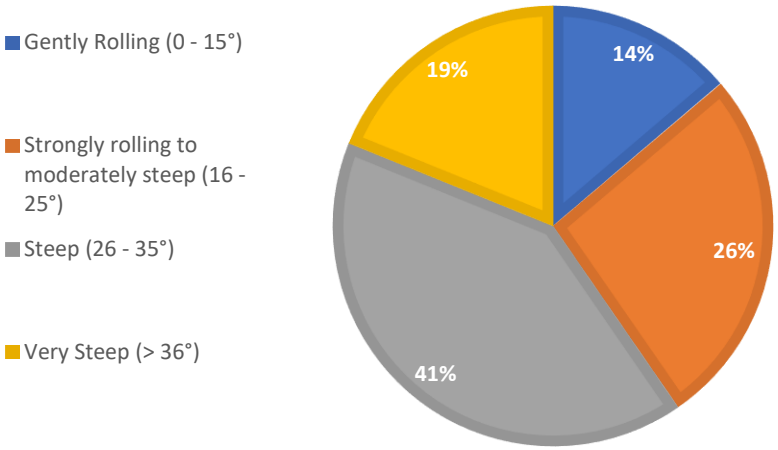

Figure 63. Relative proportions of landsliding on slopes within different slope angle classes within the Whanganui flood corridor.

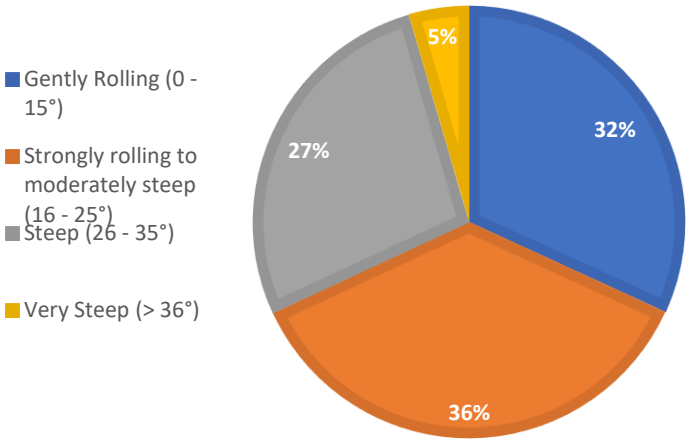

Figure 64. Relative proportions of landsliding on slopes within different slope angle classes within the Whangaehu flood corridor.

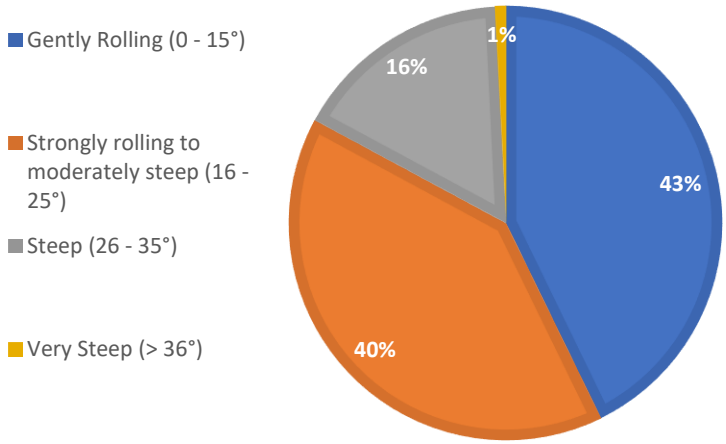

Figure 65. Relative proportions of landsliding on slopes within different slope angle classes within the Turakina flood corridor.

A limitation of the slope angle analysis in this study is here acknowledged due to the landslide mapping not including a separation of landslide source region from debris deposits. However, although source regions were not differentiated in this research, results indicate the predominant slope angle classes which were impacted by both landslide source zones and tail debris during the June 2015 rainstorm event. A further limitation is recognized here. The slope aspect data presented in this study is potentially biased due to the slope angle ratios of all slopes within the area of interest not being taken into account and compared against the angle of slope on which landslides occurred. However, this research shows the relative proportion of landslide affected slopes within each slope angle class with regards to total number of landslides.

5.2.3.2 Aspect

A summary of landslide aspect preference data for each of the three flood corridors is shown in Figures 66, 67 and 68, which shows the aspect of landslide affected slopes as a percentage of total number of landslides within each flood corridor. A strong aspect preference resides on north-facing slopes (NW, N, NE) within all three flood corridors with east-facing slopes also strongly impacted by landsliding in the Whangaehu and Turakina corridors. South-facing, as well as west-facing slopes, within all corridors showed minor slope aspect preference. The proportion of southern slopes ranged from 1% - 4% and south-western slopes aspect preference ranged between 1% - 3%.

A limitation of this study in regards to aspect data is that the relative proportions of all slopes within each aspect category was not considered in the following analysis, thus there is likely a bias caused by local topography of the aspect of all slopes within the three flood corridors. However, the data indicates the proportion of landslides in each aspect class relative to the total number of landslides within each flood corridor.

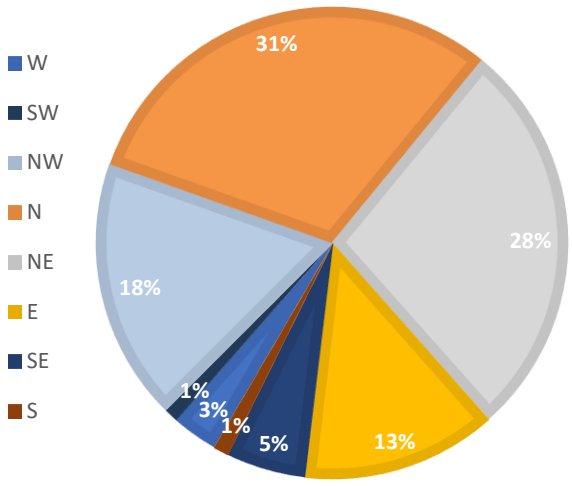

Figure 66. Aspect distribution of landslides within the Whanganui flood corridor. Areas generally show landsliding preference on north-facing slopes (NW, N, and NE).

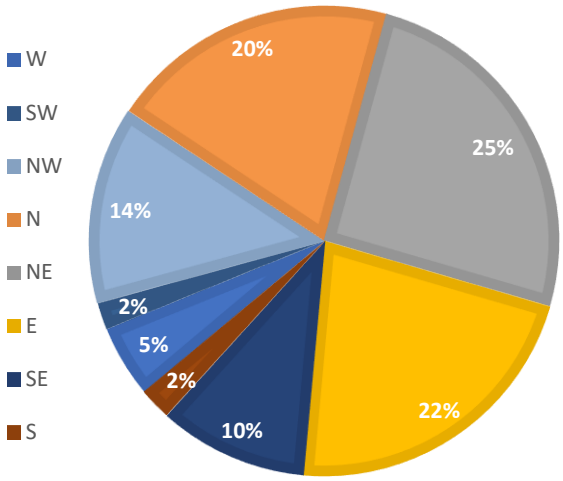

Figure 67. Aspect distribution of landslides within the Whangaehu flood corridor. Areas generally show landsliding preference on north-facing slopes (NW, N, and NE) as well as east-facing slopes.

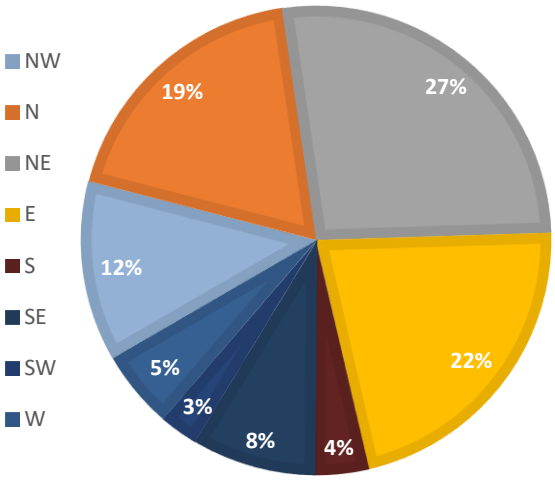

Figure 68. Aspect distribution of landslides within the Turakina flood corridor. Areas generally show landsliding preference on north-facing slopes (NW, N, and NE) as well as east-facing slopes.

5.2.3.3 Geology

Graphical summaries of landslide and rock type data within the Whanganui, Whangaehu and Turakina flood corridors are represented in Figures 69, 70 and 71, which show the total number of landslides that occurred on different rock units in each flood corridor. Data reveal that debris, gravel, mudstone, and sandstone were the main rock units that were impacted by slope erosion during the June 2015 rainstorm event. Results indicate that landslide occurrence was common on terrain underlain by mudstone within all three flood corridors with sandstone also strongly affected within the Turakina and Whangaehu corridors. Landsliding was also

relatively common on terrain underlain with debris and gravel within the Whangaehu and Turakina corridors.

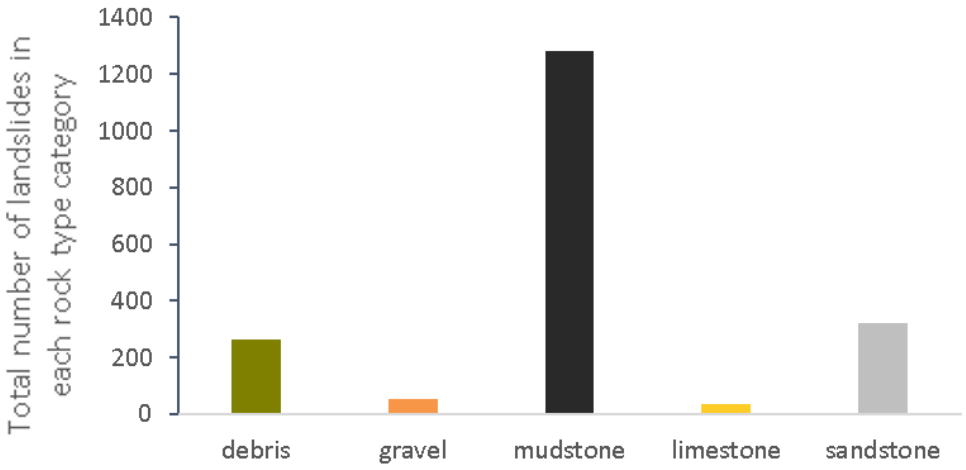

Figure 69.Landslide distribution across rock type classes within the Whanganui flood corridor shows mudstone to be the predominant lithological rock type on which landslips occurred.

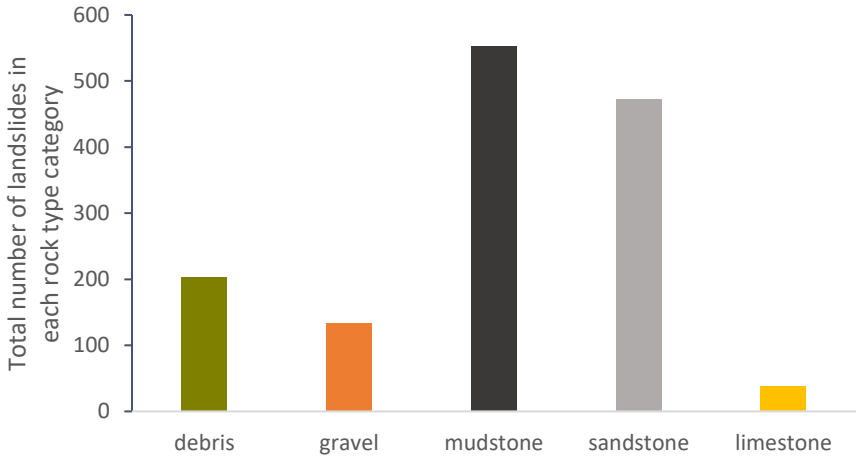

Figure 70. Landslide distribution across rock type classes within the Whangaehu flood corridor shows mudstone and sandstone to be the predominant lithological rock type on which landslips occurred.

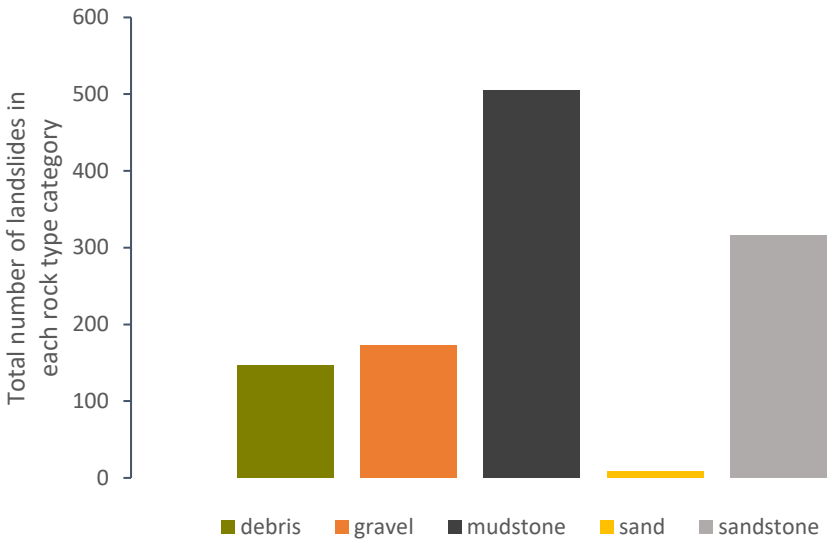

Figure 71. Landslide distribution was most extensive within mudstone and sandstone regions within the Turakina flood corridor.

5.2.3.4 Landcover

Landcover played a significant role in governing where landsliding occurred. For example, Figures 72 and 73 show GeoEye imagery of vegetated regions versus land under pasture. Whilst forested regions remained relatively stable during the June 2015 rainstorm event, large regions of pastured slopes have been destabilised. A summary of vegetation and landslide data within each flood corridor is represented in Figures 74, 75 and 76. The percentage of landslide damage on pasture ranged from 39 % -98%. Pastured land predominated areas of landsliding within the Turakina corridor with only 2% of landslides occurring within areas covered by other vegetation types. Areas in native bush ranged from 16% – 5% in the Whanganui and Whangaehu corridors respectively.

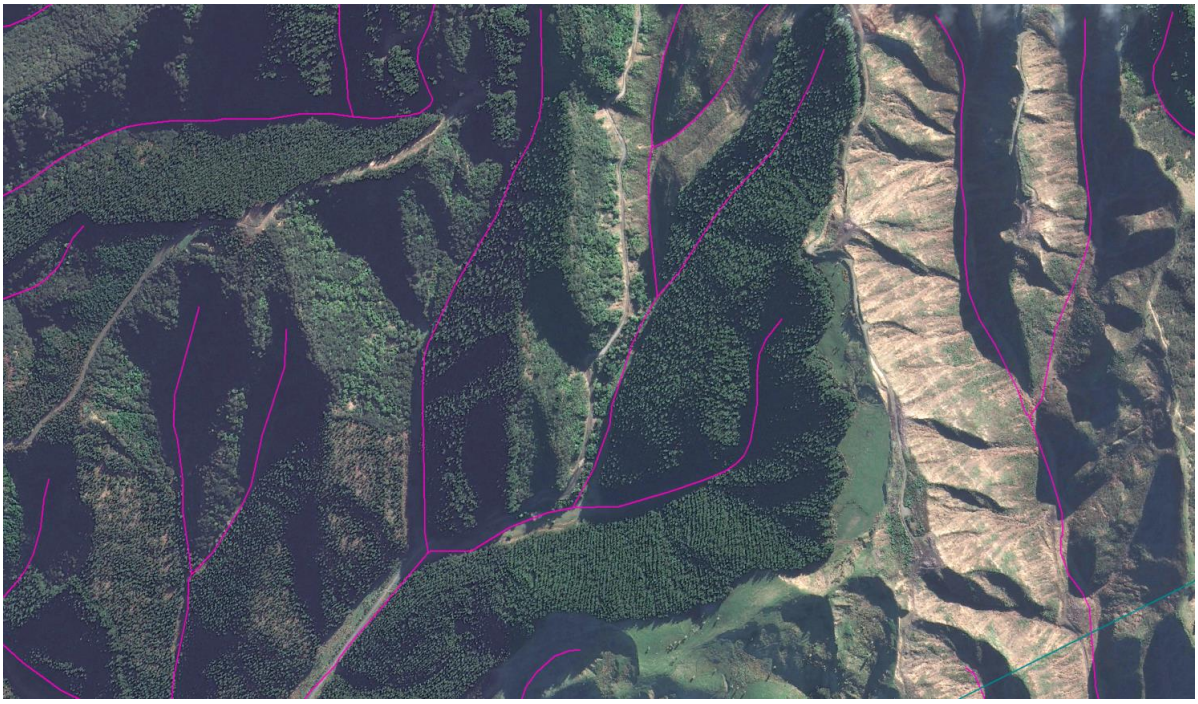

Figure 72. Landslide distribution was extensive within regions of high producing exotic grassland within all flood corridors.

Figure 73. Forested regions remained relatively stable during the June 2015 rainstorm event.

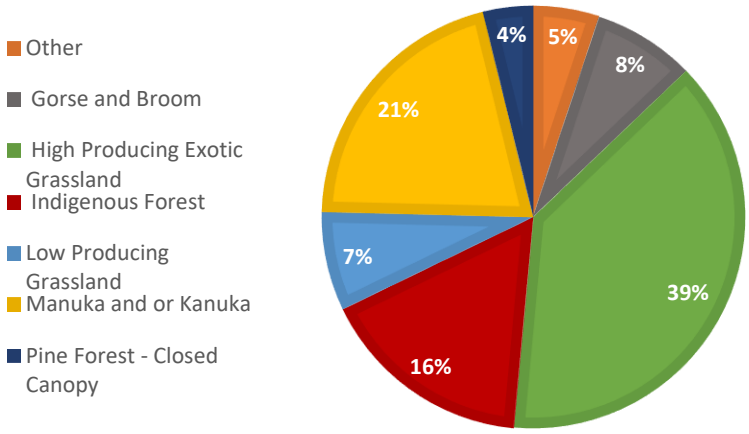

Figure 74. Landslide distribution was extensive within regions of high producing exotic grassland within the Whanganui flood corridor.

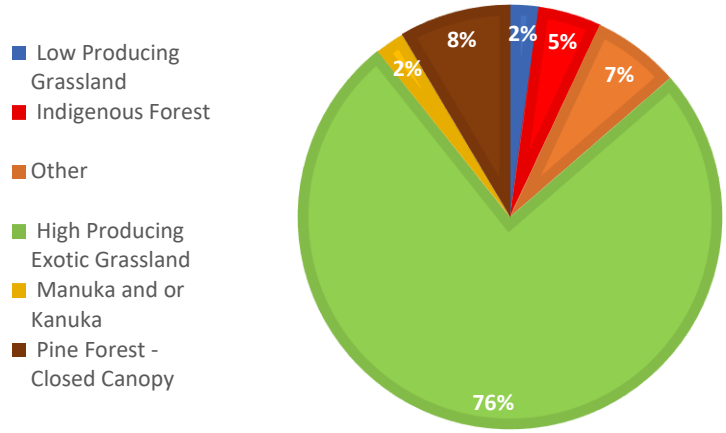

Figure 75. Landslide distribution was most extensive within regions of high producing exotic grassland within the Whangaehu flood corridor.

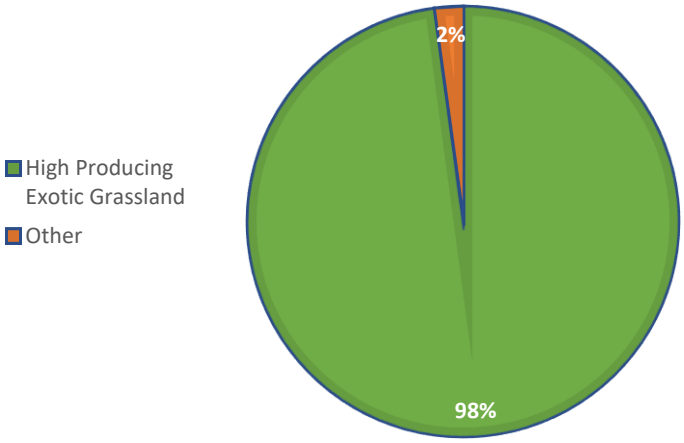

Figure 76. Landslide distribution was extensive within regions of high producing exotic grassland within the Turakina flood corridor.

Chapter 6 – Results of the 2015 Flood Drape Deposits

6.1 Introduction

The reader is referred to Appendix A for a summary of flood drape sample data from samples taken within each flood corridor and in various places along cross-sections where flood deposits had been draped over a relatively expansive area and at sites where vertical layering was discovered. Grain size (D_{50}), sample locations, sample descriptions and location descriptions, height above wetted channel, distance from coast, distance from wetted channel (proximal or distal) as well as total flood drape sample thickness calculations are included within the three catchment tables in Appendix A.

6.2 Flood Drape

Vast quantities of overbank deposits were laid down during the June 2015 rainstorm and flood event on the Whanganui, Whangaehu and Turakina floodplains. The manually digitized aerial extent of overbank sediments draped across the floodplains of these flood corridors is graphically displayed in Figure 77.

6.2.1 Distribution and extent

Calculation of the flood drape aerial extents within the three flood corridors is displayed in Tables 6, 7 and 8. The aerial extent was calculated to be 0.6389 km^2, 19.78 km^2, and 3.39 km^2 within the Whanganui, Whangaehu and Turakina flood corridors respectively. The Whanganui flood drape aerial extent is greatly underrepresented due to imagery constraints which did not allow for the mapping of large portions the lower reaches of the Whanganui River or the river mouth where vast quantities of overbank deposits were laid down.

Digital mapping of the aerial extent of the flood deposits enabled the establishment of 'common' zones of sedimentation which include around channel confluence zones (Figure 78), out on the main floodplain, lowland zones, and at interior and outer banks of bends. Figure 79 shows the distribution of overbank deposits along the Whangaehu (to the north) and Turakina floodplains where floodwaters spread out and often ponded in terrain depressions so that suspended sediments fell from suspension to be deposited in discrete zones that are disconnected from the main flood drape zones.

The vast quantities of relatively fine sediments carried down these flood corridors were draped like a thin blanket across 'common' zones of sedimentation with sample thicknesses ranging from 2 cm (Wh01) to 73 cm (Wg27).

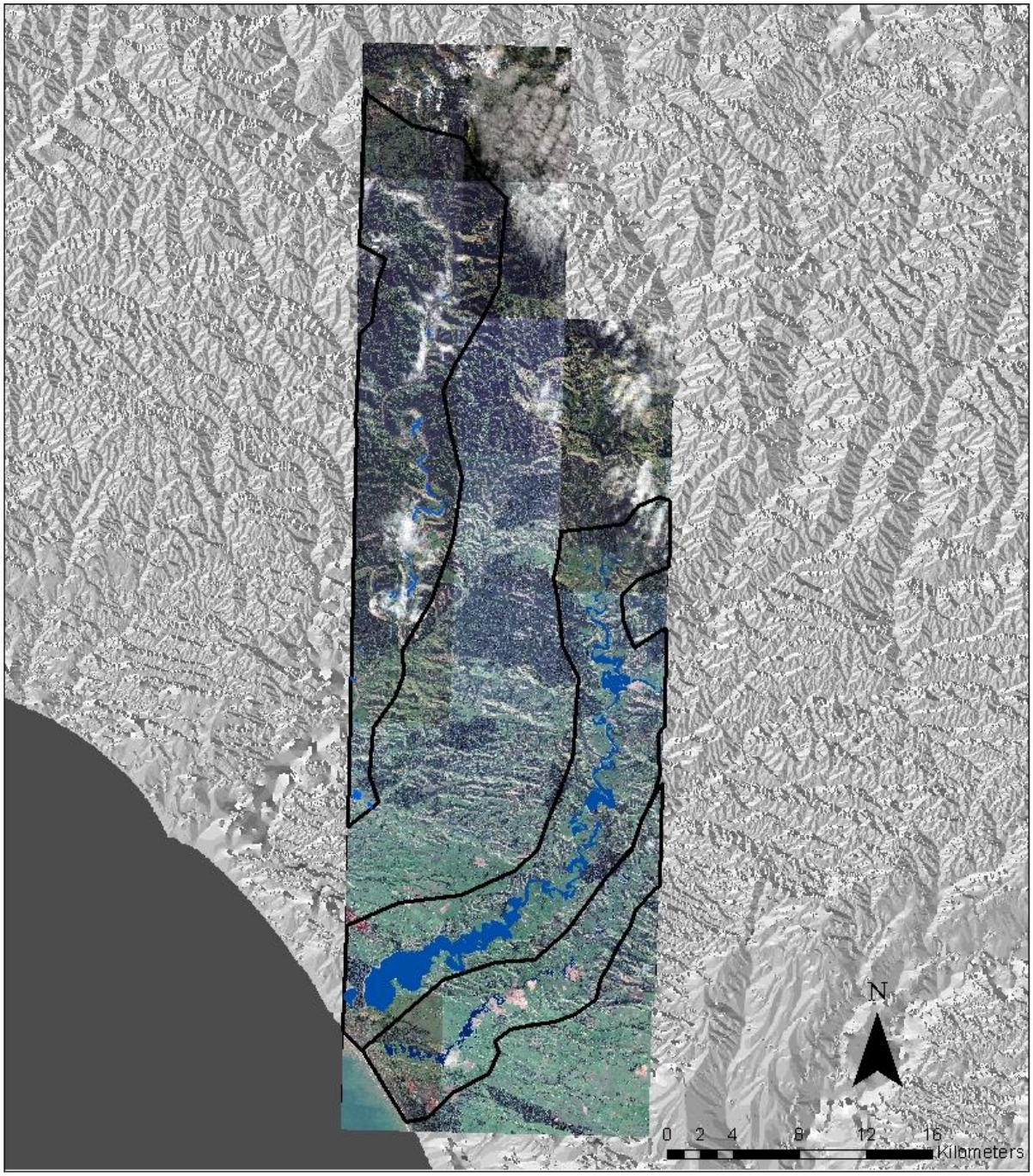

Figure 77. Distribution and extent of flood drape deposits laid down during the June 2015 flood event with the three flood corridors of interest.

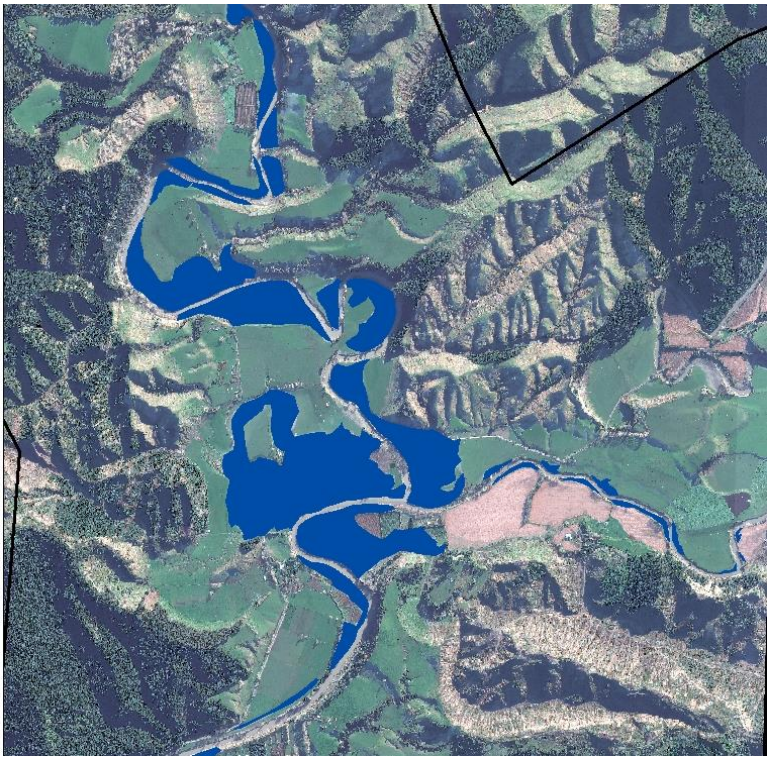

Figure 78. Distribution and extent of flood drape deposits at the confluence of the Whangaehu River and Mangawhero River.

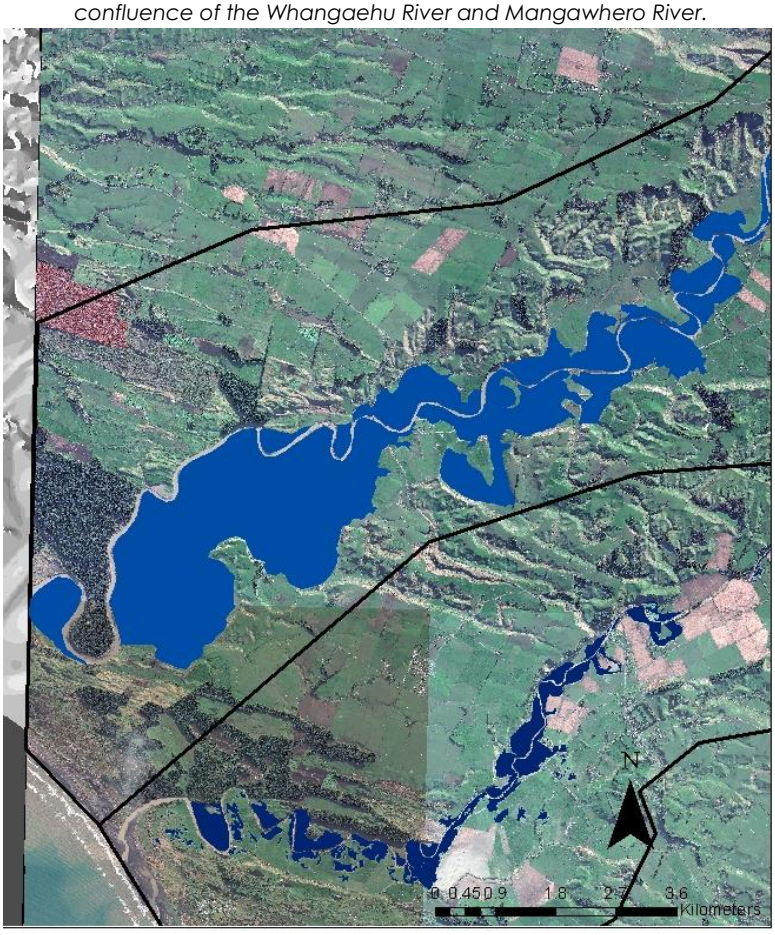

Figure 79. Distribution and extent of flood drape deposits at the confluence of the Whangaehu River and Mangawhero River.

6.3 Laser Particle Size Analysis of Flood Drape Sediments

Grain size data was examined in relation to sample elevation, sample distance from the wetted channel and distance from the coast in order to determine the hydraulic processes that transported and deposited sediments during the June 2015 flood event.

Analysis of the distribution of sediment grain sizes in relation to height above the wetted channel (Figure 80, 81, 82) shows a weak to moderate correlation of sediment fining as flood drape sample height above the wetted channel increases within the Whangaehu and Turakina flood corridor samples. However, within the Whanganui flood corridor sample sites, the relationship is much weaker with D_{50} values within the silt to fine sand ranges at all sample height elevations. There was little evidence of grain size fining with increased sample elevation within sediment samples of the Whanganui flood corridor. Further sampling with a more focussed approach toward grain size variation in regards to elevation above the wetted channel edge would aid in determining the relationship between these variables.

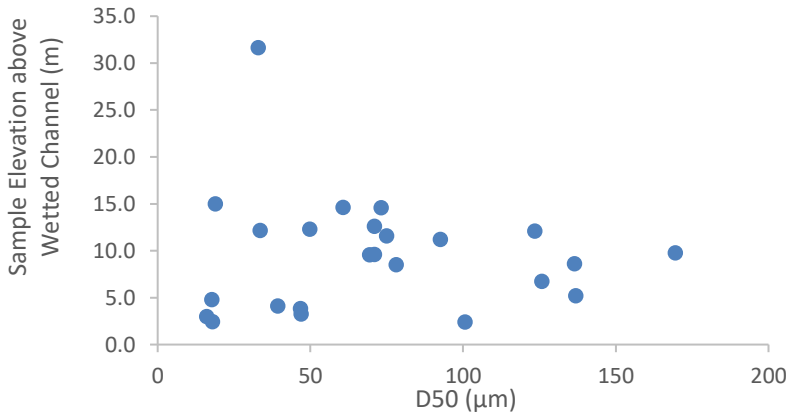

Figure 80. Elevation of the June 2015 flood drape samples relative to the wetted channel taken from within the Whanganui flood corridor.

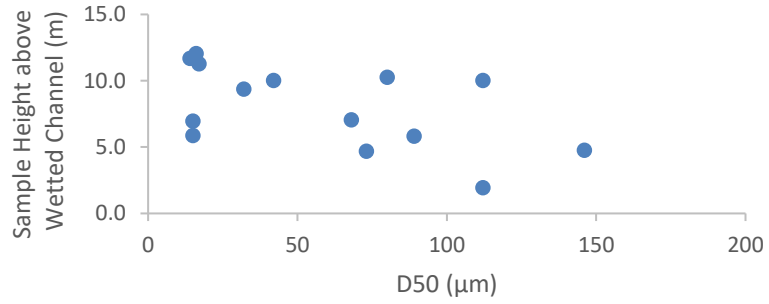

Figure 81. Elevation of the June 2015 flood drape samples relative to the wetted channel taken from within the Whangaehu flood corridor. Sample Wh10 was not included as it showed evidence of layering.

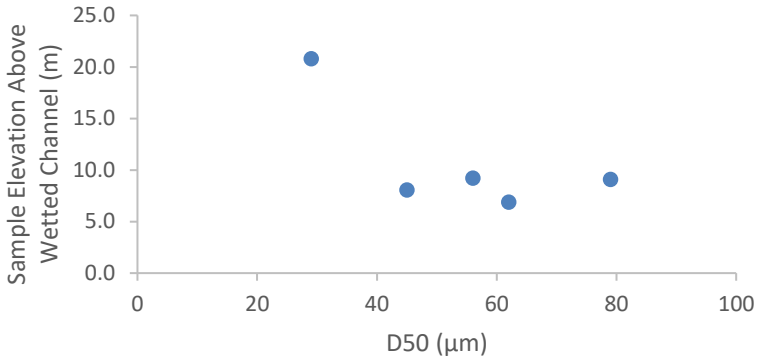

Figure 82. Elevation of the June 2015 flood drape samples relative to the wetted channel taken from within the Turakina flood corridor. Sample T02 was not included as it showed evidence of layering.

Analysis of the distribution of sediment grain sizes across the floodplain of the Whanganui River reveals that there is fining out of particle sizes within more distal zones of the deposited sediments with D50 values predominantly including silt sized particles (Figure 83). Results from sample sites more proximal to the channel indicate a relatively diverse particle-size distribution with grain sizes ranging from170 µm (fine sand) to 16 µm (fine silt) (Figure 83). Figure 83 demonstrates that coarse and relatively finer particles had been deposited closer to the channel whilst only relatively finer grades have been laid down further out from the wetted channel. Samples taken from cross-sections along the flood drape within the Whanganui flood corridor, from the most distal extent to the channel wetted edge show trends in overbank fining of grain sizes (Figures 84, 85 and 86). Similar results are seen from sample sites from within the Whangaehu flood corridor (Figures 87, 88, 89, and 90). Although the Turakina flood corridor contains a relatively small number of sample sites, there is also evidence of overbank fining from within proximal to distal flood drape sites (Figure 91).

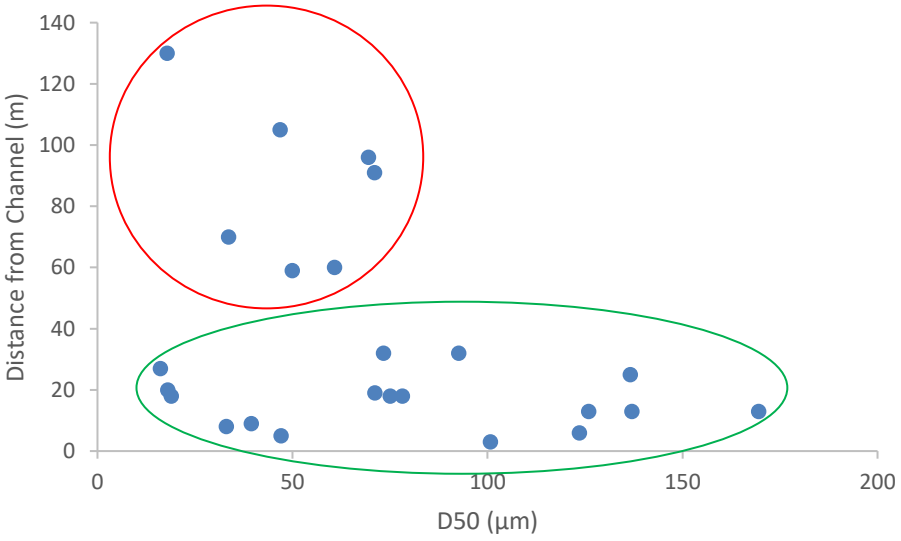

Figure 83. Fining of June 2015 flood drape sediments across the Whanganui floodplain. The plot above includes cross sectional data but grain sizes of vertical layering samples was not included. Analysis shows distal samples (circled in red) to encompass D50 (µm) values of less than 80 µm only, whilst proximal samples (outlined in green) include D50 (µm) values ranging from 170 µm (fine sand) to 16 µm (fine silt).

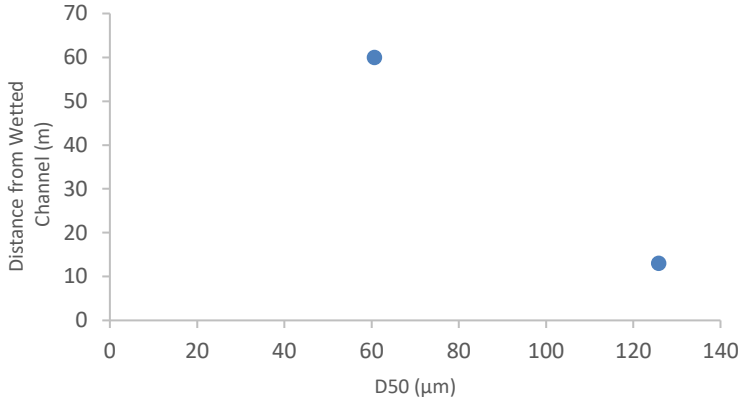

Figure 84. Particle-size distribution across cross section Wg 13 and Wg 14 at Riverine Lodge. Distal to the channel the median grain-size has fined out to be in the coarse silt range of particles whilst closer to the channel fine sand predominates the D50 grain size class.

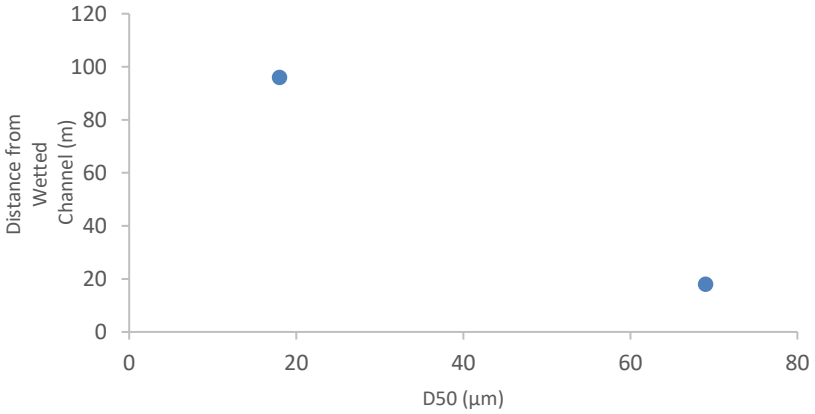

Figure 85. Particle-size distribution across cross section Wg 18 and Wg 19 at Parakino. Distal to the channel the median grain-size has fined out to be in the medium silt range of particles whilst closer to the channel very fine sand, nearing the coarse silt grain size class range, predominates the D50 grain size class.

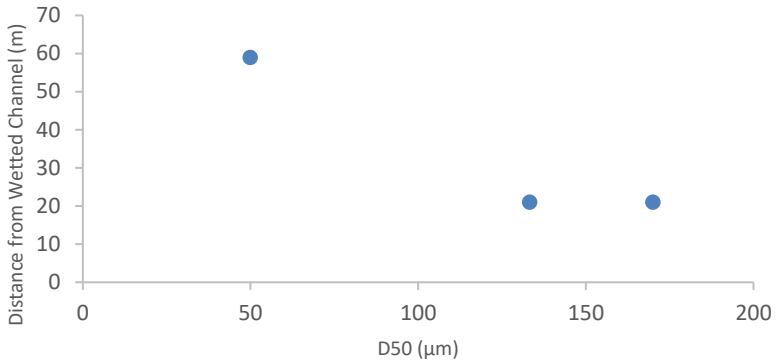

Figure 86. Particle-size distribution across cross section Wg 21 and Wg 22 at Kawhaiki. Distal to the channel the median grain-size has fined out to be in the coarse silt range of particles whilst closer to the channel fine sand predominates the D50 grain size class. Two potential vertical layers were evident within the proximal sample site, however grain size analysis revealed relatively close particle sizing within the fine sand grain size class.

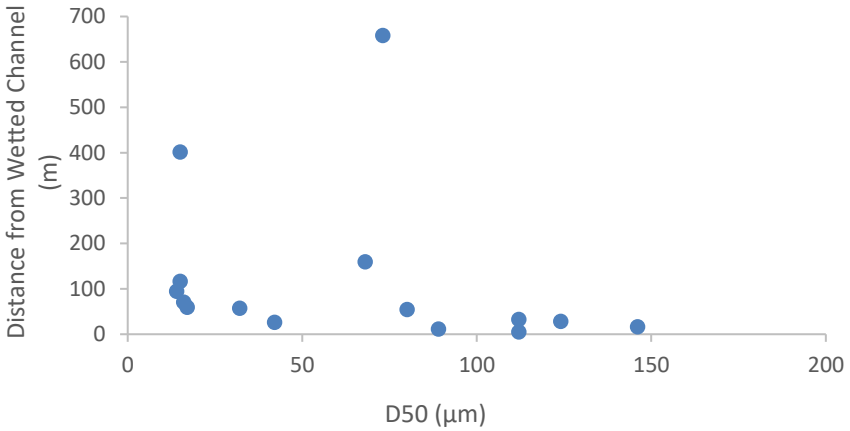

Figure 87. Fining out of June 2015 flood drape sediments across the Whangaehu floodplain. The sample outlier was measured at 658m from the streambank and was situated on the outer bend of the Whangaehu River so that overbank flow (and potentially water depth, turbulence, and velocity as well as SSC) was likely to have been relatively higher in this low-lying zone. The morphology of the river would have dictated dispersion of flood waters further across the floodplain and the sediment transport capacity of this water was potentially higher than other morphological zones of the floodplain. It is recognised that further sampling of the outer bends of this floodplain would be needed to support this assumption.

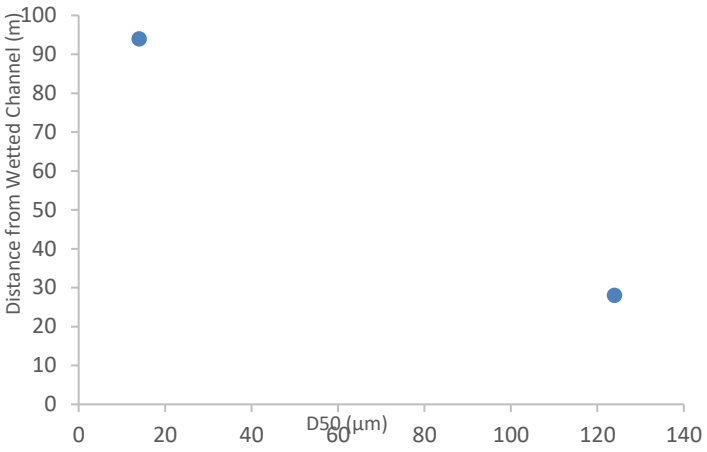

Figure 88. Samples Wh9 and Wh10 taken from a cross section across the Whangaehu flood drape shows fining out of sediment grain sizes from largest sized grains proximal to the wetted edge to relatively smaller grains (fine silt) distal to the channel.

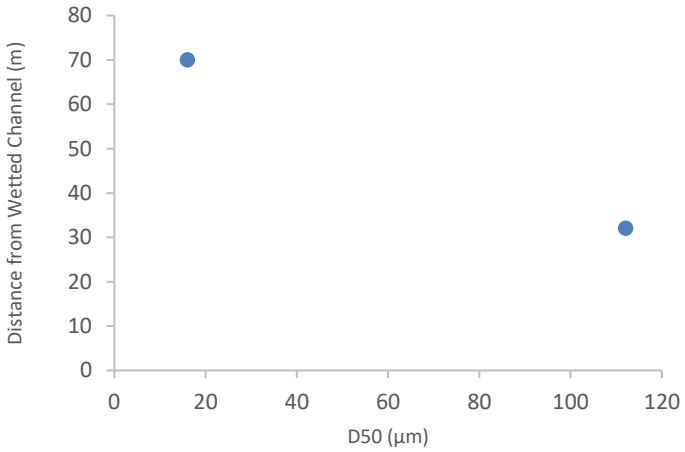

Figure 89. Samples Wh13 and Wh14 taken from a cross section across the Whangaehu flood drape shows fining out of sediment grain sizes from largest sized grains proximal to the wetted edge to relatively smaller grains (fine silt) distal to the channel.

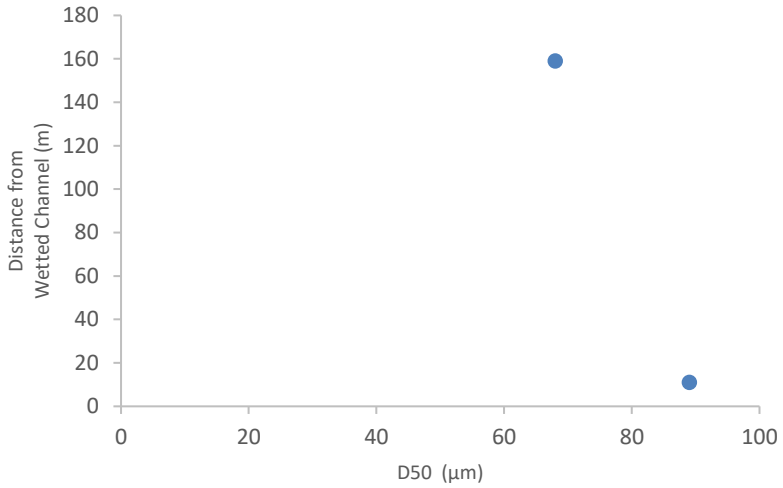

Figure 90. Samples Wh1 and Wh3 taken from a cross section across the Whangaehu flood drape shows fining out of sediment grain sizes from largest sized grains proximal to the wetted edge to relatively smaller grains (fine silt) distal to the channel.

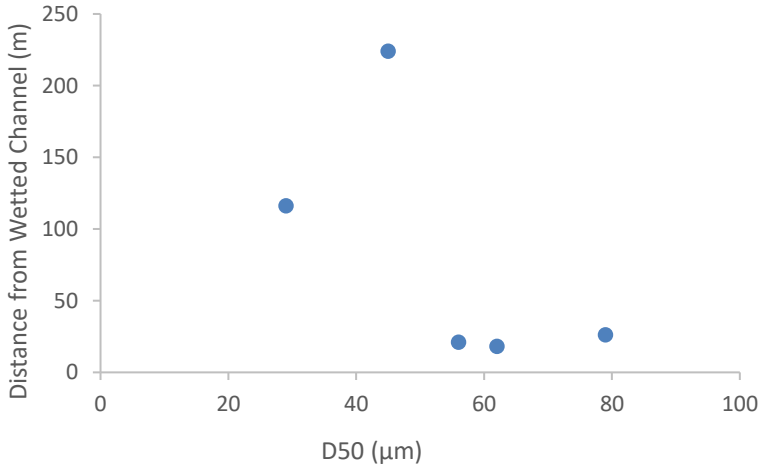

Figure 91. Fining of June 2015 flood drape sediments across the Turakina floodplain. Sample T02 was not included in the above analysis as it showed evidence of layering.

Analysis of the distribution of particle grain sizes in relation to distance from the coast shows a minor correlation between these variables within three flood corridors sampled in this study. Although all D_{50} particle size values within this research are within the silt and sand grain size classification classes (based on Wentworth, 1922), statistical analysis of grain size results reveal that there is a slight trend of downstream fining of particle sizes. In general, relatively larger sized D_{50} values tend to have been sampled from the flood drapes in the upper reaches of the flood corridors, further away from the river mouth of each of the three main rivers of this study, whilst smaller D_{50} grain size values tend to be clustered closer to the coast (Figures 92, 93 and 94). The downstream fining analysis did not take into consideration the spatial extent across the floodplain of each sample therefor there is potential for lateral grading to have influenced these results.

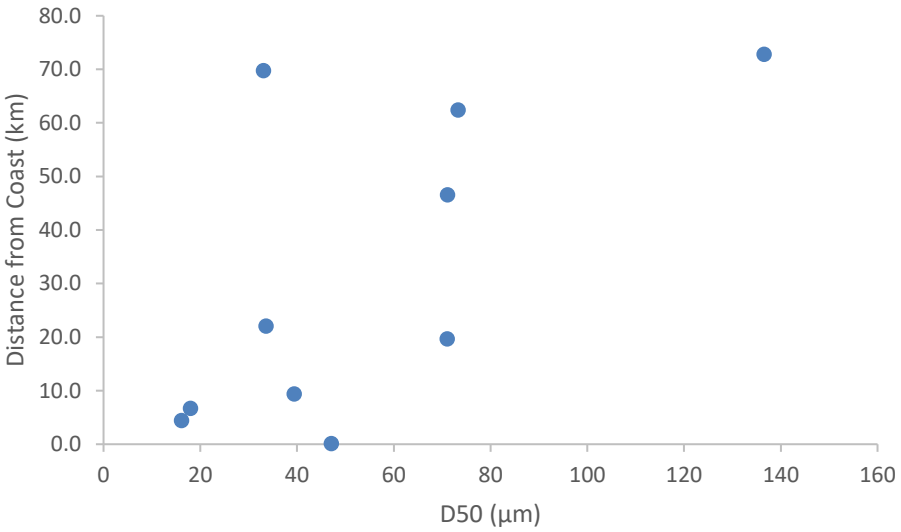

Figure 92. Downstream fining of the June 2015 flood drape within the Whanganui flood corridor. Samples taken from cross sections and sample sites with layering were not included in the downstream fining analysis.

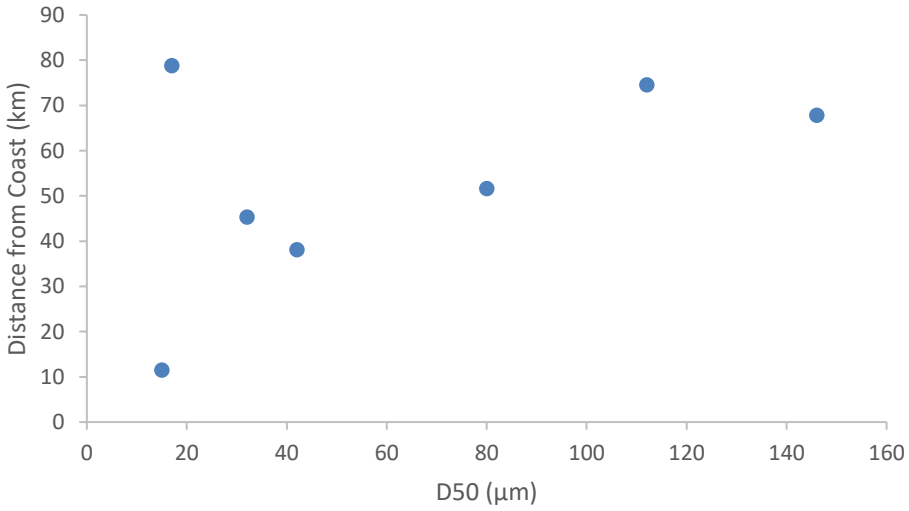

Figure 93. Downstream fining of the June 2015 flood drape within the Whangaehu flood corridor. Samples taken from cross sections were not included in the downstream fining analysis.

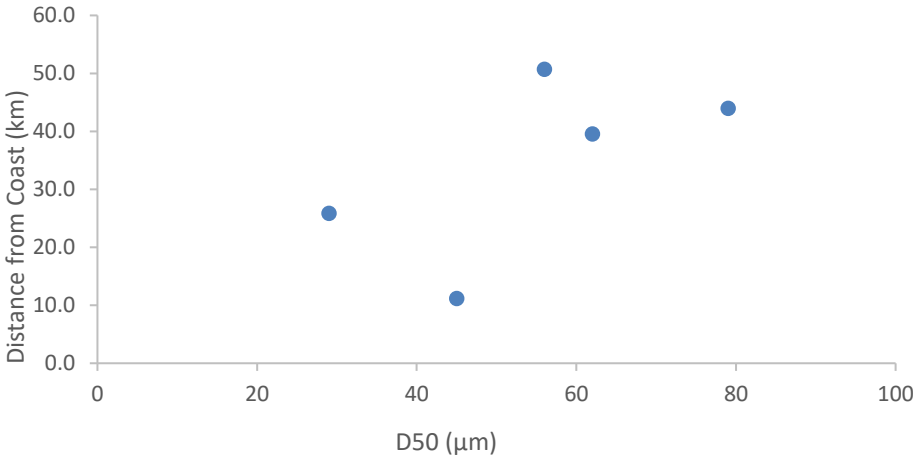

Figure 94. Downstream fining of the June 2015 flood drape within the Turakina flood corridor. Sample T02 was not included as it showed evidence of layering.

6.4 Stratigraphic layering within the 2015 flood drape

Moving from the upper reaches of the flood corridor and working down towards the river mouth, the following stratigraphic logs display vertical layering sequences that were found within the flood drape of the Whanganui River (Figures 95 through to 105). The layering units found within the flood deposits of the Whanganui flood corridor show two discrete sedimentary layers consisting of a relatively finer grained base unit (generally with a D_{50} value within the silt or mud classification category) overlain with a sedimentary layer consisting of a comparatively larger fine sand grain size unit. Samples Wg22 and Wg30 are not consistent with this trend and are likely a result of differing sedimentary and hydraulic processes.

The flood and sediment flux hydrographs taken at the Te Rewa monitoring site on the Whanganui River show that four distinct sediment pulses occurred within the Whanganui catchment (Figure 106). Analysis of turbidity data from monitoring stations at Ohura at Tokorima and Whanganui at Te Maire reveal that the Ohura did not contribute much in the way of sediment during the June 2015 flood event (B. Watson, personal communication, December 2, 2015). Rather a majority of the suspended sediment which was transported within the Whanganui fluvial network was sourced from the lower catchment (B. Watson, personal communication, December 2, 2015). This is supported by the distribution of rain shown in the 48 hr rainfall totals map as well as the 48 hr Average Recurrence Intervals for rain that fell over 19-21 June 2015 within the Whanganui, Whangaehu and Turakina catchments.

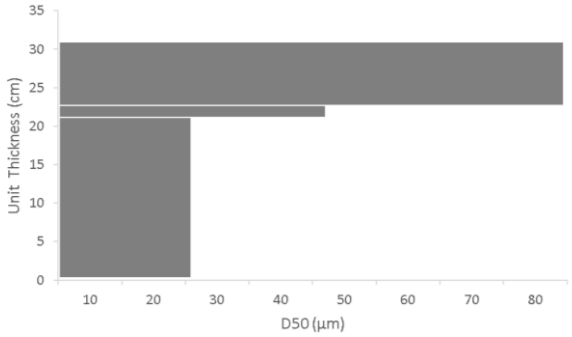

Figure 95. Vertical layering with sample site Wg10.

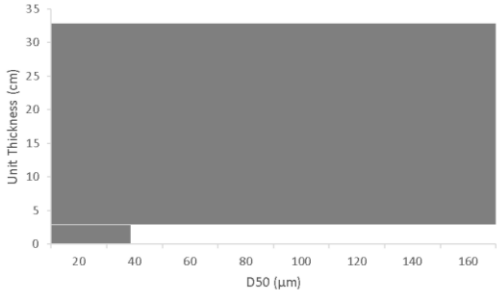

Figure 96. Vertical layering with sample site Wg11.

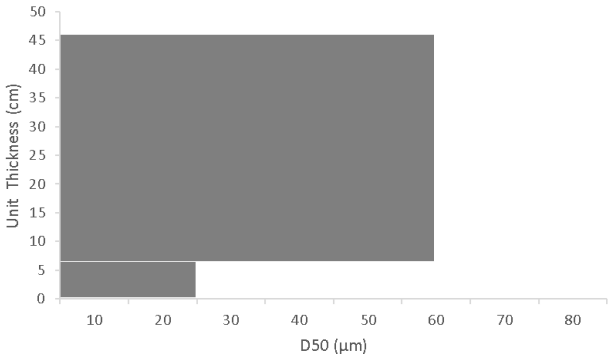

Figure 97. Vertical layering with sample site Wg12.

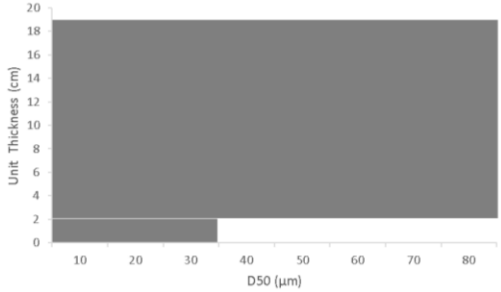

Figure 98. Vertical layering with sample site Wg16.

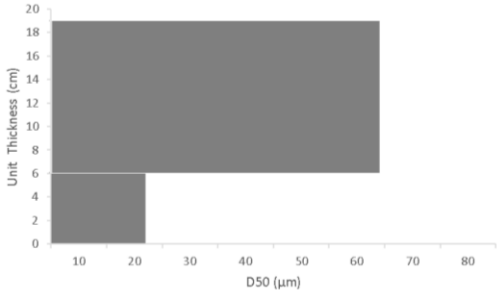

Figure 99. Vertical layering with sample site Wg20.

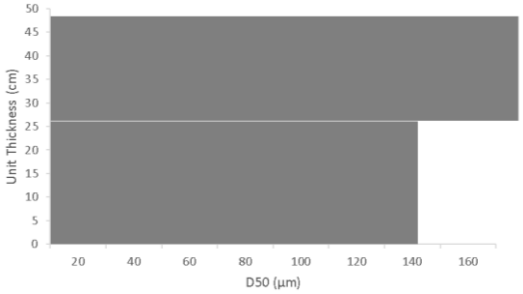

Figure 100. Vertical layering with sample site Wg22.

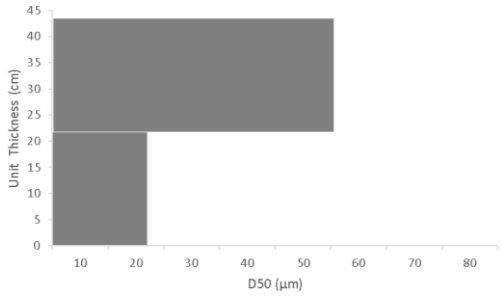

Figure 101. Vertical layering with sample site Wg25.

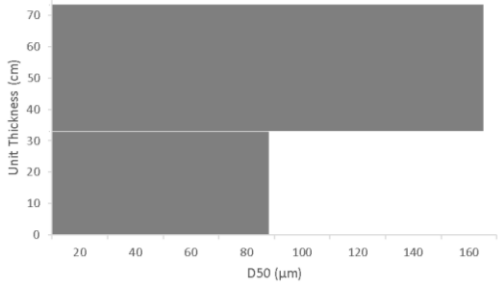

Figure 102. Vertical layering with sample site Wg27.

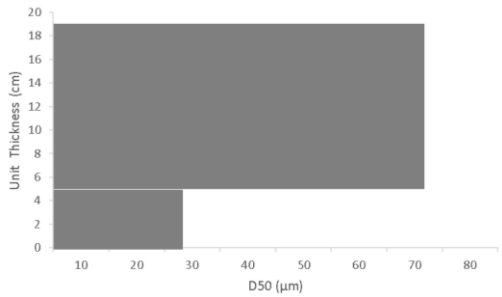

Figure 103. Vertical layering with sample site Wg29.

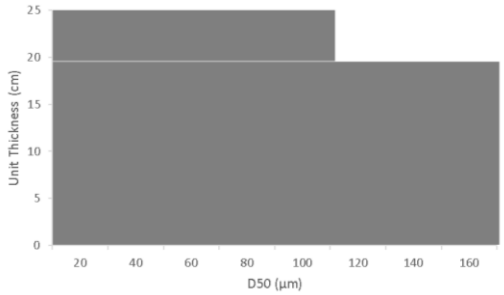

Figure 104. Vertical layering with sample site Wg30. The layering sequence within this sample site is not consist with the pattern of grading up which is displayed in all other layering sites. Both the base and top Wg30 samples consist of D_{50} values within the very fine to fine grained sand without a marked difference in grain sizes when compared to the other vertical layering sites. It has therefore been removed from the discussion and conclusion section.

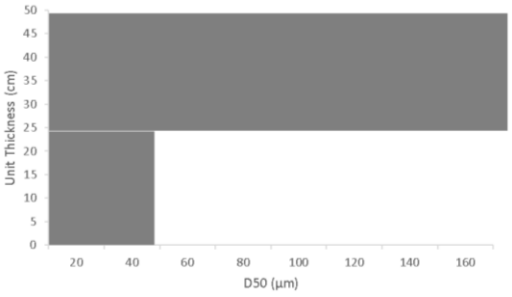

Figure 105. Vertical layering with sample site Wg31.

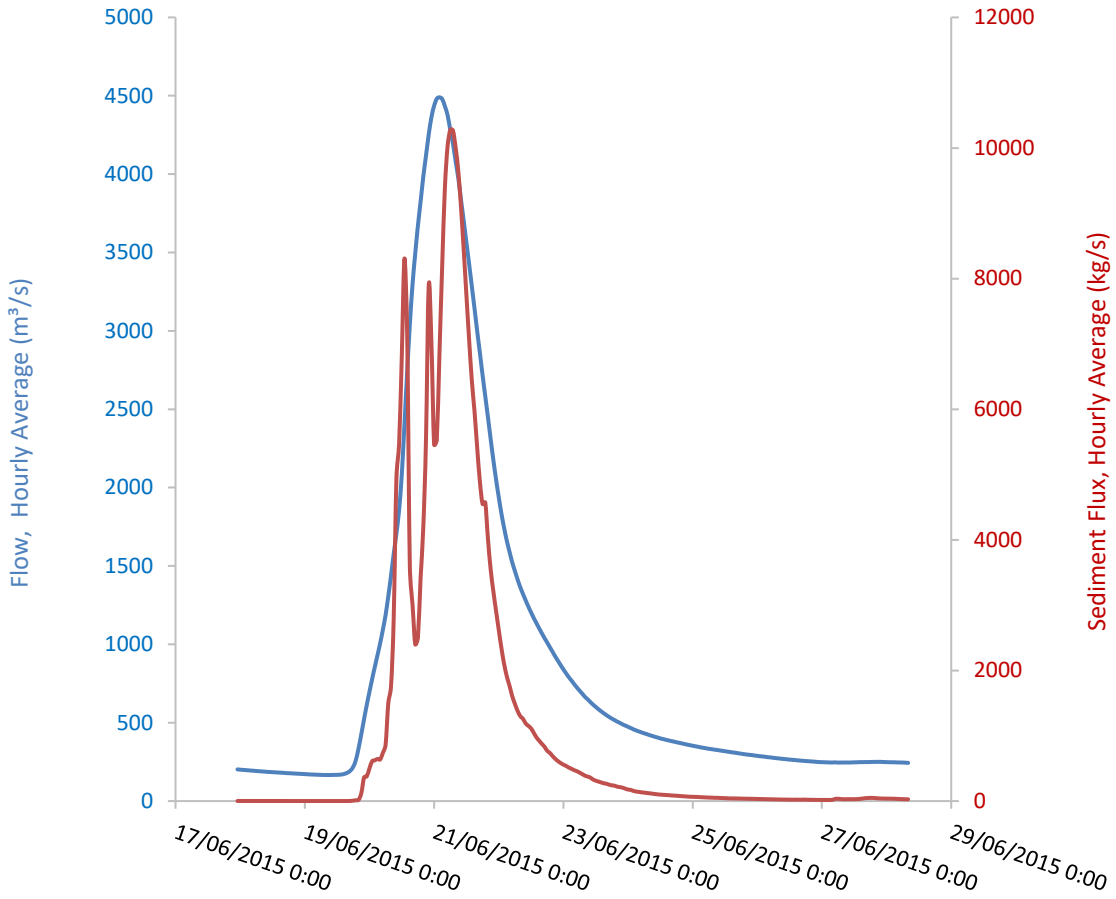

Figure 106. Flood and sediment flux hydrograph for the June 2015 flood event in the Whanganui River at Te Rewa (data courtesy of HRC, 2015).

Sediments from the volcanic regions of the Maunganui o te Ao contributed to the first distinct sediment pulse, whilst the main sediment pulse peak is thought to have come from mudstone regions (B. Watson, personal communication, December 2, 2015). Sediments from the Te Maire and Ohura regions were transported at the tail end of the flood hydrograph as displayed by the minor sediment peak on the recession of the main mudstone sediment peak (B. Watson, personal communication, December 2, 2015) (Figure 106).

Chapter 7 – Discussion

Of the 4510-total number of landslides digitally mapped within the three flood corridors of interest, the number of landslides connected to the fluvial network was 1,889 (42%). The total landslide areal extent within the three flood corridors was calculated to be 4,424,602 m^2, of which 2,811,632 m^2 (64%) was identified as being coupled with the channel. Within the Whanganui flood corridor region, a total number of 1952 landslides were mapped, of which 42% were identified as being coupled. Broken down into areal extent, the Whanganui flood corridor contained a total landslide area (buffered and coupled) of 1,941,289 m^2, of which 69% was identified as being connected to the fluvial system. Within the Whangaehu flood corridor zone, a total number of 1400 landslides were delineated, of which 38% were identified as being coupled with the fluvial network. A total landslide area of 1,621,126 m^2 was mapped within the Whangaehu corridor, of which 59% was identified as being connected to the fluvial system. Within the Turakina flood corridor, a total number of 1158 landslides were identified, of which 47% were connected to the fluvial network. A total landslide area of 862,187 m^2 was mapped within the Turakina corridor, of which 60% was designated coupled with the river system. These results substantiate the general trend of coupled landslides being comparatively larger in area than buffered landslides. Additionally, coupled landslides, in many cases, had debris-tails which were relatively longer (Figures 54 and 61) and in some cases, many small landslides along hillslopes adjacent to the fluvial network had amalgamated to such a degree that the combined outcome was a slope face almost entirely eroded by landsliding and connected to the river system (Figure 62). Furthermore, these results indicate a highly connected slope-channel system existed within all three flood corridors during the June 2015 storm event.

Deforestation and conversion of large tracts of land to pasture within the three flood corridors of interest played a significant role in influencing hillslope instability and susceptibility to erosion during the June 2015 rainstorm event. This finding correlates with research by Horizons Regional Council (2004) and Dymond *et al* (2006) on landsliding as a consequence of the 2004 rainstorm event in the Manawatu-Wanganui region. Landslide distribution and extent was strongly related to landcover type within all flood corridors in this research. Landslide distribution was extensive on *high producing exotic grassland* and *low producing grassland*, with 46%, 78% and 98% of landslides occurring on these landcover types within the Whanganui, Whangaehu and Turakina flood corridors respectively. In research on erosion under different landcover types after Cyclone Bola, Hicks (1991) revealed that the rate of landsliding under pasture was around ten times greater than under forested (native and exotic) slopes. Crozier *et al* (2008) found similar results in research conducted after the 2004 rainstorm event in the Manawatu and Wanganui hill-country where native bush and exotic forest provided some protection against hillslope instability. The percentage of landslide damage on forested (*indigenous*

forest and *pine forest – closed canopy*) slopes as opposed to areas covered by other vegetation types was calculated at 20% and 13% in the Whanganui and Whangaehu flood corridor zones respectively. Furthermore, in the Whanganui flood corridor the percentage of landslide damage on hillslopes with *Manuka and or Kanuka* landcover type was 21%. This suggests that the rainfall intensity and/or duration during the June 2015 rainstorm event was such that a threshold was exceeded destabilising hillslopes under *indigenous forest, pine forest – closed canopy* and *Manuka and or Kanuka,* producing landslides under these landcover types. Additionally, a vast majority of the Turakina and Whangaehu flood corridors are under pasture (Figures 20 and 23), whilst the Whanganui flood corridor (Figure 11) has a much smaller proportion of pastured land within the flood corridor region, which helps to explain the difference in ratio of landsliding under pastured slopes within the three flood corridors.

In addition to high intensity rainfall and vegetation cover, further physical terrain attributes recognised as important factors in governing storm-triggered landsliding that occurred during the June 2015 disturbance event include slope angle and aspect and lithology. Within the Whanganui flood corridor, a large proportion (41%) of landslide damage occurred on slopes classed as *steep (26° - 35°)*. Additionally, the proportion of landslide damage within slopes classed as *very steep (>36°)* was 19%. Due to the steepness of these slopes, sediment was expected to be delivered relatively efficiently to the fluvial system during the June 2015 rainstorm event. Comparatively smaller proportions of landslide damage occurred on slopes classed as *steep (>36°)* and *very steep (>36°)* within the Whangaehu flood corridor, with percentages of 27% and 5% respectively. The Turakina flood corridor had an even smaller proportion of landslide damage on *steep (>36°)* and *very steep (>36°)* slopes with percentages of 16% and 1% respectively. However, research by Dymond *et al* (2006) on modelling landslide susceptibility in the Manawatu-Wanganui region highlighted that although steep slopes tend to be relatively more susceptible to landslide damage and are more competent in delivering sediment to the fluvial network, considering there are so many low to moderate angle slopes in the region, significant sediment from those hillslopes still reaches the river systems during extreme rainfall events. This supports the spatial analysis finding that landslides on slopes within the *gently rolling (0°-15°)* and *strongly rolling to moderately steep(16°-25°)* classes were in many cases connected to the fluvial network during the June 2015 high magnitude storm event.

Landslide aspect preference showed a strong predilection for north-facing slope failures (NW, N, NE), with ratios of 77%, 59% and 58% in the Whanganui, Whangaehu and Turakina flood corridors respectively. East-facing slopes were also moderately impacted in the Turakina and Whangaehu areas of interest with ratios of 22% in both flood corridor regions. Additionally, results show that south-facing slopes were much less prone to failure which is unexpected as south-facing slopes are generally wetter, and with wet antecedent conditions, ground conditions were already near saturation point. Additionally, during the height of the storm the main rainfall and

airflow over the region came from the south which would initially lead one to think that the directional impact of rainfall would cause south-facing slopes to be much more affected by landsliding. These findings are similar to those made in research by Hancox *et al* (2005) on landslide slope aspect ratios resulting from the 2004 rainstorm event in the Manawatu-Wanganui region. Prior regolith stripping of south-facing slopes rendering them less vulnerable or factors such as thermal expansion and weathering of north-facing slopes could potentially have controlled the preference for north-facing slope-aspect location (Hancox *et al,* 2005). As highlighted in the 2004 rainstorm research by Hancox (2005), further investigation would need to be carried out into soil thickness and previous landsliding on south-facing slopes which would help clarify the questions around slope aspect preference.

A significant proportion of landsliding occurred on mudstone and sandstone rock types within all flood corridors of interest. Within the Whanganui flood corridor, mudstone was considerably the predominant rock type with a proportion of 66% and sandstone at 16%. Landsliding within the Whangaehu flood corridor occurred on mudstone at a ratio of 40% and sandstone 34%. Within the Turakina flood corridor the ratio was similar to neighbouring Whangaehu catchment, with 44% of landsliding occurring on mudstone and 28% on sandstone. Landslide susceptibility research by Dymond *et al* (2006) in the Manawatu-Wanganui region suggests that all mudstone and sandstone hillslopes within the region, no matter what the slope angle, are susceptible to landsliding.

These findings support research by Hancox *et al* (2006) on the 2004 rainstorm event in the Manawatu-Wanganui region which revealed slope angle, slope aspect and height, vegetation cover and lithology as the most significant factors affecting hillslope instability during this disturbance event.

The combination of high intensity rainfall falling upon already saturated, highly erodible slopes with inadequate landcover that surround the fluvial network, resulted in many of the relatively larger landslides being connected to the river system. This combination also facilitated relatively long runout distances of landslide debris-tails in many of the mapped hillslope failures. Spatial analysis revealed that physical coupling of the slope and channel domain remained relatively consistent throughout the entirety of the three flood corridors until the flood plain zone was reached. Analysis also revealed that the three flood corridors of interest were all highly connected between sediment sources on hillslopes and river networks and the propagation of sediment throughout the fluvial system was highly efficient during the June 2015 disturbance event so that extensive flood drape was laid down along the flood plains, at confluences of tributaries and main trunks, along the inner banks of meander bends, in usually disconnected depressions in lowland zones where post flood ponding occurred and along streambanks in the upper reaches of the flood corridors (Figure 60).

Field observations revealed that channel margins within all three flood corridors succumbed to widespread streambank erosion and draw-down processes where

entire sections of non-cohesive streambank had slumped and substantial desiccation cracks had developed between steps of slumped bank. Extensive streambank erosion occurred in particular along unvegetated channel margins constructed of alluvial deposits and along the outer bank of meander bends where cut bank erosion was widespread and extensive. This supports research by Brooks *et al,* 2013, Daly *et al,* 2015, and Bridge, 2003 who reveal that bank erosion rates, streambank stability and stable channel geometry, is heavily influenced by the binding effect of vegetation. Along channel margins consisting of bedrock, and in particular along outer meander bends consisting of bedrock, scouring and vegetation stripping was extensive. Although no quantitative measurements were taken, the extent of streambank erosion observed in the field likely contributed substantially to the sediment load within the flood waters during the June 2015 storm and flood event.

Spatial analysis identified common zones of flood drape deposition within all three flood corridors at confluence zones, on the inner bends of channels, lowland areas along streambanks in the upper reaches of the flood corridors, in terrain depressions and along the flood plains where flood waters dispersed, and water velocities decreased. The median grain size of samples taken from flood drape deposits laid down during the June 2015 flood event were all within the fine sand, silt, and mud particle size ranges (refer Appendix A). This reflects the geological nature of the three adjacent watersheds whereby relatively weak, uncompacted mud and sand marine deposits dominate the rock types of the region. The sheer quantity of deposited sediment is a reflection of the highly erodible nature of the hill country within the three flood corridors, the significant degree of connectivity between the slope-channel environments that transpired during the June 2015 storm event and the competency with which flood waters transported these relatively fine-grained sediments. During a disturbance event of such a magnitude as the June 2015 event, the three catchments within this study can be regarded as being both longitudinally and laterally efficient and effective sediment delivery systems.

The general trend of a grading down sequence of distinct vertical layers within the Whanganui flood drape is surmised to be a consequence of a combination of changes in inundation height and velocity as well as changes in sediment flux over the duration of the flood (Figure 106). Major sediment pulses from various main tributaries within the Whanganui watershed produced large scale variances in sediment concentration as the flood progressed. The flood and sediment flux hydrographs show that four discrete sediment pulses occurred within the Whanganui catchment over the duration of the flood. A majority of the high intensity rainfall fell over the lower reaches of these catchments, so it follows that sediment source areas correspond with these zones. Volcanic sediments originating from the Maunganui o te Ao tributary region are thought to have contributed to the first discrete sediment pulse, whilst the main distinct sediment peak is thought to have come from mudstone regions of the Whanganui catchment. Sediments from the Te Maire and Ohura regions, further up in the watershed are thought to have been transported at

the tail end of the flood hydrograph. There is a distinct time lag in sediment pulses from the different source regions with the first sediment peak arriving before the peak discharge and the largest pulse in suspended load arriving shortly after the peak flow, once the flood was abating. It could follow then that sediments from the volcanic regions potentially did not contribute to any great degree to overbank deposits due to the pulse arriving on the rising limb of the flood hydrograph well before the flood peak occurred. This is due to flood waters potentially may not have been flowing across the floodplain at that stage height or if flows had reached bank full discharge, the competency of flood waters, whilst discharges are rising, is also increasing and deposition rates are likely to have been low within the floodplain environment. This is supported in research by Hicks *et al* (1997) that indicates that sedimentation rates along a floodplain can decline as flood discharges increase due to the rising competency of flood flows across the floodplain. The main sediment pulse, which is thought to be sourced from mudstone regions occurred during the waning stage of the flood, when the water level was beginning to fall, overbank flood flow was starting to decrease, and turbulence and water velocities were declining as flood waters spilled across the floodplain. This was potentially the mechanism which produced the basal silt/mud layer within the vertical layering of the Whanganui flood drape samples. The Ohura and Te Maire sediment pulse, which also arrived on the tail end of the flood hydrograph potentially contributed to the second vertical layer of sand which was laid down on top of the basal silt layer.

In terms of lateral fining out of flood deposits, both sand and silt particles were laid down proximal to the channel margins whilst only relatively finer grades were deposited further out from the wetted channel (Figures 83-91). These results demonstrate lateral depositional grading across the floodplains and attest to a decrease in the sediment carrying capacity once flood waters began to flow across the floodplain and water velocities declined. Analysis of flood drape samples from the Whangaehu and Turakina flood corridors show similar results of lateral fining out of particle grain sizes. The grain size distributions in relation to longitudinal fining towards the river mouths (Figures 92-94) show a slight relationship between these variables with typically larger particle sizes found within the upper flood corridor when compared with floodplain sample grain sizes. However, the downstream fining analysis did not take into consideration lateral grading across the flood plains. Therefore, overbank lateral fining potentially has influenced the validity and reliability of these results and further sampling with a more focussed approach on longitudinal fining would need to be conducted for any definitive conclusion to be made in regards to longitudinal fining resulting from the June 2015 flood event in these catchments. Church (2002) explains how fluvial systems are sediment sorting machines, whereby a wide range of grain sizes enter the upper catchment but as stream competence declines downstream, typical sediment sizes become finer, so it is feasible that downstream fining of sediments did occur at some point along the flood hydrograph during the June 2015 flood event. However, in an event such as the June 2015 flood, stream competence was likely relatively high throughout much of the duration of the flood and with sediment, for the most part, entering the

catchments in an already relatively fine-grained state due to the geological nature of these watersheds, longitudinal fining may not have occurred until the waning stages of the flood if at all.

Predicted climatic changes such as increased precipitation and intensity, shifting rain bearing weather systems and cyclone tracks, as well as greater variations in precipitation and temperature (Crozier, 2010) will govern geomorphic change of the landscape and influence fundamental processes of fluvial geomorphology such as sediment source, transfer, and depositional zones as well as flow regimes. By analysing various compartments within fluvial systems, such as hillslopes, the channel network, and floodplains, and how these geomorphic components are linked through processes that move water and sediment between them, this research provides an insight into how these process-response systems interact and respond to change during extreme rainstorm events and gives an indication as to how this landscape will respond in the future as climate and land-use evolves. Findings from this research, as well as research by Ministry for Primary Industries (2015) on the June 2015 rainstorm event and analysis by Horizons Regional Council (2004) on the 2004 rainstorm event in the Manawatu-Wanganui region, indicate that the predominant sediment source zones resulting from major rainstorm events correlate with regions of highest intensity rainfall. Increased landslide activity and sediment generating events are an anticipated consequences of human-induced climate change (Crozier, 2010; Fryirs, 2013) and with alterations to the climate set to continue, and the magnitude and prevalence of rainstorms expected to increase in some areas of New Zealand, it is paramount to understand how the landscape evolves in response to extreme storm events so that future adverse effects can be mitigated.

Although destabilisation and landsliding occurred under forest covered slopes during the June 2015 extreme rainfall event, in the Whanganui and Whangaehu catchments in particular, this does not negate the effectiveness of utilizing reforestation or other vegetation planting tools to reduce sediment generation from erodible pasture in the future. Spatial analysis demonstrated that hillslopes planted in exotic forest or covered by native bush were considerably less prone to slope failure in comparison to pastured slopes. This supports findings by Crozier *et al* (2008) and Dymond *et al* (2006) from research of the 2004 rainstorm event in the Manawatu-Wanganui region which revealed that unsustainable land use of hill country was a major contributing factor in hillslope failure during the 2004 event. Research by Page *et al* (2000) on the implications of long term anthropogenic erosion for future land use in the Gisborne region of New Zealand, suggests an effective strategy to reduce overall sediment yield is targeted reforestation of different land types and erosion processes and found that a 50% reduction in sediments derived from landsliding could be accomplished within the Waipaoa catchment through reforestation of 12% of the land area if hillslopes are prioritized on the premise of landslide susceptibility. Dymond *et al* (2006) suggest a comprehensive catchment-wide approach of managing slopes through their vegetation cover by utilizing tools such as farm forestry, space-planted trees, reforestation, retirement or riparian planting, channel planting or gully wall planting in the Manawatu-Wanganui region. By applying the

findings from research such as this on the June 2015 rainstorm event in the Manawatu-Whanganui region, as well as conclusions made from the 2004 storm event (Hancox *et al*, 2005), and identifying hill country most susceptible to erosion based on attributes such as landcover, lithology, slope angle and height as well as aspect, and applying tools such as the various revegetation techniques suggested by Dymond *et al* (2006), hill-slope erosion can be mitigated into the future as the climate changes.

Chapter 8 – Conclusions

The landscape within the mid to lower reaches of the Whanganui, Whangaehu and Turakina drainage basins was activated and extensively modified during the June 2015 rainstorm and flood event. This study investigated the degree to which various geomorphic units within these catchments actively contributed to the sediment cascade during the June 2015 disturbance event and examined the degree of connectivity within the slope-channel environment in the areas of interest. Manual digitisation of landslides found that a relatively greater aerial extent of landslides were coupled with the fluvial network in comparison to buffered landslides, indicating highly connected slope-channel networks within the three flood corridors of interest.

Landcover played a significant role in governing where landsliding occurred. Whilst forested regions remained relatively stable during the June 2015 rainstorm event, large regions of pastured slopes were destabilised. Pastured land predominated areas of landsliding within all three flood corridors of interest, with 98% of all landslides within the Turakina flood corridor occurring on pastured slopes. Furthermore, landslide distribution and extent analysis in relation to physical terrain attributes revealed north-facing, as well as eastern-facing slopes predominated slope aspect preferences. Slope failures on natural slopes within all areas of interest were shown to occur within all slope angle class ranges. However, in the Whanganui flood corridor the *strongly rolling to moderately steep* and *steep* classes predominate slopes affected by landsliding. The *gently rolling, strongly rolling to moderately steep* and *steep* classes have a relatively even proportion of slopes affected by landsliding within each of these classes within the Whangaehu flood corridor. A majority of landslide affected slopes were within angles ranging from 0° - 25° with the *gently rolling* and *strongly rolling to moderately steep* classes predominate slopes affected by landsliding with the Turakina area of interest. The *very steep* slope class contained a minority of landslide affected slopes with approximately 1% of all landslides being within the > 36° slope angle range. Additionally, results indicate that landslide occurrence was most common on terrain underlain by mudstone within all three flood corridors with sandstone also strongly affected within the Turakina and Whangaehu corridors. The highly dissected, relatively 'soft' rock hill country within these catchments is a governing factor in the stability of land slopes with human intervention, such as deforestation increasing the likelihood of slope instability.

Flood drape deposition sampling and analysis reveal general trends in particle size distribution across the floodplain, and down the catchment whereby processes of sediment fining took place as flood waters decreased in velocity and turbulence and the carrying capacity of floodwaters declined along distal zones. Vertical stratification within the flood drape of the Whanganui River is surmised to be a product of a combination of changing suspended sediment concentrations due to discrete sediment pulses occurring at different stages of the flood as well as

processes of overbank flow along the waxing and waning stages of the flood hydrograph.

Analysis of slope-channel coupling, and the processes of sediment transport and deposition show a highly dynamic and active sediment cascade is in operation within all three catchments whereby sediment is effectively eroded and transported throughout the fluvial system during infrequent high magnitude disturbance events such as the June 2015 rainstorm and flood event.

References

Asselman, N.E.M. (1999). Suspended sediment dynamics in a large drainage basin: the River Rhine. *Hydrological Processes. 13:10,* (1437-1450).

Baca, P. (2008). Hysteresis effect in suspended sediment concentration in the Rybárik basin, Slovakia. *Hydrological Sciences Journal. 53:1*, 224-235

Ballance, P. (2017). *New Zealand Geology: an illustrated guide.* Geoscience Society of New Zealand Miscellaneous Publication 148.

Basher, L. (2013). Erosion processes and their control in New Zealand. In J Dymond (Eds.), *Ecosystem services in New Zealand – conditions and trends* (pp. 363-374). Manaaki Whenua Press.

Beaglehole, D. (2015). 'Whanganui places - Whanganui River', Te Ara - the Encyclopedia of New Zealand. Retrieved 8 May 2017 http://www.TeAra.govt.nz/en/whanganui-places/page-5.

Bell, J. (2013). Whangaehu-Mangawhero River Scheme Audit. *Horizons Regional Council*.

Benito, G. & Thorndycraft, V.R. (2005). Paleoflood hydrology and its role in applied hydrological sciences. *Journal of Hydrology, 313,* 3-15.

Blackham, M (Ed) (2015). Understanding and predicting floods and their impacts. *Water and Atmosphere,* National Institute of Water and Atmospheric Research Ltd: Wellington.

Blackwood, P. & Bell, J. (2016). Lower Whanganui River Flood Protection Investigations: Review of the June 2015 Flood and Update of Design Flood Level Estimates. *Horizons Regional Council.* Report No. 2016/EXT/1482.

Bridge, J.S. (2003). *Rivers and Floodplains: Forms, processes, and sedimentary record.* Oxford: Blackwell Science Ltd.

Brierley, G.J. & Fryirs, K.A. (2005). *Geomorphology and River Management.* Oxford: Blackwell Publishing.

Brooks, S.M., Crozier, M.J., Glade, T.W., & Anderson, M.G. (2004). Towards Establishing Climatic Thresholds for Slope Instability: Use of a Physically based Combined Soil Hydrology-slope Stability Model. *Pure and Applied Geophysics. 161,* 881–905.

Brooks, K. N., Ffolliott, P. F. & Magner, J. A. (2013). *Hydrology and the Management of Watersheds*. Iowa: John Wiley & Sons, Inc

Castro-Bolinaga, C.F. & Fox, G. A. (2018). Streambank erosion: Advances in monitoring, modelling and management. *Water. 10,* (10), 1346.

Charlton, R. (2008). *Fundamentals of Fluvial Geomorphology.* Great Britain: TJ International Ltd.

Chivers, M (n.d.) ArcUser Online: Differential GPS Explained. Retrieved 3 July 2016 from http://www.esri.com/news/arcuser/0103/differential1of2.html

Church, M. (2002). Geomorphic thresholds in riverine landscapes. *Freshwater biology, 47,* 541-557.

Churchill, R.R. (1982). Aspect-induced differences in hillslope processes. *Processes and Landforms, 7,* 2.

Coastal Systems Ltd (n.d.) River mouth environments example: Turakina River mouth dynamics. Retrieved 10 October 2016 from http://www.coastalsystems.co.nz/EnvironmentExamples/Environments%20Example%20of%20rivermouth%20dynamics%20-%20Turakina.pdf

Conley, B. (2015, June 21). Whanganui's Worst Flooding. *Whanganui Chronicle.* Retrieved February 12, 2021 from https://www.nzherald.co.nz/whanganui-chronicle/news/whanganuis-worst-flooding/QM7QQ2LOPLPPKOSZ2DXFVV4GEI/

Crozier, M.J. (1999). Prediction of rainfall-triggered landslides: a test of the antecedent water status model. *Earth Surface Processes and Landforms 24,* 825-833.

Crozier, M.J.; Hancox, G.T.; Dellow, G.D.; Perrin, N.D. (2008). Slip sliding away. p. 198-201 IN: Graham, I.J. (ed.) *A continent on the move: New Zealand geoscience into the 21st century.* Wellington: Geological Society of New Zealand in association with GNS Science. Geological Society of New Zealand miscellaneous publication 124.

Crozier, M.J. (2010). Deciphering the effect of climate change on landslide activity: A review. *Geomorphology, 124,* 3-4.

Daly, E.R., Miller, R.B. & Fox, G. A. (2015). Modeling streambank erosion and failure along protected and unprotected composite streambanks. *Fluvial Eco-Hydraulics and Morphodynamics, Advances in Water Resources*

Davie, T. (2008). *Fundamentals of Hydrology.* Routledge: Oxford

Department of Conservation (2006). Flora and fauna of Whanganui National Park. Retrieved March 11, 2017 from http://www.doc.govt.nz/documents/about-doc/concessions-and-permits/conservation-revealed/flora-fauna-whanganui-national-park-lowres.pdf.

De Ruyter, J. (2001). The Whangaehu River and Mangawhero River. A report on flooding and erosion hazards. *Horizons Regional Council.*

De Ruyter, J. (2002). The Turakina River: a report on flooding and erosion hazards. *Horizons Regional Council.*

Di Francesco, S., Biscarini, C., Manciola, P. (2016). Characterization of a Flood Event through a Sediment Analysis: The Tescio River Case Study. *Water. 8,* 308.

Douglas, G.B., McIvor, I.R., Manderson, A.K., Koolaard, J.P., Todd, M, Braaksma, S. & Gray, R.A.J. (2013) Reducing shallow landslide occurrence in pastoral hill country using wide-spaced trees. *Land Degradation and Development, 24,* 103-114.

Dymond, J. &Shepard, J. (2006). Highly erodible land in the Manawatu-Wanganui region. *Landcare Research Contract Report*: 0607/027 prepared for Horizons Regional Council.

Dymond, J.R., Ausseil, A., Shepard, J.D. & Buettner, L. (2005). Validation of a region-wide model of landslide susceptibility in the Manawatu-Wanganui region of New Zealand. *Geomorphology, 74,* 70-79.

Environmental Systems Research Institute (2016). Interpolate Polygon to Multipatch. Retrieved 20 September 2016 from https://desktop.arcgis.com/en/arcmap/10.3/tools/3d-analyst-toolbox/interpolate-polygon-to-multipatch.htm

Ferguson, R. I. (1981). Channel forms and channel changes. *British Rivers,* (pp. 90–125). London: Allen and Unwin.

Ferguson, R. & Ashworth, P. (1991). Slope-induced changes in channel character along a gravel-bed stream: the Allt Dubhaig, Scotland. *Earth Surface Processes and Landforms, 16,* 65-82.

Fleming, C. (1953). *The Geology of Wanganui Subdivision*. New Zealand Geological Survey, Bulletin 52. Government Printer, Wellington.

Fryirs, K.A. (2013). (dis)Connectivity in catchment sediment cascades: A fresh look at the sediment delivery problem. *Earth Surface Processes Landforms, 38*, 30-46.

Fryirs, K.A. & Brierley, G.J. (2001). Variability in sediment delivery and storage along river courses in Bega catchment, NSW, Australia: Implications for… *Geomorphology, 38* (237–265).

Fryirs, K. & Brierley, G. (2012). *Geomorphic analysis of river systems: An approach to reading the landscape*. West Sussex: Wiley-Blackwell.

Fryirs, K., Brierley, G., Preston, N., & Kasai, M. (2007a). Buffers, barrier, and blankets: The (dis)connectivity of catchment-scale sediment cascades. Catena, 49-67.

Fuller, I.C. & Marden, M. (2011). Slope–channel coupling in steepland terrain: A field-based conceptual model from the Tarndale gully and fan, Waipaoa catchment, New Zealand. *Geomorphology, 128,* 3-4, p 105-115.

Gao, J. & Maro, J. (2010). Topographic controls on evolution of shallow landslides in pastoral Wairarapa, New Zealand, 1979-2003. *Geomorphology,* 114, 373-381

Glade, T. (2003). Landslide occurrence as a response to land use change: a review of evidence from New Zealand. *Catena, 51,* 297-314.

Guzzetti, F., Peruccacci, S., Rossi, M. & Stark, C.P. (2007). The rainfall intensity–duration control of shallow landslides and debris flows: an update. *Landslides 5,* 3–17.

Guzzetti, F., Mondini, A.C., Cardinali, M., Fiorucci, F, Santangelo, M. & Chang, K. (2012). Landslide inventory maps: new tools for an old problem. *Earth Science Review, 112*, (1-2) 73-89.

Haddadchi, A. & Hicks, M. (2021). Interpreting event-based suspended sediment concentration and flow hysteresis patterns. *Journal of Soils and Sediments, 21,* 1, 592-612.

Haddadchi, A. & Hicks, M. (2020). Understanding the effect of catchment characteristics on suspended sediment dynamics during flood events. *Hydrological Processes, 34,* 7, 1558-1574.

Hancox, G.T. and Wright, K. (2005a). Analysis of landsliding caused by the 15-17 February 2004 rainstorm in the Wanganui-Manawatu hill country, southern North Island, New Zealand. *Institute of Geological & Nuclear Sciences science report* 2005/11. 64p.

Hancox, G.T & Wright, K. (2005b). Landslides caused by the February 2004 rainstorms and floods in southern North Island, New Zealand. *Institute of Geological and Nuclear Sciences science report* 2005/10. 32p.

Hanton & Andersen Design & Print (1995). Memories of Old Wanganui volume 1. Hanton & Anderson Limited.

Hanton & Andersen Design & Print (2001). Memories of Old Wanganui volume 4. Hanton & Anderson Limited.

Hanton & Andersen Design & Print (2005). Memories of Old Wanganui volume 5. Hanton & Anderson Limited.

Hanton & Andersen Design & Print (2009). Memories of Old Wanganui volume 7. Hanton & Anderson Limited.

Hensley, K. J. & Ayers, P. D. (2018). Estimating Streambank Erosion Rates with a GPS-Based Video Mapping System. *Journal of the American Water Resources Association, 54,* 6.

Heron, D.W. (custodian) 2014: Geological Map of New Zealand 1:250 000. *GNS Science Geological Map 1.* Lower Hutt, New Zealand. GNS Science

Hicks, E.L., (1991). Erosion under pasture, pine plantations, scrub, and indigenous forest: a comparison from Cyclone Bola, *New Zealand Forestry, 26,*

Hicks, M., Davies, T. Erosion, and sedimentation in extreme events. In Mosley, M.P. & Pearson, C.P. (Eds.) (1997). *Floods and Droughts: The New Zealand Experience.* Christchurch: New Zealand Hydrological Society.

Hicks D.M., Shankar U., McKerchar A.I., Basher L., Jessen M., Lynn I., Page M. (2011). Suspended sediment yields from New Zealand rivers. *Journal of Hydrology (NZ) 50,* 81–142.

Hoey, T.B. & Bluck, B.J. (1999). Identifying the controls over downstream fining of river gravels. *Journal of Sedimentary Research, 69,* 1, 40-50.

Horizons Regional Council (2002). The Turakina River: A report on flooding and erosion hazard. *Horizons Regional Council.*

Horizons Regional Council (2004). Storm: Civil Emergency Storm and Flood Report February 2004. *Horizons Regional Council.*

House, P. K., Webb, R. H., Baker, V. R. & Levish, D. R. (2002). Ancient Floods, Modern Hazards: Principles and Applications of Paleoflood Hydrology. Washington DC: Water Science and Application 5.

Hume, T., Ovenden, R. & MacDonald, I. (2012). Coastal stability in the South Taranaki Bight - Phase 1. Historical and present-day shoreline change. Prepared for Trans-Tasman Resources Ltd. National Institute of Water & Atmospheric Research Ltd: Hamilton. Report no. HAM2012-083

Jones, Lewin & Macklin, M. (2010). Flood series data for the later Holocene: Available approaches, potential and limitations from UK alluvial sediments. *The Holocene 20* (7), 1123-1135.

Keen-Zebert, A. (2016). Downstream Fining. Retrieved February 12, 2021 from http://buffalorivergeoscience.org/blog/2016/11/29/downstream-fining.

Keesstra, S.D., Davis, J., Masselink, R.H., Casali, J., Peeters, E.T.H.M. & Dijksma, R. (2019). Coupling hysteresis analysis with sediment and hydrological connectivity in three agricultural catchments in Navarre, Spain. *Journal of Soils and Sediments*, *19,* (1598–16121).

Knight, J. & Evans, M. (2017). The sediment stratigraphy of a flood event: An example from the Sabie River, South Africa. *Catena, 151,* 87-97.

Kuo, C. W. & Brierley, G. (2013). The influence of landscape configuration upon patterns of sediment storage in a highly connected river system. *Geomorphology 180–181*, 255–266.

Lo´czy, D. (Ed). (2013). *Geomorphological Impacts of Extreme Weather.* New York: Springer Geaography

Manville, V., Segschneider, B., Newton, E., White, J.D.L, Houghton, B.F. & Wilson, C.J.N. (2009). Environmental impact of the 1.8 ka Taupo eruption, New Zealand: Landscape responses to a large-scale explosive rhyolite eruption. *Sedimentary Geology 220, 3–4*, 318–336.

Marden, M., Herzig, A., & Basher, L. (2014). Erosion process contribution to sediment yield before and after the establishment of exotic forest: Waipaoa catchment, New Zealand. *Geomorphology 226,* 162-174.

Matsumoto, D., Sawai, Y., Yamada, M., Namegaya, Y., Shinozaki, T., Takeda, D., Fujino, S., Tanigawa, K., Nakamura, A. & Pilarczyk, J. (2016). Erosion and sedimentation during the September 2015 flooding of the Kinu River, central Japan. *Scientific Reports,* 6: 34168.

McColl, S.T. (2014). Landslide Causes and Triggers. In *Landslide Hazards, Risks, and Disasters,* 17 - 42.

Ministry for Primary Industries (2015). June 2015 Taranaki and Horizons Regions Storm. Primary Sector Impact Assessment MPI Technical Paper No. 2015/28.

Mosley, M.P. & Pearson, C.P. (Eds.) (1997). *Floods and Droughts: The New Zealand Experience.* Christchurch: New Zealand Hydrological Society.

New South Wales Government. (2019). Gully Erosion. Retrieved February 8, 2021 from https://www.environment.nsw.gov.au/topics/land-and-soil/soil-degradation/gully-erosion

National Geographic (2019). Retrieved January 18, 2021 from https://www.nationalgeographic.com/culture/2019/04/maori-river-in-new-zealand-is-a-legal-person/.

National Park Service. (2019). *Mass Wasting.* Retrieved February 12, 2021 from https://www.nps.gov/subjects/erosion/mass-wasting.htm.

Page, M., Trustrum, N. & Gomez, B. (2000). Implications of a century of anthropogenic erosion for future land use in the Gisborne-East coast region of New Zealand. *New Zealand Geographer, 56(2),* 13.

Phillips, C. & Daly, C. (2008). *Willows or natives for stream bank erosion control: a survey of usage in New Zealand regional councils.* Landcare ICM Report No. 2008-2009/01.

Philpott, J. (2007). Whangaehu and Mangawhero Rivers Scheme. Development of management plan and rating system. *Horizons Regional Council.*

Pietron, J., Jarsjo, J., Romanchenko, A.O., & Chalov, S.R. (2015). Model analyses of the contribution of in-channel processes to sediment concentration hysteresis loops. *Journal of Hydrology, 527,* (576-589).

Pillans, B. (1990). Late Quaternary Marine Terraces South Taranaki – Wanganui. New Zealand Geological Survey Miscellaneous Map Series Map 18. Lower Hutt: New Zealand Geological Survey.

Pillans, B. (1994). Direct marine-terrestrial correlations, Wanganui Basin, New Zealand: The last 1 million years. *Quaternary Science Reviews, 13,* 3, pp. 189-200.

Ponziani, F., Pandolfo, C, Stelluti, M. Berni, N. Brocca, L. & Moramarco, T. (2011). Assessment of rainfall thresholds and soil moisture modelling for operational hydrogeological risk prevention in the Umbria region (central Italy). *Landslides* 9(2),229-237.

Queensland Government. (2020). Types of Erosion. Retrieved February 8, 2021 from https://www.qld.gov.au/environment/land/management/soil/erosion/types#:~:text=Sheet%20erosion%20occurs%20when%20a,it%20concentrates%20down%20a%20slope.

Renwick, J., Anderson, B., Greenaway, A., Ngaru King, D., Mikaloff-Fletcher, S., Reisinger, A. & and Rouse, H. (2016). Climate change implications for New Zealand. The Royal Society of New Zealand.

Ritter, D.F., Kochel, R.C. & Miller, J.R. (2011). *Process Geomorphology.* Illinois: Waveland Press Inc.

Rosser, B.J., Ross, C.W. (2011). Recovery of pasture production and soil properties on soil slip scars in erodible siltstone hill country, Wairarapa, New Zealand. *New Zealand Journal of Agricultural Research, 54,* (1), 23-44.

Schwendel, A.C. & Fuller, I.C. (2011). Connectivity in forested upland catchments and associated channel dynamics: The eastern Ruahine Range. *Journal of Hydrology (NZ) 50* (1): 205-225

Shand, R.D., Shepherd, M.J. & Bailey, D.G. (2001). *Morphological investigations along the Wanganui Coast: 1990 – 1998.* A report prepared for the Wanganui District Council and the Wanganui Port Company: Ocean Terminals Ltd.

Smith, W. (2016, 23 February). Flood photograph in Massey professors evaluate past Whanganui floods to help gauge future events. *Stuff*. Retrieved February 12, 2021 from https://www.stuff.co.nz/manawatu-standard/news/77165941/massey-professors-evaluate-past-whanganui-floods-to-help-gauge-future-events.

Sparling G.P., Ross, D., Trustrum, N. & Arnold, G. (2003). Recovery of topsoil characteristics after landslip erosion in dry hill country of New Zealand, and a test of the space-for-time hypothesis. *Soil Biology and Biochemistry, 35,* 12.

Switzer, A.D. (2013). Measuring and analysing particle size in a geomorphic context. In: Shroder, J. (Editor in Chief), Switzer, A.D., Kennedy, D.M. (Eds), *Treatise on Geomorphology*. Academic Press, San Diego, CA, vol. 14, Methods in Geomorphology, pp. 224-242.

Tait, A., Bell, R., Burgess, S., Gray, W., Ladd, M., Mullan, B., Ramsay, D., Reid, S., Thompson, C., Todd, M., Watson, M. & Wratt, D. (2005). Meteorological Hazards and the Potential Impacts of Climate Change in the Manawatu-Wanganui Region. Prepared for Horizons Regional Council. *National Institute of Water and Atmospheric Research Ltd*.

Thomas, M.F. (2001). Landscape sensitivity in time and space – an introduction. *Catena 42*, 83–98.

Thornberry-Ehrlich, T. L. (2019). *Mass wasting processes diagram*. Retrieved February 12, 2021 from https://www.nps.gov/subjects/erosion/mass-wasting.htm

Tonkin & Taylor Consulting Engineers (1978). Water Resources of the Wanganui River. Prepared for the Rangitikei-Wanganui Catchment Board

Townsend, T., Vonk, A. & Kamp, P.J.J. (2008). *Geology of the Taranaki Region*. Institute of Geological & Nuclear Sciences, Lower Hutt, New Zealand.

Trimble (2016). Trimble GPS Tutorial - How Differential GPS works. Retrieved 10 July 2016 from http://www.trimble.com/gps_tutorial/dgps-how.aspx

Van der Neut, M (1996). Sequence Stratigraphy of Plio-Pleistocene Sediments in Lower Turakina Valley, Wanganui Basin, New Zealand. A thesis in partial fulfilment of the requirements for the degree of Master of Science in Quaternary Science at Massey University.

Watson, A.J., Basher, L.R. (2006). *Stream bank erosion: a review of processes of bank failure, measurement and assessment techniques, and modelling approaches.* Landcare ICM Report No. 2005-2006/01.

Watson, B., Rose, M. & Hicks, M. (2017). Turbidity. *National Environmental Monitoring Standards, 1.2.*

Watson, M., Williams, G., Williams, E., & Sewell, P. (1998). Whanganui River investigations of bank erosion and instability. *Wanganui District Council, Manawatu Wanganui Regional Council and Transit NZ*

Williams, G.P. (1989). Sediment concentration versus water discharge during single hydrologic events in rivers. *Journal of Hydrology, 111,* (89-106).

Appendix A

Sample ID	Catchment	Northing	Easting	Total thickness (cm)	D50 (µm)	Distance from Coast (km)	Sample Elevation Height Above Wetted Channel (m)	Distance from Wetted Channel (m)	Sample Description	Site Description
wg1	Whanganui	1778617	5619634	49	124	86.2	12.1	6	Fine sand, light grey/brown, no layering visible	TL, proximal. Moderate/severe streambank erosion on TL bank. Fresh landsliding on TR coupled with channel. Sample taken at Jerusalem.
wg2	Whanganui	1778778	5619740	51	75	86.0	11.6	18	Fine sand and silt, medium grey/brown, no layering visible, homogenous profile	TL, proximal. Severe/moderate streambank erosion on both banks as well as heavy deposition. Bar has formed within river. Severe landsliding between Jerusalem and Ranana on steep slopes of both sides of channel - vegetated with scrub/gorse and patches of native bush at base and peaks of slopes. Landslide/channel coupling extensive. Weak, unconsolidated siltstone/mudstone with blue/grey micaceous layers - 70+ m deep, undeformed layers
wg3	Whanganui	1780947	5616129	19	101	76.8	2.4	3	Fine sand and silt. No layering visible	TL, proximal. This site and Wg4 and Wg5 are part of a cross-section from closest to channel here at Wg3 to more distal at Wg5. Streambank erosion evident. No landsliding visible.
wg4	Whanganui	1780949	5616137	37	137	76.8	5.2	13	Fine sand and silt. No layering visible	TL, proximal. This sample site was taken approxiamtely in the middle of the cross section between Wg3 and Wg5. Streambank erosion evident. No landsliding visible.
wg5	Whanganui	1780954	5616156	32	93	76.8	11.2	32	Fine sand and silt (predominantly silt)	TL, distal. This site along with Wg3 and Wg4 are part of a cross-section from proximal at Wg3 to more distal here at Wg5.
wg6	Whanganui	1784514	5614801	28	137	72.8	8.6	25	Fine sand and silt, medium grey/brown, no layering visible	TL, proximal. Whatauma Stream directly US of this site. Severe streambank erosion and several large landslides on both sides of channel which are coupled with the river. Landslides in pastured regions.
wg7	Whanganui	1786261	5612891	16	33	69.8	31.6	8	Fine sand and silt, light brown/grey, no layering	Small gravel bar forming in channel on TL near bend. Pasture on TL with landsliding. Native bush on TR, minor landsliding. Near Te Aunui Stream confluence which is choked with flood deposits.
wg8	Whanganui	1784911	5606646	31	73	62.4	14.6	32	Fine sand and silt, no layering, homogenous deposits.	TL, distal. Abundant streambank erosion on both banks. Pasture on TL with landsliding. Native bush on TR, no landsliding visible.
wg9	Whanganui	1784753	5604034	24	170	59.9	9.8	13	Fine sand and silt, no layering, light brown/grey	TL, proximal. Streambank erosion on both banks. Minor landsliding on TL below road. Native bush above road with no visible landslides. River debris caught in trees approximately 10m high at this site.
wg10 base	Whanganui	1782226	5601825	32	22	56.1	17.6	50	Layering evident. Top - fine sand and silt, grey/brown. Middle - black/grey silt. Bottom - blue/grey silt.	TL, distal. Relatively low laying in relation to channel, gently sloping site at small 'free camping' area surrounded by bush/scrub
wg10 mid	Whanganui	1782226	5601825	32	43	56.1	17.6	50	Layering evident. Top - fine sand and silt, grey/brown. Middle - black/grey silt. Bottom - blue/grey silt.	TL, distal. Relatively low laying in relation to channel, gently sloping site at small 'free camping' area surrounded by bush/scrub
wg10 top	Whanganui	1782226	5601825	32	81	56.1	17.6	50	Layering evident. Top - fine sand and silt, grey/brown. Middle - black/grey silt. Bottom - blue/grey silt.	TL, distal. Relatively low laying in relation to channel, gently sloping site at small 'free camping' area surrounded by bush/scrub
wg11 base	Whanganui	1783611	5600229	33	30	53.8	10.1	45	Layering evident. Top - light	Native bush/pasture. Landsliding evident on pasture. Rock

									brown/grey fine sand and silt. Bottom - grey silt.	escarpments in native bush areas.
wg11 top	Whanganui	1783611	5600229	33	163	53.8	10.1	45	Layering evident. Top - light brown/grey fine sand and silt. Bottom - grey silt.	Native bush/pasture. Landsliding evident on pasture. Rock escarpments in native bush areas.
wg12 base	Whanganui	1783315	5600255	46	22	54.0	14.0	35	Layering evident. Top - fine sand and silt. Light brown/grey. Bottom - silt, mottled	TL (Atene). Extensive slumping/drawdown along streambank. Obvious flood drape on failure surface. At base of slump is a layer of exposed consolidated conglomerate, signifying downcutting or lateral erosion of channel. TL is on inside of bend and is where deposition would usually occur but during this flood the energy transported the riverbed gravels to expose this consolidated surface. TR is on outside of bend and erosion of bedrock is occurring within channel.
wg12 top	Whanganui	1783315	5600255	46	65	54.0	14.0	35	Layering evident. Top - fine sand and silt. Light brown/grey. Bottom - silt, mottled	TL (Atene). Extensive slumping/drawdown along streambank. Obvious flood drape on failure surface. At base of slump is a layer of exposed consolidated conglomerate, signifying downcutting or lateral erosion of channel. TL is on inside of bend and is where deposition would usually occur but during this flood the energy transported the riverbed gravels to expose this consolidated surface. TR is on outside of bend and erosion of bedrock is occurring within channel.
wg13	Whanganui	1784846	5597080	7	61	48.9	14.6	60	Fine sand and silt. No layering visible	TL, distal. Riverine Lodge site. Pasture paddock along a broad bend in channel. Poplars along streambank.
wg14	Whanganui	1784801	5597081	13.5	126	48.9	6.7	13	Fine sand and silt. No layering evident.	TL, proximal. Sample taken along same transect as above, closer to channel
wg15	Whanganui	1785096	5595625	13	71	46.6	12.6	19	Fine sand and silt. No layering, light grey/brown, homogenous. Small amount of mottling <5%.	TL, proximal. Extensive streambank erosion on TR bank into alluvial sediments. This bank is lower lying and is pastured with no stabilizing features. TR on inside bend with extensive flood drape. TL bank is cutting down into bedrock.
wg16 base	Whanganui	1784027	5595380	19	30	44.7	12.6	57	Layering visible. Top - very fine sand and silt, grey/brown, some mottling at layer contact. Bottom - silt, grey, mottling	TL, distal. Pasture strip between road and channel. Extensive deposition as well as slumping/erosion along streambank.
wg16 top	Whanganui	1784027	5595380	19	84	44.7	12.6	57	Layering visible. Top - very fine sand and silt, grey/brown, some mottling at layer contact. Bottom - silt, grey, mottling	TL, distal. Pasture strip between road and channel. Extensive deposition as well as slumping/erosion along streambank.
wg17	Whanganui	1783982	5595384	41	78	44.7	8.5	18	Fine sand, light grey/brown. No layering.	TL, proximal. Sample taken from same site as above but closer to channel. Willows along streambank. Relatively thick sediment drape under canopy which has distinct ridges and channels on surface. TR extensive streambank erosion occurring in alluvium. No landslide/channel coupling evident.
wg18	Whanganui	1783959	5591778	8	19	40.9	15.0	18	Silt, light brown/grey, mottling, no layering.	TL, distal. Parakino. Low lying pasture. TR streambank erosion and coupled landsliding evident.
wg19	Whanganui	1784021	5591827	35	69	40.9	9.6	96	Fine sand and silt, no layering.	TL, proximal. Parakino. Sample taken from same site as above but closer to the channel. Slumping/streambank erosion evident as well as extensive deposition.
wg20 base	Whanganui	1783709	5590857	19	17	39.8	12.1	70	Layering evident. Top - fine sand and silt, light grey/brown.	TL, distal. Pungarehu Marae. On TR landslide/channel coupling evident as well as streambank erosion. Podocarp lowland

									Bottom - silt, light grey, mottling	forest on TR whilst TL is pasture. Area profiled and sampled is an extensive slumped region along alluvium streambank.
wg20 top	Whanganui	1783709	5590857	19	59	39.8	12.1	70	Layering evident. Top - fine sand and silt, light grey/brown. Bottom - silt, light grey, mottling	TL, distal. Pungarehu Marae. On TR landslide/channel coupling evident as well as streambank erosion. Podocarp lowland forest on TR whilst TL is pasture. Area profiled and sampled is an extensive slumped region along alluvium streambank.
wg21	Whanganui	1778456	5589796	5	50	25.8	12.3	59	No layering, silt, light grey/brown, faint mottling	TL, distal. Kawhaiki. TR bank consists of very steep slopes vegetated with native bush and small regions of pines. Small, localised landslides coupled with channel. TL consists of road, pasture, and small settlement. Resident from this property estimates 6 floods since 1980 have inundated the road. Several river terraces visible. Stream bank erosion on TL.
wg22 base	Whanganui	1778441	5589836	49	133	25.8	7.3	21	Layering evident. Top - medium grained sand - light grey/brown. Bottom - fine sand and silt, light grey/brown, faint mottling	TL, proximal. Kawhaiki. Sample taken from same site as above but closer to the channel.
wg22 top	Whanganui	1778441	5589836	49	170	25.8	7.3	21	Layering evident. Top - medium grained sand - light grey/brown. Bottom - fine sand and silt, light grey/brown, faint mottling	TL, proximal. Kawhaiki. Sample taken from same site as above but closer to the channel.
wg23	Whanganui	1780051	5585698	6	71	19.7	9.6	91	Silt, no layering, distinct mottling	TL, distal. Kawhaiki. Area proximal to channel has been cultivated for crops. Streambank erosion on TL. Both sides of channel surrounded by lowland flat/undulating pasture. Predominantly willows along banks.
wg24	Whanganui	1780123	5582756	6	18	16.1	4.8	130	Silt, no layering, light brown/grey	TL, distal. Old two-story Victorian villa DS of Upokongaro. Three river terraces visible. Slight 'basin' in first terrace where extensive deposition has occurred. Landowner said this site has been inundated at least six times in the last 45 years. Willows vegetate riverbank region. Extensive deposition, little erosion evident.
wg25 base	Whanganui	1780022	5582754	43	18	16.1	2.9	35	Layering evident. Top - fine sand/silt, light grey/brown, faint mottling. Bottom - silt, grey, distinct mottling	TL, proximal. Sample taken from same site as above but closer to the channel.
wg25 top	Whanganui	1780022	5582754	43	50	16.1	2.9	35	Layering evident. Top - fine sand/silt, light grey/brown, faint mottling. Bottom - silt, grey, distinct mottling	TL, proximal. Sample taken from same site as above but closer to the channel.
wg26	Whanganui	1779054	5581570	13	47	14.4	3.8	105	No layering, silt, light brown/grey, faint mottling	TL, distal. 'Sparrows Cliff' site. Willows along channel. Area of low lying, flat land on first river terrace, pasture.
wg27 base	Whanganui	1779036	5581660	41	79	14.4	2.9	15	Layering evident. Top - fine sand and silt. Light grey/brown. Bottom - silt and fine sand (more silt than above layer), light brown/grey	TL, proximal. Sample taken from same site as above but closer to the channel.
wg27 top	Whanganui	1779036	5581660	32	157	14.4	2.9	15	Layering evident. Top - fine sand and silt. Light grey/brown. Bottom - silt and fine sand (more silt than above layer), light brown/grey	TL, proximal. Sample taken from same site as above but closer to the channel.
wg28	Whanganui	1777987	5586354	10	34	22.1	12.2	70	No layering, silt, faint mottling	TR, distal. Papaiti. Ohorere property. Extensive deposition, very little erosion on TR.

										Poplars/willows along streambank. TL is pasture with extensive streambank erosion/slumping and deposition. Erosion less severe where plantings (willow) occur. 2015 flood reached base of third river terrace - at least 2-3m higher than 2004 flood.
wg29 base	Whanganui	1780629	5584679	19	23	18.3	8.0	42	Layering evident. Top - fine sand and silt, light grey/brown. Bottom - grey silt with organic detritus, distinct mottling.	TR, proximal. Flood waters reached base of third river terrace. TR and TL willows/ poplars along streambanks with small localised slumping. Extensive deposition on both banks. TR flat, open pasture.
wg29 top	Whanganui	1780629	5584679	19	67	18.3	8.0	42	Layering evident. Top - fine sand and silt, light grey/brown. Bottom - grey silt with organic detritus, distinct mottling.	TR, proximal. Flood waters reached base of third river terrace. TR and TL willows/ poplars along streambanks with small localised slumping. Extensive deposition on both banks. TR flat, open pasture.
wg30 base	Whanganui	1777367	5581727	25	161	12.7	5.1	11	Layering evident. Top - fine/medium sand and silt, grey/orange/brown , mottled. Bottom - dark grey sandy silt, slight mottling esp. near decomposing roots at base of layer.	TR, proximal. Very little erosion visible along streambanks. Extensive deposition. TR has flax/willows planted and rip rap boulders to inhibit erosion
wg30 top	Whanganui	1777367	5581727	25	104	12.7	5.1	11	Layering evident. Top - fine/medium sand and silt, grey/orange/brown , mottled. Bottom - dark grey sandy silt, slight mottling esp. near decomposing roots at base of layer.	TR, proximal. Very little erosion visible along streambanks. Extensive deposition. TR has flax/willows planted and rip rap boulders to inhibit erosion
wg31 base	Whanganui	1776570	5581077	49	26	11.7	2.6	10	layering evident. Top - fine sand, light grey/brown. Quartz, ferromagnesium rich. Bottom - silt, dark grey, organic detritus, distinct mottling.	TR, proximal. Minor streambank erosion/slumping.
wg31 top	Whanganui	1776570	5581077	49	170	11.7	2.6	10	layering evident. Top - fine sand, light grey/brown. Quartz, ferromagnesium rich. Bottom - silt, dark grey, organic detritus, distinct mottling.	TR, proximal. Minor streambank erosion/slumping.
wg32	Whanganui	1775237	5579078	10	39	9.4	4.1	9	Silt, no layering, faint mottling	TR, proximal. TR is higher than floodplain on TL. TL flood waters/energy dispersed extensive, thick deposits along Anzac Pd and Kowhai Park
wg33	Whanganui	1775567	5576865	12	18	6.7	2.4	20	Silt, light grey/brown, no layering, faint mottling.	TL, proximal. No erosion along streambanks as rip rap extensive along this reach. 200 m US extensive landsliding of Durie Hill cliff face as well as Shakespeare Cliff (these are situated along broad outer bend of channel). Also localised streambank erosion 200 m US at bend where concrete drums were emplaced to inhibit erosion.
wg34	Whanganui	1773907	5575142	6.5	16	4.4	3.0	27	Silt, no layering, faint mottling, light grey/brown	TL, proximal. Landgaurd Bluff. River is relatively wide at this site, so flood waters were not as high at this point in comparison to upper reaches. No streambank erosion visible. Deposition extensive, especially on TR where floodplain is lower
wg35	Whanganui	1769880	5576415	5	47	0.1	3.3	5	Silt, light grey/brown, distinct mottling abundant throughout	TR, proximal. Site located DS of wharf at river mouth. Extensive deposits have built up in channel from Sailing Club to the Coastguard. Much of the flood drape has been cleared but this

										site appears to be untouched - below a bank adjacent to Tregenna St/Short St intersection.

ID	Catchment	Northing	Easting	Total thickness (cm)	D50 (µm)	Distance from Coast (km)	Sample Elevation Height Above Wetted Channel (m)	Distance from Wetted Channel (m)	Sample Description	Site Description
Wh1	Whangaehu	5569617	1784855	2	68	11.5	7.1	159	No layering, silt, light grey, distinct mottling	TR, distal. DS SH3 bridge. Relatively flat paddock newly planted with maize. Streambank erosion evident along TR bank and slumping in localised unplanted areas. Willows sparsely planted along TR.
Wh2	Whangaehu	5569553	1784933	8	15	11.5	7.0	116	No layering, silt, light grey, distinct mottling	TR. Sample taken from the same cross section as above and below samples (middle sample).
Wh3	Whangaehu	5569470	1784867	31	89	11.5	5.8	11	No layering, fine sand, light grey, diffuse mottling.	TR, proximal. Deposition of fines and gravel on TL whilst this bank has slumped. Pasture on TL.
Wh4	Whangaehu	5569215	1787105	9.5	73	15.4	4.7	658	No layering, silt, distinct mottling, grey/brown	TL, distal. John Wilkie property. Samples taken from narrowest point in floodplain - two ridges on either side of channel jut out to create a bottleneck. Railway line built 1940-1945. Road raised 2004. Landowner said both railway and road which are on raised bases can dam flood waters during floods. Rail bridge and two culverts are the only areas that flood water can go under the raised railway bridge. Landowners woolshed was inundated by floods in 2015, 2013, 2006. 2004.
Wh5	Whangaehu	5569725	1787921	12	15	15.4	5.9	401	No layering, silt, distinct mottling.	TL, proximal. Sample taken from the same cross section as above but closer to the channel.
Wh6	Whangaehu	5578040	1794499	10	42	38.0	10.0	26	Fine sand and silt, grey/brown, faint mottling, no layering	TL, proximal. Kaiangoroa beside bridge. Moderate slumping/streambank erosion along both banks. Willows/poplars sparsely planted long both sides of channel. Wide floodplain on both sides of channel with extensive deposition - some of which is being cleared.
Wh7	Whangaehu	5581041	1795806	25	32	45.3	9.4	57	Fine sand and silt, grey/brown, faint mottling, no layering	TL, distal. Adjacent to new Mangamahu Bridge. Floodwaters reached second river terrace and partway up third. Wide floodplain region, pastured, poplars/willows along banks. Much debris in river, water is extremely turbid.
Wh8	Whangaehu	5583507	1794646	31	80	51.6	10.3	54	Layering evident. Top - fine sand and silt, light brown/grey, no mottling. Bottom - grey silt, mottled where organics are decomposing	TR, distal. Streambanks planted with willows/poplars with forestry plantation further back - landsliding evident in forestry region. TR has extensive streambank erosion/slumping and large area of deposition. TL minor streambank erosion, extensive deposition also.
Wh9	Whangaehu	5587744	1795085	2	14	61.0	11.7	94	No layering, grey silt.	TR, distal. Mangawhero tributary. Pastured floodplain on both banks, channel incised into alluvium therefor there is substantial streambank erosion/slumping on both banks. Deposition extensive on TR
Wh 10	Whangaehu	5587676	1795096	18	124	61.0	11.4	28	Layering evident. Top - fine sand and silt, light brown/grey. Bottom - silt, grey, distinct mottling	TR, proximal. Mangawhero tributary. Sample taken from the same cross section as above site but closer to the channel. North facing pastured slopes in distance contain substantial landsliding.

									around decomposing roots	
Wh 11	Whangaehu	5587378	1801563	32	146	67.8	4.8	16	Medium/fine sand and silt, grey/brown, no layering	TL, proximal. Below Mangamahu Rd, in valley with relatively small floodplain. TL extensive streambank erosion into alluvium with moderate deposition. Landslides evident on surrounding moderate/steep slopes - no channel/slope coupling visible. TR bank is predominantly cutting into bedrock with some erosion along cliff face.
Wh 12	Whangaehu	5589928	1802354	3	112	74.5	1.9	5	Fine sand and silt, light grey/brown, distinct mottling	TL, proximal. Vegetated with willows. Very little erosion/deposition. TR bank has been steeply incised by channel and is bedrock. TR vegetated with kanuka, toi toi, poplar, coprosma, ferns, pine
Wh 13	Whangaehu	5589116	1795067	10	16	63.6	12.0	70	Light grey/brown silt, distinct mottling.	TL, distal. Mangawhero River. Polsons Farm on Te Rimu Rd. Pastured paddock surrounded by moderate/steep slopes and a bluff at north-eastern edge. Gravel road was inundated, and extensive deposition occurred which has since been cleared. Banks space planted with poplars, alder, and pine saplings. Much streambank erosion/slumping along both banks. Deposition more extensive on TL as lower. Landsliding on TR bluff
Wh 14	Whangaehu	5589077	1795068	55	112	63.6	10.0	32	Fine sand, light grey/brown, mottling at base where organics are decomposing	TL, proximal. Mangawhero River. Sample taken from same site as above but closer to the channel. Much organic debris in channel. Streambank erosion extensive. Slope channel coupling.
Wh 15	Whangaehu	5592235	1795851	8	17	78.8	11.3	59	Light grey/brown silt, mottling, no layering	TL, distal. Site is a small depression of pasture below the Parapara Rd - likely first river terrace. Extensive streambank erosion into alluvium. Closer to the channel deposits of sand were found but were over 0.5 m deep. Landowner said this came from a large landslide on his property (Polsons).

ID	Catchment	Northing	Easting	Total thickness (cm)	D50 (µm)	Distance from Coast (km)	Sample Elevation Height Above Wetted Channel (m)	Distance from Wetted Channel (m)	Sample Description	Site Description
T01	Turakina	5564243	1787435	6	45	11.2	8.1	224	No layering present, silt, light grey/brown, no mottling	TL distal. Pasture, relatively flat near river mouth. Extensive slumping/streambank erosion/drawdown of banks within alluvium on both sides. Willows/poplars along both banks. No slope/channel coupling evident.
T02	Turakina	5566150	1788388	14	176	13.7	6.2	43	Layering evident - 11cm grey/light brown sand above 3cm grey silt, distinct mottling	TR distal. DS SH3 bridge. Pasture. Surrounded by moderately steep slopes. 3 river terraces evident. Drape reached base of second terrace. Streambank erosion/ slumping/drawdown evident. Alluvium remobilised. No slope/channel coupling.
T03	Turakina	5570345	1795377	16	29	25.8	20.8	116	No layering present, silt, light grey/brown, distinct mottling throughout	TL distal. Moderate streambank erosion on both sides. No slope/channel coupling evident. TL bank slightly lower so deposition dominant on this side.
T04	Turakina	5574439	1799000	14	62	39.5	6.9	18	No layering evident, fine sand/silt, grey/brown, no mottling.	TL, distal. Poplar/willow dense along streambanks. Sample taken from depression along floodplain. Desiccation cracks in new drape.
T05	Turakina	5576943	1799556	13	79	44.0	9.1	26	No layering present, distinct mottling,	TR, proximal. Adjacent to Cranston farmhouse bridge. Willows dense along streambanks.

									light grey/brown	
T06	Turakina	5579248	1801391	3	56	50.7	9.2	21	No layering, light grey/brown silt, diffuse mottling present	TR, proximal. Deeply incised surrounded by near vertical, vegetated cliffs. TR bank lower and alluvium. Pasture surrounded by native bush. Extensive TR streambank erosion. Large amount of woody debris in river.